AFRL-RQ-WP-TR-2016-0131

DEMONSTRATION OF NOVEL SAMPLING TECHNIQUES FOR MEASUREMENT OF TURBINE ENGINE VOLATILE AND NON-VOLATILE PARTICULATE MATTER (PM) EMISSIONS

Edwin Corporan

Fuels and Energy Branch
Turbine Engine Division

Matthew DeWitt and Chris Klingshirn

University of Dayton Research Institute

Meng-Dawn Cheng

Oak Ridge National Laboratory

Richard Miake-Lye, Jay Peck and Zhenhong Yu

Aerodyne Research Inc.

John Kinsey

Environmental Protection Agency

Berk Knighton

Montana State University

SEPTEMBER 2016
Final Report

AIR FORCE RESEARCH LABORATORY
AEROSPACE SYSTEMS DIRECTORATE
WRIGHT-PATTERSON AIR FORCE BASE, OH 45433-7541
AIR FORCE MATERIEL COMMAND
UNITED STATES AIR FORCE

NOTICE AND SIGNATURE PAGE

Using Government drawings, specifications, or other data included in this document for any purpose other than Government procurement does not in any way obligate the U.S. Government. The fact that the Government formulated or supplied the drawings, specifications, or other data does not license the holder or any other person or corporation; or convey any rights or permission to manufacture, use, or sell any patented invention that may relate to them.

This report was cleared for public release by the USAF 88th Air Base Wing (88 ABW) Public Affairs Office (PAO) and is available to the general public, including foreign nationals.

Copies may be obtained from the Defense Technical Information Center (DTIC) (http://www.dtic.mil).

AFRL-RQ-WP-TR-2016-0131 HAS BEEN REVIEWED AND IS APPROVED FOR PUBLICATION IN ACCORDANCE WITH ASSIGNED DISTRIBUTION STATEMENT.

*//Signature//

DONALD K. MINUS
Program Manager
Fuels and Energy Branch
Turbine Engine Division

//Signature//

MIGUEL A. MALDONADO, Branch Chief
Fuels and Energy Branch
Turbine Engine Division
Aerospace Systems Directorate

//Signature//

CHARLES W. STEVENS
Lead Engineer
Turbine Engine Division
Aerospace Systems Directorate

This report is published in the interest of scientific and technical information exchange and its publication does not constitute the Government's approval or disapproval of its ideas or findings.

*Disseminated copies will show "//Signature//" stamped or typed above the signature blocks.

REPORT DOCUMENTATION PAGE

Form Approved
OMB No. 0704-0188

1. REPORT DATE *(DD-MM-YY)*	2. REPORT TYPE	3. DATES COVERED *(From - To)*
September 2016	Final	11 December 2009 – 30 June 2016

4. TITLE AND SUBTITLE

DEMONSTRATION OF NOVEL SAMPLING TECHNIQUES FOR MEASUREMENT OF TURBINE ENGINE VOLATILE AND NON-VOLATILE PARTICULATE MATTER (PM) EMISSIONS

5a. CONTRACT NUMBER
FA8650-10-2-2934

5b. GRANT NUMBER

5c. PROGRAM ELEMENT NUMBER
Multiple (cooperative)

6. AUTHOR(S)

Edwin Corporan (AFRL/RQTF)
Matthew DeWitt and Chris Klingshirn (University of Dayton Research Institute)
Meng-Dawn Cheng (Oak Ridge National Laboratory)
Richard Miake-Lye, Jay Peck and Zhenhong Yu (Aerodyne Research Inc.)
John Kinsey (Environmental Protection Agency)
Berk Knighton (Montana State University)

5d. PROJECT NUMBER
Multiple (cooperative)

5e. TASK NUMBER

5f. WORK UNIT NUMBER
Q0HS

7. PERFORMING ORGANIZATION NAME(S) AND ADDRESS(ES)

Fuels and Energy Branch (AFRL/RQTF)
Turbine Engine Division
Air Force Research Laboratory, Aerospace Systems Directorate
Wright-Patterson Air Force Base, OH 45433-7541
Air Force Materiel Command, United States Air Force

University of Dayton Research Institute
300 College Park Ave
Dayton, OH 45469-0001

8. PERFORMING ORGANIZATION REPORT NUMBER
ESTCP Project WP-201317

9. SPONSORING/MONITORING AGENCY NAME(S) AND ADDRESS(ES)

Air Force Research Laboratory
Aerospace Systems Directorate
Wright-Patterson Air Force Base, OH 45433-7541
Air Force Materiel Command
United States Air Force

Environmental Security Technology Certification Program
4800 Mark Center Drive, Suite 17D08
Alexandria, VA 22350-3605

10. SPONSORING/MONITORING AGENCY ACRONYM(S)
AFRL/RQTF

11. SPONSORING/MONITORING AGENCY REPORT NUMBER(S)
AFRL-RQ-WP-TR-2016-0131

12. DISTRIBUTION/AVAILABILITY STATEMENT

DISTRIBUTION STATEMENT A: Approved for public release. Distribution is unlimited.

13. SUPPLEMENTARY NOTES

PA Case Number: 88ABW-2016-0148; Clearance Date: 15 Jan 2016. The U.S. Government is joint author of this work and has the right to use, modify, reproduce, release, perform, display, or disclose the work.

14. ABSTRACT

This project consists of demonstrating the performance and viability of two devices to condition aircraft turbine engine exhaust to allow the accurate measurement of total (volatile and non-volatile) particulate matter (PM) emissions by promoting condensation of volatile species. A device to separate volatile from non-volatile species from turbine engine exhaust was also evaluated for the measurement of only non-volatile PM. These measurements are needed to assess the environmental burden of military aircraft for regulatory purposes. Non-volatile PM are those found at the engine exit temperature and pressure conditions, whereas volatile PM are those formed from organic and sulfur compounds via gas-to-particle reactions in the atmosphere. The total PM devices were evaluated by comparing the PM characteristics to those found in plume samples using exhaust from a T63 turboshaft and an F117 turbofan engine. Results show that the devices can partially simulate the thermophysical processes in the plume that lead to the formation of volatile PM. However, several of the performance criteria for these devices were not met. A vapor particle separator met the performance goals and shall be considered for non-volatile PM systems after further evaluations.

15. SUBJECT TERMS

Turbine engine emissions, non-volatile and volatile PM, PM environmental regulations

16. SECURITY CLASSIFICATION OF:			17. LIMITATION OF ABSTRACT:	18. NUMBER OF PAGES	19a. NAME OF RESPONSIBLE PERSON (Monitor)
a. REPORT	b. ABSTRACT	c. THIS PAGE			Donald K. Minus
Unclassified	Unclassified	Unclassified	SAR	90	19b. TELEPHONE NUMBER *(Include Area Code)* N/A

Table of Contents

Section **Page**

List of Figures

Figure **Page**

List of Tables

Acknowledgments

The authors are grateful to the Environmental Technology Security Certification (ESTCP) office for funding this project, and to the Turbine Engine Division of the Aerospace Systems Directorate Air Force Research Laboratory (AFRL) for its support via in-house facilities, manpower and emissions measurement capabilities. We appreciate the efforts of Joe Mantz, Tyler Hendershott, Sam Tanner, Robert Casselberry, Rhonda Cook from the University of Dayton Research Institute (UDRI) for their technical support during the demonstrations on the C-17 aircraft and T63 engines, and to Zach West of UDRI and Matt Wagner of AFRL for their support on the facility and experimental system setup and data acquisition during the demonstration on the T63 engine. Also our appreciation to Alex Briones of UDRI for the Computational Fluid Dynamics (CFD) modeling the dilution chamber mixing characteristics. Thanks to the Air Mobility and Air Force Reserve Commands for approving the use of the C-17 aircraft for the second demonstration and special thanks to Lt Col Jay Smeltzer, SMSgt Jason Gumm and MSgt Scott Stein of the 445th Air Lift Wing at Wright-Patterson Air Force Base for assisting in the coordination of the demonstration and their logistical support during the campaign.

The efforts of John Storey, Scott Curran, Teresa Barone, Steve Allman, Brian Bischoff and Shannon Mahurin of Oak Ridge National Laboratory (ORNL) to develop the VPS during this and SERDP project WP-1627 are greatly appreciated. Also, the work of Erik Kabela (also from ORNL) in support of the demonstration on the C-17 is acknowledged.

The condensation dilution probe (CDP) was developed under an Air Force Small Business Innovation Research (SBIR) contract (contract number: FA9101-08-C-0013), and the support of Robert Howard, the AEDC SBIR technical monitor, is greatly appreciated.

The efforts of UDRI were supported by the USAF under the Cooperative Research Agreement FA8650-10-2-2934.

1. EXECUTIVE SUMMARY

This project consists of demonstrating the performance and viability of three devices to condition aircraft turbine engine exhaust for the measurement of non-volatile and/or total (volatile and non-volatile) particulate matter (PM) emissions. These measurements are needed to assess the environmental burden of military and commercial aircraft to verify compliance with future regulations. Non-volatile PM are those found at the engine exit temperature and pressure conditions, whereas volatile PM are those formed from organic and sulfur compounds via gas-to-particle reactions in the atmosphere. Accurate measurement of non-volatile PM is challenging due to the harsh environment found at the engine exit plane. Reliable measurements of volatile PM are even more difficult as these are formed in the exhaust plume and are influenced by fuel composition, ambient conditions and composition of the volatile species.

Two devices, the dilution chamber (DC) and the condensation dilution probe (CDP), were evaluated to assess their effectiveness in conditioning turbine engine exhaust for total PM emissions measurements. Both were designed to promote the condensation of volatile species and thus, the formation of volatile PM (simulating ambient dilution), which can then be characterized along with non-volatile PM using conventional aerosol instruments. During operation, the PM exhaust sample was collected at the engine exit using one or multiple probes and transported through heated lines to the condensation devices. The DC diluted with mainly ambient air, while the CDP diluted with temperature and humidity controlled nitrogen. The dilution ratios for both the DC and CDP were controlled to match the levels found in the plume (set for this demonstration at 20 m from the engine exit plane). Exhaust from two engines, a T63 and an F117 (C-17 aircraft), were used to evaluate the devices.

A vapor particle separator (VPS), a device to separate volatile and non-volatile species from turbine engine exhaust, was evaluated for the measurement of only non-volatile PM. The performance of the device was assessed in the laboratory by sampling tetracontane (C_{40}) particles and during field demonstrations using turbine engine exhaust.

PM physical and chemical properties were measured at the exit of the condensation devices at several engine settings, and compared to measurements made in the engine plume. Significant challenges were faced during both demonstrations, which included: inclement weather and limited test time (both for the C-17), sampling system issues and difficulty in obtaining steady emissions data at the plume. Despite the challenges, it was evident that the devices were able to promote the formation of volatile PM, therefore simulating ambient gas-to-particle processes. However, the concentration of particles formed from volatile species was significantly lower than those sampled at plume locations, especially when the engine was operated with high sulfur content fuel. Since neither condensation device met all of the performance objectives set for the project, it is concluded that these technologies are not currently ready to use for compliance relevant measurements.

Based on the set performance criteria, the VPS met the objectives of the project. Evaluations against the criteria set by the SAE E31 committee (ARP 6320) for volatile particle removers (VPR) shall follow to further validate its use for non-volatile PM measurement. This includes volatile removal efficiency, pressure control, and particle penetration requirements.

2. INTRODUCTION

2.1 BACKGROUND

The U.S. EPA has the authority under the Clean Air Act (CAA) to protect human health and welfare from the effects of air pollution by establishing and ensuring compliance of the National Ambient Air Quality Standards (NAAQS). The NAAQS apply to seven air pollutants, referred to as criteria pollutants. Due to its harmful environmental and health impacts, particulate matter (PM) [specifically particles less than 10 and 2.5 μm in aerodynamic diameter (PM_{10} and $PM_{2.5}$)], have been identified as criteria pollutants [1]. Both PM_{10} and $PM_{2.5}$ include volatile and non-volatile PM (defined below) emitted from mobile and stationary sources. Accordingly, the U.S. EPA and international environmental agencies continue to implement more stringent air quality standards to limit PM emissions. For instance, in regions that do not meet the NAAQS requirements, the individual states need to develop and adopt strategies to be included in their EPA-mandated State Implementation Plan (SIP) to bring the area into compliance. The type of strategy employed depends on the area's designation stage and severity as well as the state of progress toward regaining attainment status. Within the SIP, states must develop measures to control and reduce emissions, and demonstrate compliance with the NAAQS within 5 years of being designated as nonattainment. In the aviation sector, these measures may include: changing airport operations (e.g., surface congestion management strategies), replacing or modifying ground support equipment, infrastructure additions (e.g., air traffic control, runways) and others. Although current aircraft turbine engines are substantially less polluting than legacy engines manufactured pre-1980s (as evidenced by the less visible smoke trail), they still emit significant quantities of very fine volatile and non-volatile particles ($PM_{2.5}$). Consequently, current and future PM regulations will likely affect the aviation sector by slowing down the growth of commercial aviation worldwide and negatively impact military operations by limiting readiness exercises and restricting the use of different types of aircraft. In the commercial sector, increased landing and takeoff fees may be assessed if pollutant allowances are exceeded [similar to the European Union (EU) Emissions Trading Scheme (ETS)] resulting in more expensive air travel for the general population. In the military, expensive fines may be incurred due to non-compliance of environmental regulations. Evidently, it is imperative that accurate and reliable aircraft turbine engine measurement techniques are developed for total (volatile + non-volatile) PM to assess the true environmental burden of aviation activities and to help determine the proper corrective action (if needed). After accurate assessments are performed, more educated decisions can be made to properly and cost-effectively control and mitigate PM emissions.

Aircraft PM is formed in the engine combustor due to incomplete combustion of fuel, and in the atmosphere through gas-to-particle transformations of organic and sulfur-based volatile components upon cooling and mixing with the atmosphere (see Figure 1). PM emitted from the engine at exit temperatures and pressures are defined as **non-volatile**, whereas those formed via gas-to-particle conversion in the atmosphere are known as **volatile** PM. Accurate measurement of non-volatile PM from aircraft engines is a daunting task due to the harsh environment found at the engine exit, particle losses during transport in sample lines, and physical and chemical transformations of the sample as it is transported to analytical instrumentation. Reliable measurements of volatile PM are even more challenging as these are formed in the exhaust plume and are greatly influenced by ambient conditions and composition of the volatile species.

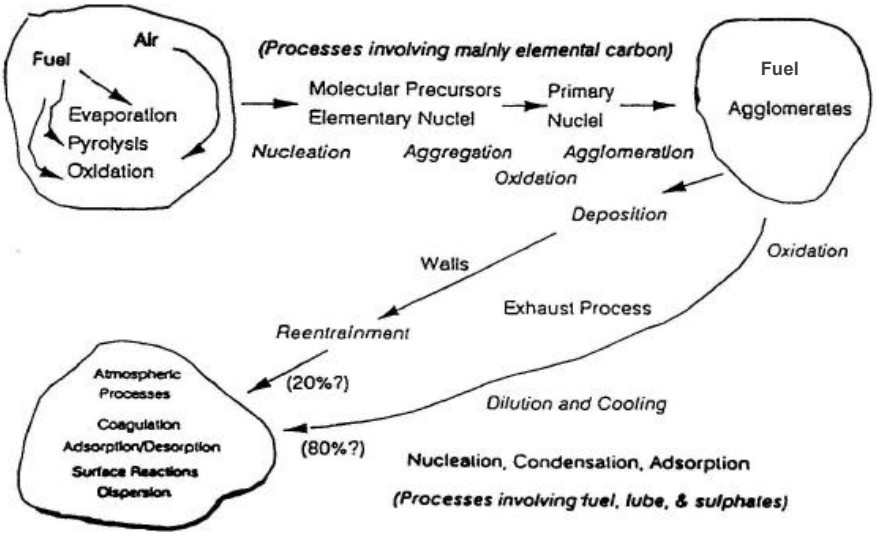

Figure 1. Formation of Volatile and non-volatile PM from engine exhaust [from Ref 2]

Historically, the SAE E-31 committee has been assigned by the Committee on Aviation Environmental Protection (CAEP) of the International Civil Aviation Organization (ICAO) to develop a standard methodology to accurately measure non-volatile particle number and mass emissions from aircraft turbine engines. This methodology could then be used to certify engines to provide an accurate estimate of PM emissions from aircraft, in the event that aircraft PM regulations are implemented. The non-volatile PM Aerospace Recommended Practice (ARP) being developed by the E-31 Committee will include proper sampling approaches, instrumentation specifications and emission index calculation procedures. One approach proposed by the committee for particle number measurement uses Annex 16 Volume II sampling principles in combination with methodology developed under the EU Particle Measurement Programme (PMP) for ground vehicles [3]. In this hybrid method, the sample is extracted at the turbine engine exit using conventional gas probes, transported to a dilution section at > 150 °C (max distance probe to dilution of 8 m), through a downstream volatile particle remover (VPR) (for number only), which includes hot and cold dilution with an evaporator, and finally to instrumentation for particle number measurements. However, several technical issues of concern must be addressed before the PMP method could be implemented for measurement of turbine engine exhaust, including: efficient removal of volatile PM, effective quantitation for particle sizes < 23 nm (currently 23 nm size cut off for PMP – not acceptable for turbine engines as these produce high concentration < 23 nm diameter particles), optimization of sampling line lengths and residence time (probe to dilution point and total length to instruments) and overall particle losses. Since volatile material can greatly affect the particle number counting robustness, a VPR is required. Unfortunately, commercial VPRs are not effective in suppressing volatile material below 23 nm and as such, may be inadequate for this application. In addition, non-volatile particle losses in commercial VPRs may also be a concern.

With the assistance of SAE-E31 members, the International Civil Aviation Organization (ICAO) recently developed a standard methodology to accurately measure non-volatile particle number and mass emissions from aircraft turbine engines. This methodology, soon to be published in Annex 16, Volume 2 of the ICAO standards, includes proper sampling approaches, instrumentation specifications and emission index calculation procedures. The method includes

the sampling system and instrumentation to measure the non-volatile PM mass and number emissions using standard gas probes sampling the engine exhaust at the exit plane. The ICAO methodology does not, however, address the volatile particles formed in the downstream plume which is important to both local air quality and impacts on global climate.

Under SERDP project WP 1627, the Oak Ridge National Laboratory (ORNL)/Air Force Research Laboratory (AFRL)/University of Dayton Research Institute (UDRI) team developed a VPS to partition volatile and non-volatile components in aircraft engine exhaust and allow volatile species to be chemically analyzed. Also under this SERDP project, a DC was developed to homogeneously dilute and condition aircraft exhaust for measurement. Under an Air SBIR program, Aerodyne Research Inc. (ARI) developed a CDP to effectively control the formation of volatile particles to simulate atmospheric processing behavior and to quantify this contribution on the total PM mass emissions. All devices have shown excellent potential when testing in laboratory and limited field environments. Further demonstrations of these devices may lead to the development of more reliable methodologies for the measurement of both volatile and non-volatile PM emissions from turbine engines, which can then be used for cost-effective determination of regional PM emissions for regulatory purposes.

2.2 OBJECTIVE OF THE DEMONSTRATION

The objective of the demonstration can be divided into four parts, listed below.

- Demonstrate reliable operation of the DC to condition PM sample collected at the engine exit plane for the characterization of non-volatile PM.
- Demonstrate the viability of the DC and CDP to simulate volatile PM formation in the atmosphere by comparing to a measurement conducted far field (e.g., 20 m). Successful demonstration will allow for the characterization of total PM at the exit plane.
- Demonstrate efficient operation and establish conditions of the VPS to remove volatile PM precursors from turbine engine exhaust. Successful demonstration may lead to inclusion of the VPS in the non-volatile ARP as a more efficient alternative to the available commercial volatile particle remover (VPR) units.
- Develop sampling methodology with the most efficient devices and provide recommendations to SAE E-31 for potential inclusion in the non-volatile PM number and mass ARP. Develop an Aerospace Information Report (AIR) as a first step towards the development of an ARP for total (volatile and non-volatile) turbine engine PM measurements.

2.3 REGULATORY DRIVERS

The EPA has promulgated the NAAQS for $PM_{2.5}$, which impacts air operations at DoD facilities and thus, squadron basing options. Each facility must perform a conformity analysis which shows that the emissions from that facility do not violate the $PM_{2.5}$ ambient air quality standard. Since $PM_{2.5}$ includes both volatile and non-volatile PM components, methods which allow for quantification of the contribution of each to the total PM are necessary. At the present time, no such information exists for military aircraft and thus new data and methodologies to obtain these data are needed.

3. DEMONSTRATION TECHNOLOGY

3.1 TECHNOLOGY DESCRIPTION

This program consists of demonstrating the viability of three devices to condition turbine engine exhaust for the analysis of non-volatile and/or total (volatile and non-volatile) PM emissions. The technologies (devices) are described below.

3.1.1 Dilution Chamber (DC) – PM measurements in diesel engines are conducted using full-flow Constant Volume Sampling (CVS) systems, which dilute and condition the entire engine sample to simulate PM dilution processes in the atmosphere. Because of the significantly higher exhaust mass flows and gas velocities, this approach is not feasible for turbine engines. For turbine engine PM sampling, the historical approach has been to sample a portion of the flow near the exhaust nozzle and dilute at the probe-tip with nitrogen. Although this methodology is believed to provide a good representation of the non-volatile PM emissions, it is complex and sample dilution downstream of the engine exit is preferable as engine manufacturers can use existing gas probes and rakes. The DC in this project was designed to provide an easy and effective (i.e., low PM loss) means of diluting a hot, PM turbine engine exhaust sample collected at the exit plane in a controlled manner, while maintaining its physical characteristics. PM samples require dilution to reduce concentrations to the range of commercial aerosol instruments and to minimize losses through sampling system lines. The DC was designed to promote condensation and thus, the formation of volatile particles (simulating ambient dilution), which can then be characterized using conventional aerosol instruments. Under several conditions, the DC may also be used to provide a non-volatile PM sample to the instruments. The DC (Figure 2) has a cylindrical design with three regions: exhaust sample injection and primary dilution zone (via an ejector and motive flow), a secondary diluent zone, and a turbulent mixing zone. Raw exhaust is extracted at the engine exit plane and drawn to the dilution chamber by the ejector via a 0.77 cm inner diameter stainless steel heated line at 150°C. Compressed ambient air or nitrogen is used as the motive (driver) flow. The raw sample residence times are typically 60 to 100 ms before reaching the ejector. Low raw sample residence times and high temperatures before dilution are desirable to maintain sample integrity and reduce particle losses and agglomeration. The sample is then diluted with compressed nitrogen or ambient air drawn into the DC with a variable speed blower. The secondary diluent enters the DC and is passed through a flow straightener before mixing with the partially diluted sample from the ejector. The mixing section downstream of the ejector is comprised of a converging/ diverging section and a homogeneous sampling zone. The DC was designed based on CFD modeling using Fluent software and the turbulent RNG k-ε RANS model approach. The radial and axial exhaust profiles were used to assess the homogeneity of the conditioned gas stream. The methodology resulted in a design with a converging/diverging section to promote convective mixing of the sample and diluent streams to overcome diffusional transport limitations. The DC has an internal diameter of 0.21 m with a cylindrical inlet length of 0.80 m. The internal diameter then rapidly converges to 0.038 m followed by a gradual divergence to the original diameter over the next 0.10 m. The diluted sample extraction point is located approximately 1.10 m downstream of the converging/diverting section throat.

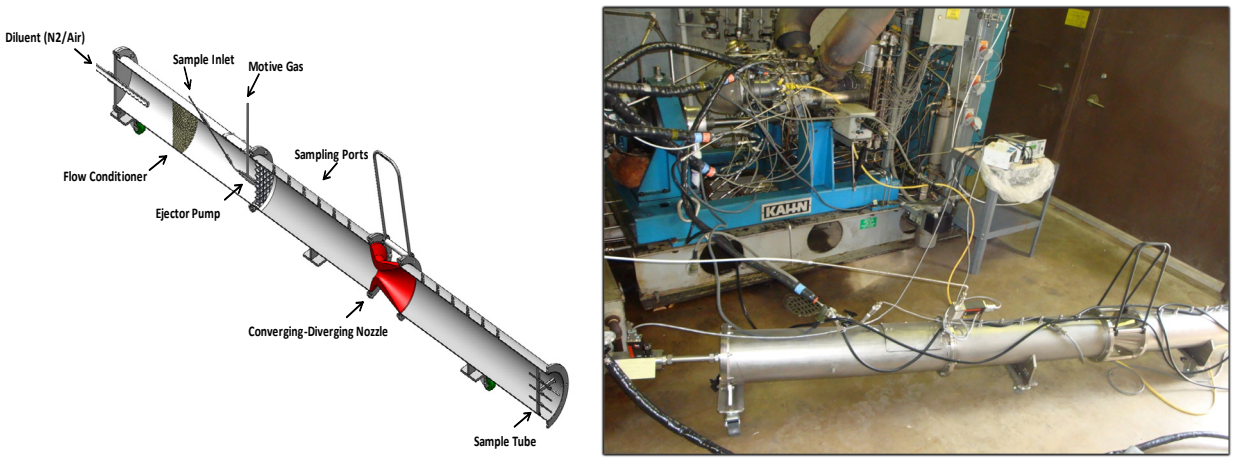

Figure 2. Schematic of DC and implementation of DC on T63 engine

An axisymmetric cross section of the DC is shown in Figure 3 with the predicted mixing characteristics for CO_2 as a function of axial and radial position for a dilution ratio of 100:1. The CFD analyses indicated that the process stream would be fully developed and homogeneous at the downstream sampling location. The concentration of CO_2, used as the representative trace gas for these calculations, is initially non-homogeneous through the cross section. However, once the stream passes through the converging/diverging section (axial distance of 1.0 m), the stream is radially homogeneous at the extraction point. During engine sampling, the diluted sample is collected in the mixing zone via a 0.635 cm SS tube, and transferred to the instrumentation through unheated carbon impregnated PTFE and SS tubing.

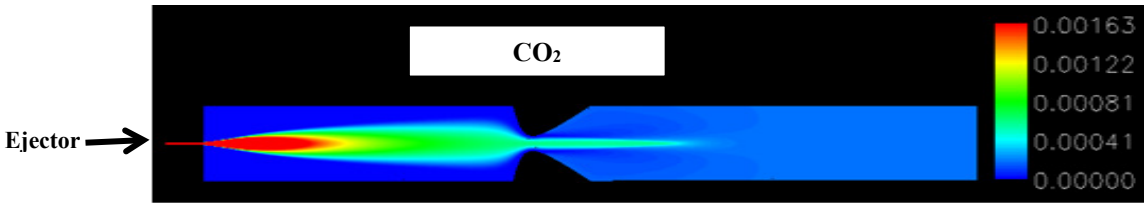

Figure 3. Axisymmetric radial CO_2 distribution as a function of axial distance in dilution chamber for a dilution ratio of 100:1

3.1.2 Vapor Particle Separator (VPS) – In order to remove volatile materials in combustion aerosol to measure only non-volatile PM, techniques like thermodenuder [4], catalytic stripping [5], and Volatility Tandem Differential Mobility Analyzer (VTDMA) [6,7] have been developed. However, none of these techniques enable the study of engine particle dynamics, molecular transfer, or evaporation process under varying temperature conditions. For example, the thermodenuder and the catalytic stripper were intended for rapid removal of volatile components from soot particles, while VTDMA was to investigate volatilization and hygroscopicity of single ambient aerosol particles. Although highly detailed, the mobility analyzer design was too slow to be suitable for volatile PM measurement. In addition, the concentrations of water vapor, unburned hydrocarbons, and particles in turbine engine exhaust are sufficiently high that the VTDMA design would not work properly.

For the past 30 years, the thermodenuder has been a popular device designed to desorb volatile species from studies of ambient particles [6, 8-17]. Thermal stripping devices have also been used on diesel engine soot and aircraft emissions [4,18,19-26]. Although volatile components were removed from the PM, the adsorbent used in these designs retained the volatile components throughout the measurement system [18]. Once the adsorption capacity is expended, the volatiles could and have been found to return to the particles or to form new particles [18]. The thermal removal efficiency has never been 100% due to the nature of sampling and thermal desorption in the exhaust flow. Distortion of the engine particle size distribution can be severe because the loss of particles in the high-temperature heating system is not uniform across the size of particles. Therefore, several fundamental issues should be addressed while sampling and measuring engine volatile PM.

In our own study [25] using commercially available thermodenuders, size-dependent loss of particles ranges from 15% to 85% was also observed. Since the losses are particle size dependent, the quantification of source emissions is very challenging, if not impossible. This is a very serious issue when the number of particles is the primary metric in emissions control and regulation (e.g., EURO5. [26]). Finally, the use of granulate charcoal adsorbent used in thermodenuders makes it infeasible to extract adsorbed vapors for quantitative analysis, and the high labor required to maintain and replace the charcoal pellets is not desirable.

To improve the understanding of the volatility of nanometer scale engine particles, a new generation of thermal separation device was designed and tested at ORNL during the earlier SERDP WP-1627 project. In the VPS construction, a microporous metallic membrane was applied for the separation of vapors and particles [25]. The metallic membrane is chemically inert and similar to that used in a previous study of water treatment [27]. Many different metallic materials have been used in the construction of the membrane. The membrane made specifically for this project is fabricated as double-layered from 306L stainless steel, and is about 400 microns thick when two layers are combined. The pore size of the top layer is from 5 to 500 nm and about 10 microns thick. The top layer is supported by a backbone structure with a pore size of 500 to 50,000 nm with a thickness less than 400 microns.

The VPS uses a cross-flow membrane separation concept filtration design to remove vapors and prevent re-condensation of desorbed vapor onto existing particles. This approach has been found to effectively separate vapor from particles at a given temperature, but also allows the collection of vapors (e.g., by canisters, solid-phase extraction cartridges, etc.) desorbed from the particles. Once particles are desorbed in the heated section, they are removed via preferential diffusion through the porous membrane via pressure and concentration differential. The collected vapors can be subsequently analyzed for chemical composition, which is an added and new capability that has not been available in current thermodenuder or catalytic strippers that have been used primarily as a volatile removers. Furthermore, operationally, the new design eliminates the need to replace the adsorbents which greatly simplifies the maintenance of the instrument. In addition, there are no complications associated with sulfur poisoning, an issue with the research catalytic strippers. The VPS design concept was awarded US Patent Number US 8,771,402 B2 on July 8, 2014.

Figure 4 shows a schematic of the main components of the VPS. In this design, a heating section approximately 30.5 cm long (a total of 38.1 cm long including the ceramic insulation) is used to precondition the exhaust sample to a set temperature prior to volatile removal. Controlled heating is provided using a 600 W radiant heater insulated by ceramic clamp-shell casing with an additional thicker layer of fiberglass insulation material. The engine sample enters the VPS through the heating section, which is followed by a section for separation of desorbed volatile species from the non-volatile particles. The heating section residence time is approximately 2.6 s estimated at the flow rate of 2 slpm, and is set to completely desorb volatiles for the range of operational temperatures as determined with design computations. The double-layer metallic microporous membrane tube has an internal diameter of 1.91 cm and 25.4 cm long. The nominal pore size of the membrane is approximately 0.4 μm and thickness about 420 μm. The membrane section is enclosed in a 5-cm diameter stainless steel tube insulated with a double-layered fiberglass blanket. The volume between the metallic membrane and the tube serves as a temporary holding space for the desorbed vapors before they are evacuated by an extraction pump, which leaves no opportunity for the vapor to re-enter the membrane and condense on the non-volatile particles or nucleate into new ones.

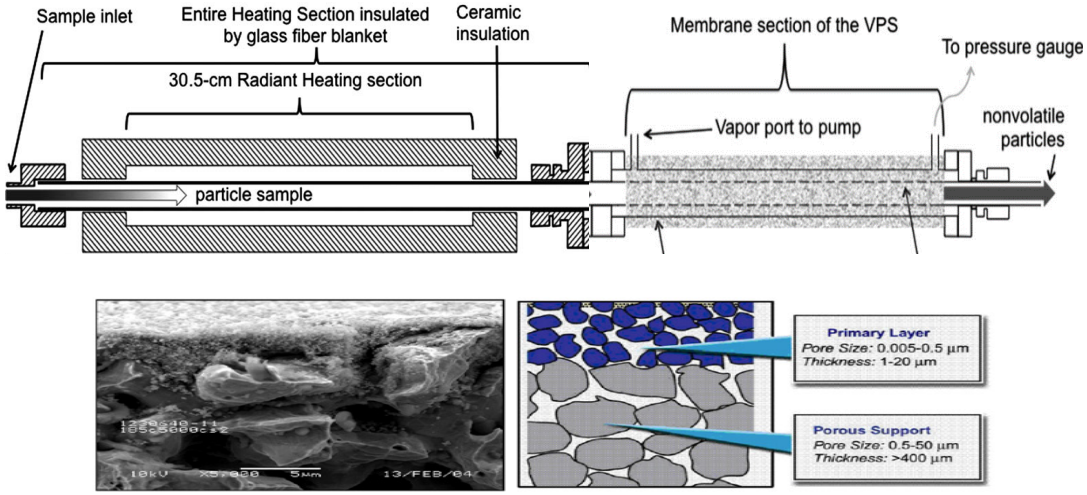

Figure 4. Schematic of the Vapor Particle Separator (VPS) and metallic membrane filter

3.1.3 Condensation Dilution Probe (CDP) – The CDP was developed by Aerodyne Research Inc. (ARI) under an Air Force SBIR project. Its objective is to simulate the environmental conditioning and volatile species condensation of volatile species in a controlled manner when extracting exhaust from the engine exit plane [28]. The CDP (referred in references as Simulated Aircraft Exhaust Plume Aging (SAEPA) probe) has been demonstrated in the laboratory test environments and sampling turbine engine exhaust on the tarmac at airports. The "probe" was developed through rigorous design case studies, modeling, and flow characterization with non-reacting flows. Shown schematically in Figure 5, the device extracts exhaust gas from the engine exit plane, and transfers the sample through a heated (> 150°C) stainless steel tube to a dilution and aging chamber. Transferring the sample through a heated tube is required to prevent microphysical reactions as well as thermophoretic loss of soot particles. The dilution/aging chamber is cylindrical with a diameter of 10 cm and a length of 1.8 m. The raw exhaust sample is

injected as a turbulent jet into the chamber at the centerline, and the dilution gas (either nitrogen or CO_2 -free air) is introduced as a sheath co-flow. The exhaust is injected as a turbulent jet into a laminar dilution co-flow because this configuration 1) mimics the jet engine plume traveling through the ambient air, 2) minimizes the effect of the chamber wall during the critical microphysical processes, and 3) produces a well defined flow. The dilution gas is conditioned to achieve the desired temperature and relative humidity prior to introduction to the chamber, and passes through a packed-bed flow straightener to provide uniform plug-flow. Within the chamber, the exhaust sample and dilution gas mix in a well-defined manner.

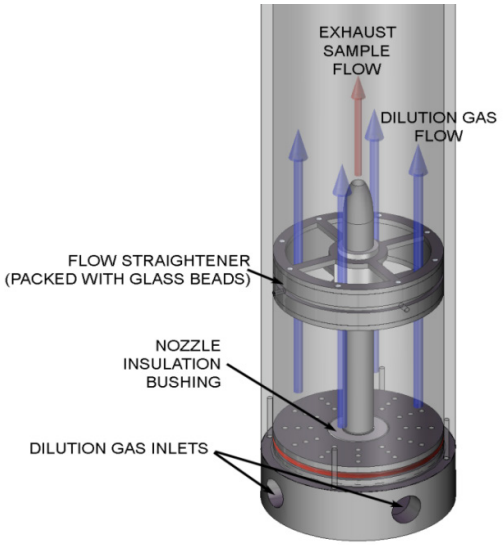

Figure 5. Schematic of the inlet region of the condensation dilution probe

3.2 TECHNOLOGY DEVELOPMENT

All three devices have been evaluated in laboratory environments, and in the case of the DC and CDP, in larger turbine engines, with very promising results. Additional characterization of these devices in more extensive field campaigns will further validate their capability and contribute to the development of standard methodologies for the reliable measurement of volatile and non-volatile PM characteristics from turbine engines. A brief discussion of the studies and primary results for the three devices is provided below.

3.2.1 DC - Sample Homogeneity Tests

The DC was evaluated in the laboratory to validate the CFD model and ensure a homogenous diluted sample at the extraction point. Characterization was performed using CO_2 calibration gas drawn into the ejector with nitrogen motive and secondary flows at conditions simulating engine exit pressures. Sample homogeneity was evaluated by extracting samples at different axial and radial locations of the DC while operating at different overall dilution ratios. Test results (Figure 6) validated the CFD results showing that the DC provides radially uniform CO_2 concentration profiles at relatively short distances from the ejector, even for a low dilution ratio of 20:1. This allows sample extraction for transport to the instruments at a single location in the DC without concern of sample quality. It is expected that PM mixing characteristics will be similar to those observed during the CO_2 tests.

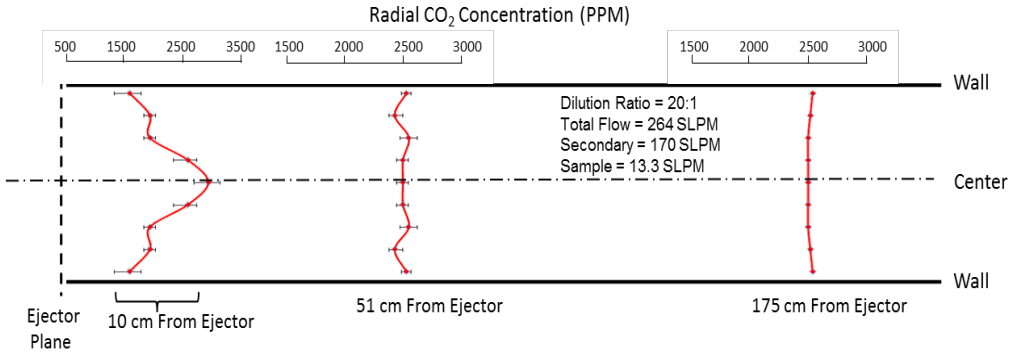

Figure 6. Measured CO_2 concentrations in DC at various radial and axial locations

Engine Evaluations

The DC was evaluated in two piggy-back alternative fuel turbine engine emissions tests during the last several years. Although valuable data were collected, limited conditions were examined as these tests were not focused on the evaluation of the DC performance.

3.2.2 DC - C-17 (F117-PW-100 Engine) Tests

C-17 emissions tests were performed in August 2010 to support the certification of the aircraft on 50/50 blends of JP-8 and Hydroprocessed Esters and Fatty Acid (HEFA) fuel [29]. For these evaluations, emissions were measured at engine powers ranging from 4 to ~63% of max thrust. PM emissions were sampled and quantified using both probe-tip and DC dilution. For the DC, the raw engine exhaust sample was extracted through a gas probe installed on a probe rake located 42 cm from the engine exhaust. The sample was drawn through a 2.4 m long, 0.77 cm diameter heated line (150°C) using a nitrogen-driven (motive flow) ejector pump. The sample was further diluted with nitrogen (secondary flow) to obtain the desired overall dilution. Since ambient air was not used as a diluent, minimal physical/chemical transformations of the PM emissions were expected. The motive and secondary dilution flows provided total dilution ratios of 19 to 50:1. The diluted sample was collected at a single point near the center of the DC at 1.10 m from the converging/diverging section and transported to dedicated Scanning Mobility Particle Sizer (SMPS) and Condensation Particle Counter (CPC) instruments via unheated 23 m long, 0.77 cm I.D. stainless steel tubing. Test results of average particle number emission indices (EI_n) (defined as number of particles produced per kg of fuel consumed) and particle size distributions using the two dilution methods are shown in Figure 7. Excellent agreement in EI_n and size distribution profiles between probe-tip and N_2-diluted dilution chamber sampling are observed throughout the test conditions evaluated. These results suggest that particle integrity is conserved in the DC and that it may be a valid tool for the characterization of mostly non-volatile PM without the complications associated with dilution at the probe-tip. Due to the dry/inert nature of the dilution N_2, there was negligible nucleation of new particles from sulfur and organic species. Dilution of the sample using atmospheric air in the DC is expected to promote the condensation of these species and the formation of PM nuclei as has been observed in far field measurements [30,31].

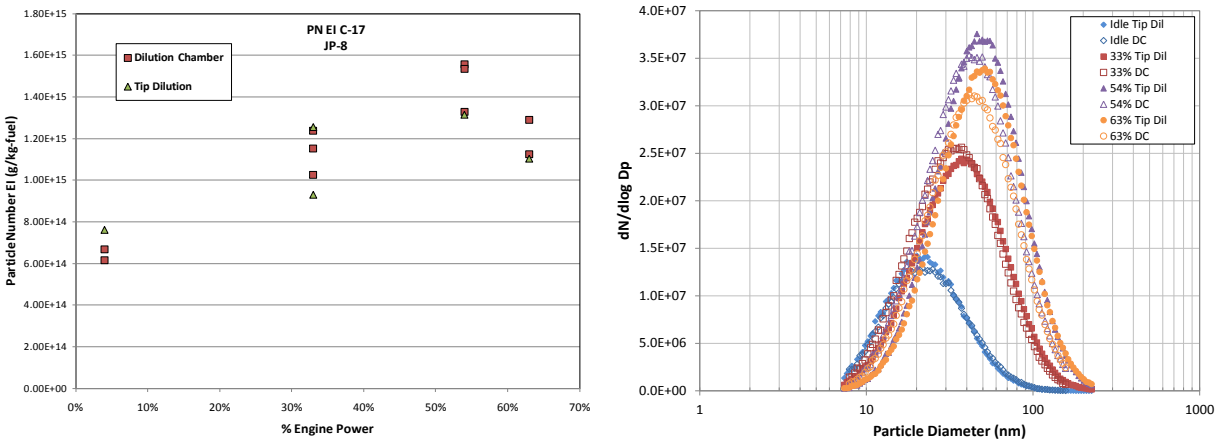

(a) (b)

Figure 7. Average PM measurements in PW-F117 engine for probe tip and N_2 diluted dilution chamber at several power settings: (a) Particle number EI, (b) Particle Size Distribution

3.2.3 DC - DC-8 (CFM56-2 Engine) Tests

A CFM56-2 engine was tested under the NASA AAFEX II [31] program to study engine emissions burning several alternative fuels. Similar to the C-17 tests, PM samples were collected at the engine exit plane and diluted at the probe-tip and in the DC. In addition, samples were obtained at approximately 30 meters downstream of the engine exit plane. For the DC, the PM samples were drawn with the ejector using N_2 as the motive gas and further diluted with atmospheric air in the secondary path. Particle size distributions and particle numbers (EI_n) for engine PM collected using the three dilution schemes are shown in Figures 8. For several power settings, the samples diluted in the DC and at 30 m downstream consistently yielded significantly higher particle numbers than for probe tip dilution, which are attributed to the condensation of volatile species. The difference between tip-diluted (1 m) and downstream (30 m) dilution was more pronounced at lower engine power due to the larger concentration of organic species prone to condensation which nucleate new particles and/or condensation sites for sulfuric acid aerosols. Reasonably good agreement was observed for the DC and 30 m size distributions; however, the nucleation mode observed at 30 m with JP-8 was not fully replicated in the DC. This may be due to the fact that the motive gas in the ejector was nitrogen and not atmospheric air, which may have limited gas-to-particle transformations.

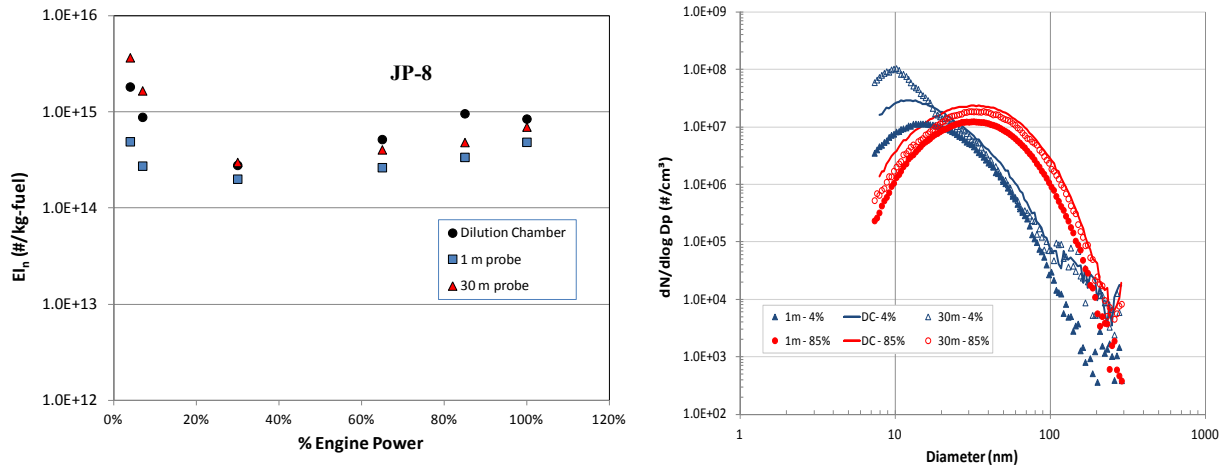

Figure 8. Impacts of PM dilution technique on particle number EI and particle size distribution for the CFM56-2 engine during the NASA-led AAFEX II tests

3.2.4 VPS

The VPS was evaluated using synthetic particles generated in an aerosol science laboratory at the Oak Ridge National Laboratory (ORNL). These synthetic particles included: 1) a non-volatile material - NaCl, 2) a semi-volatile material Dioctyl Phthalate (DOP) ($C_{24}H_{38}O_4$), and 3) an aviation emissions community-agreed test material, tetracontane (C_{40}) ($C_{40}H_{82}$). After successful development of the VPS instrument through SERDP WP 1627, the VPS was further tested with aircraft engine exhaust in this demonstration. Technology development activities are summarized in this section, and additional information can be found in the WP1627 project report and several journal manuscripts [25,32, 33].

3.2.4.1 VPS Validation Experiments in Laboratory Conditions

The vapor pressure of NaCl at 20°C is almost zero, and 1.82 mmHg at 586.99°C. It is approximately $1x10^{-2}$ mmHg at 20°C for DOP, and $1.74x10^{-7}$ mmHg at 25°C for tetracontane. The non-volatile materials are commonly considered to have vapor pressure equal or less than 10^{-4} mmHg at the room temperature. Therefore, NaCl and C_{40} particles are considered non-volatile particles by such a definition, while DOP particles are semi-volatile.

Evaluation of the VPS in laboratory conditions was designed to understand: 1) particle transmission efficiency at non-heated condition, 2) ability to evacuate desired gas phase species, and 3) removal efficiency of particles as a function of temperature including PMP VPR temperature setpoint of 350°C. Since, 1) is the most critical data needed for this demonstration project that focuses on the current demonstration, only the transmission efficiency results are presented.

3.2.4.2 Particle Transmission Efficiency

Transport of particles of size less than 100 nm can be problematic in the measurement of aircraft engine emissions [25, 32, 33]. At normal sampling rate, the nm size particles undergo losses through the sampling tube attributed to diffusion and thermophoretic mechanisms. Both mechanisms are a function of temperature (T), since particle diffusivity, D, is a linear function of air temperature and defined in Eq. (1) as follows:

$$D = Cc\ [kT/6\pi\mu D_p] \quad (1)$$

Where Cc is the Cunningham correction factor, k is the Boltzmann constant, μ is the dynamic viscosity and D_p is the particle diameter. The thermophoretic force is defined in Eq. (2) as follows:

$$F = -p\lambda D_p^2 \Delta T/T \quad (2)$$

Where p is the gas pressure, λ is the gas mean free path, D_p is particle diameter, ΔT is the temperature gradient, and T is the absolute temperature of the particle. Both diffusion and thermophoretic forces are linear functions of the temperature. Since the particles are immersed in a uniform temperature field in the VPS heating region, and the temperature gradient between air and particles is minimal, the particles basically experience virtually no thermal gradient and the thermophoretic force is negligible in the VPS design.

Experimentally, the particle transmission loss of the VPS at room temperature was evaluated by comparing the size distributions of particles obtained at the VPS outlet to those from a bypass tube of the same length. An ideal volatile particle remover would exhibit a 100% transmission and no loss of particles. Test results displayed in Figure 9 show that the particle transmission efficiency of DOP particles through the VPS is virtually identical to that of the bypass tube for room temperature tests (no heating applied). The slight difference could be only found at the 6 nm region where the bypass tube had about 2% higher count. This was the smallest size the instrument could measure at that particular setting. This example is obtained using particles made from 0.01%w DOP solution (i.e., 1 g of DOP material in 99 g of ethyl alcohol) at the room temperature of 21°C. The loss of test particles through the VPS appears to be beyond the detection ability of the SMPS. Similar performance was observed when testing with NaCl, C_{40} and other materials. Therefore, it was evident that the VPS did not contribute to any measureable loss of non-volatile particles due to diffusional mechanisms.

As the heating section temperature is increased, the chance of particle loss of any materials increased because particles (even non-volatile) might be vaporized. The transmission efficiency in this case would be lower due to multiple loss mechanisms, not solely due to diffusional impaction. During testing, it became clear that heated section temperature was interfering with the intended measurement of particle transmission loss at elevated temperatures, and it was decided to abandon studies at the high temperature to assess particle transmission efficiency.

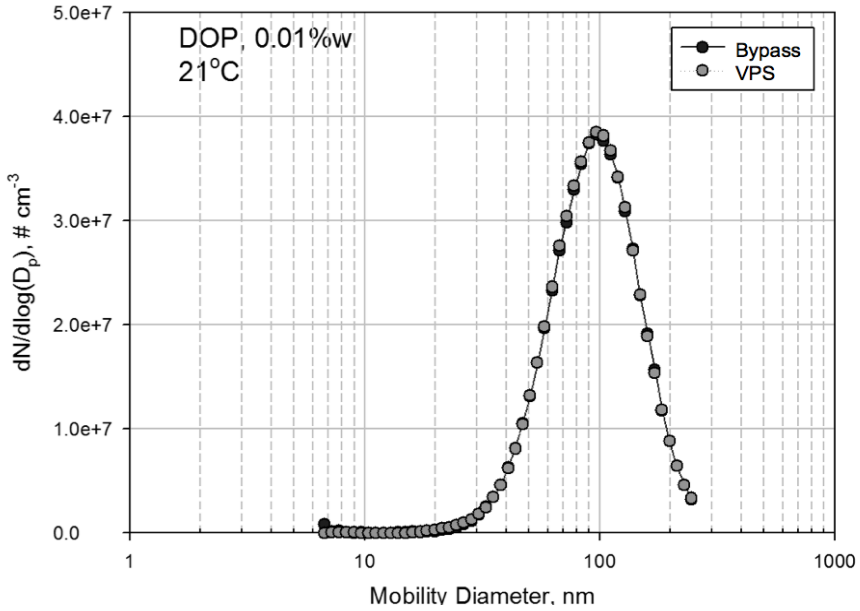

Figure 9. Plot of particle size distributions of VPS vs VPS bypass

3.2.4.3 C_{40} Particle Removal Efficiency

Tests of the removal efficiency under the laboratory conditions were performed using the particles mentioned above. Figure 10 shows a schematic of particle generating system used throughout the laboratory experiments. The C_{40} test particles were generated by using the evaporation-condensation technique (Figure 11) as the particle source, which replaced the TSI Model 3076 nebulizer shown in Figure 10. To generate the particles, C_{40} powder was placed in a quartz boat inside a furnace (not shown) and the evaporated tetracontane molecules were condensed in a stainless steel cylindrical chamber. The generated particles were sampled by the VPS, aerosol monitor, and electrical precipitator for SEM imaging. The generated aerosol stream was monitored using a TSI 3068B aerosol electrometer for concentration stability. The particles were charged by a Kr-85 neutralizer before entering the electrometer. The averaging time for each data point generated by the electrometer was ten seconds. MicroRaman spectroscopy of the C_{40} particles generated was conducted and the Raman vibration spectrum confirmed the particles were pure tetracontane.

The number concentration of the generated C_{40} particles fluctuated at start up then stabilized at approximately $1x10^5$ particles per mL of air. When the concentration stabilized, the VPS experiments were performed.

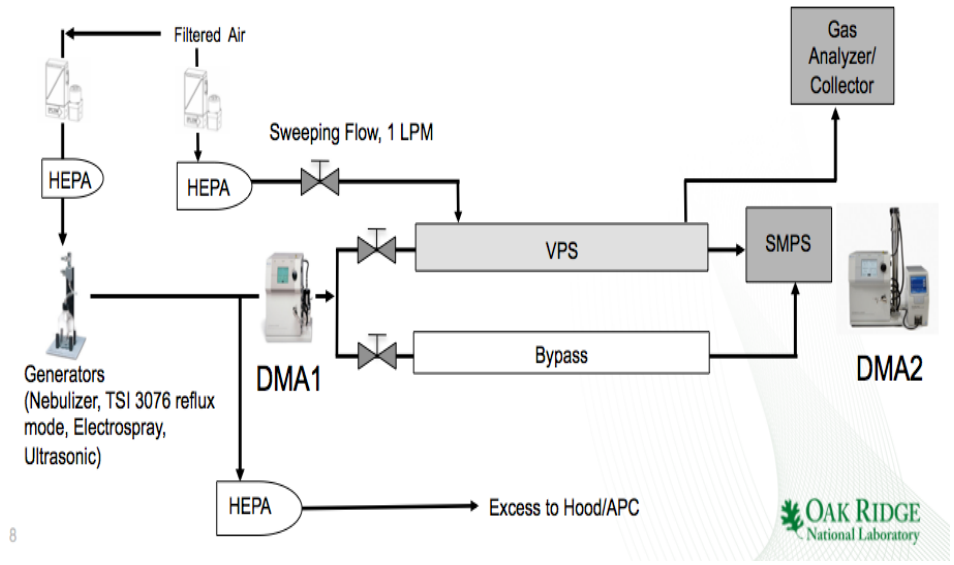

Figure 10. Schematic of experimental verification of particle setup

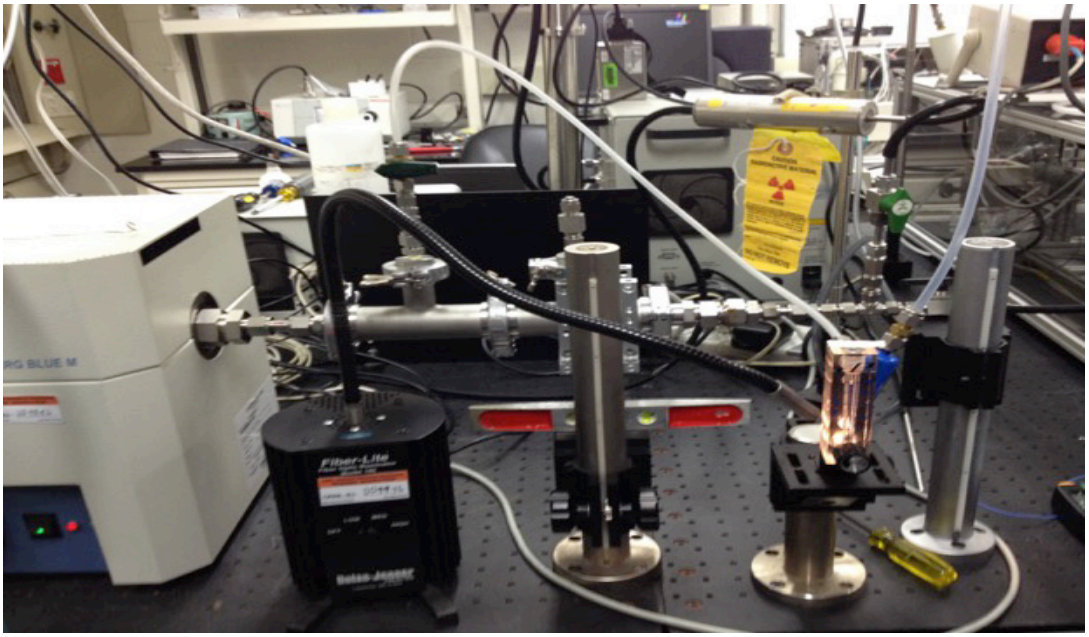

Figure 11. PMP VPR Evaporation-Condensation Setup for volatile PM generation

The particle number concentration as a function of particle size and temperature for C_{40} particles is displayed in Figure 12. The "source" term refers to the mono-dispersed C_{40} particles generated by evaporation-condensation method and then size-selected by DMA1 in Figure 10. The geometric standard deviation for the source sample was 1.036, which is essentially monodisperse. Regarding the particle removal measurements, the results show that all 89-nm C_{40} particles were removed at 350°C, which is the design temperature of PMP, with an efficiency of greater than 99.99%. This test demonstrated that the conditions in the heated section (temperature and residence time) were sufficient to completely volatilize the C_{40} particles and the membrane

section provided selective removal of the vapor-phase components. A similar experiment with C_{40} particles smaller than 15-nm did not produce statistically significant results due to the relatively low concentration of particles produced. However, the efficient (~99.99%) removal of 15 nm and smaller C_{40} particles at 350°C is anticipated based on the observations in Figure 12. This is an indication that C_{40} particles, produced by evaporation-condensation, do not realistically mimic the thermographic behavior of engine-generated volatile particles.

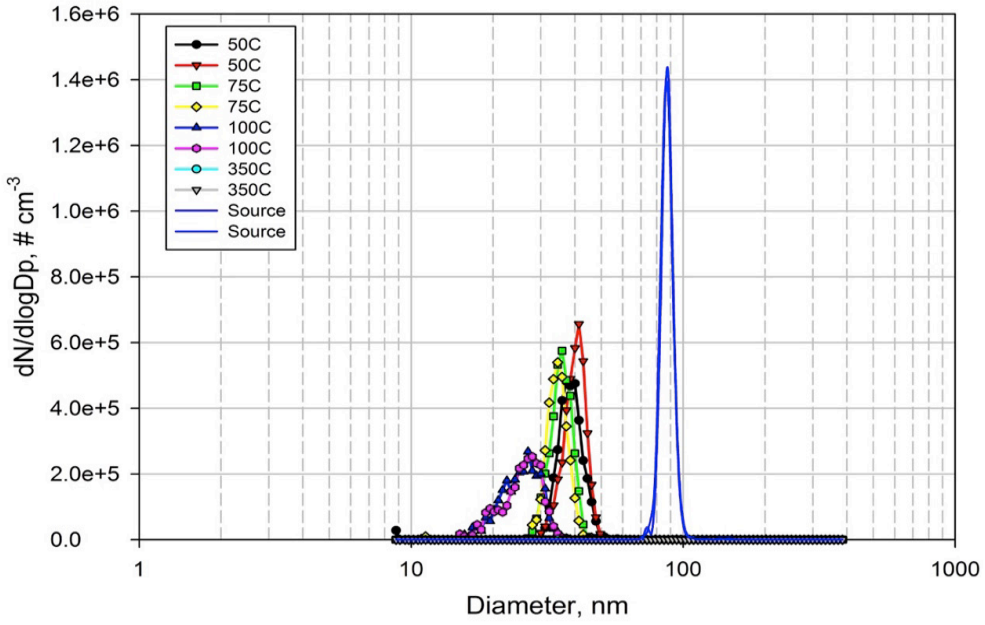

Figure 12. Concentrations of tetracontane particles as a function of temperature and size

3.2.5 CDP

The CDP system was developed under a previous Air Force program. During development it was deployed at two venues for field testing. First, it was tested in a lean-direct inject (LDI) combustor rig at the CE-5 combustor test cell at NASA Glenn Research Center (GRC) [28]. The exhaust gas samples were extracted at high-pressure/temperature conditions with a probe embedded inside the flame tube. The sample went through a 0.5 mm critical orifice to reduce the pressure and through a shut-off valve that can be remotely operated. The sample was transferred to the CDP via a 3 m long, 12.7 mm o.d. stainless steel tube maintained at 150°C. Downstream of the CDP, a 15 m long, 12.7 mm o.d. stainless steel tube maintained at room temperature was used to deliver the conditioned sample to the instruments. The second venue was Chicago Midway Airport (MDW), where the CDP was tested using in-service, on-wing CFM56-7 aircraft engines as part of a more comprehensive measurement activity (MDW-10)[28]. MDW-10 consisted of sampling exhaust from four CFM56-7 engines operating near idle conditions. Exhaust gas samples were extracted at 1 m from the engine exit using a gas probe, and transported to the CDP via a ~20 m heated (150°C) line.

A suite of characterization instruments for particle size, number and chemical speciation measurements, where used to support the CDP evaluations during field deployments. To compare

with conventional probe technologies, a conventional particle probe (tip-dilution) with a condensation particle counter (CPC) and an Engine Exhaust Particulate Sizer (EEPS) were used during the CE-5 testing. Figure 13 shows the particle size distribution for both the combustor rig and MDW-10 tests. For the CE-5 test samples through the CDP system, the particle size distribution typically showed two distinct peaks, one around 15 nm and the other near 35 nm, whereas the conventional particle probe displayed only one peak around 35 nm. The 15 nm peak was assigned to nucleation mode PM formed by gas-to-particle conversion, and the 35 nm peak to soot. For this measurement, the combustor inlet temperature was 225°C, exit temperature was 1110°C, and the combustor pressure was 1 MPa. JP-8 fuel was burned at the overall equivalence ratio of 0.42. The particle size distribution shows the changes in response to sample fraction (f) (sample flow divided by total flow) and total flow rate (sample + dilution). The number concentration was corrected by the diluted and raw CO_2 concentrations to eliminate the first-order effect of dilution. The differences in particle number are attributed to microphysics. Flow residence time in the CDP and the sample fraction were adjusted by varying the dilution flow rate, so the sample fraction and the residence time are not independent. Results indicate that the nucleation mode of volatile PM increases in magnitude from having a peak at approximately 10-15 nm to peaking in the 15-20 nm range as the sample fraction and/or residence time was increased. The soot mode is apparent at low sample fraction and/or residence time, but becomes encompassed under the nucleation mode as the nucleation mode grows in size. For the MDW-10 tests, the particle size data shows that the nucleation peak magnitude (volatile PM contribution) becomes larger as the sample fraction is increased (indicated by the higher CO_2 level) while the size does not noticeably change.

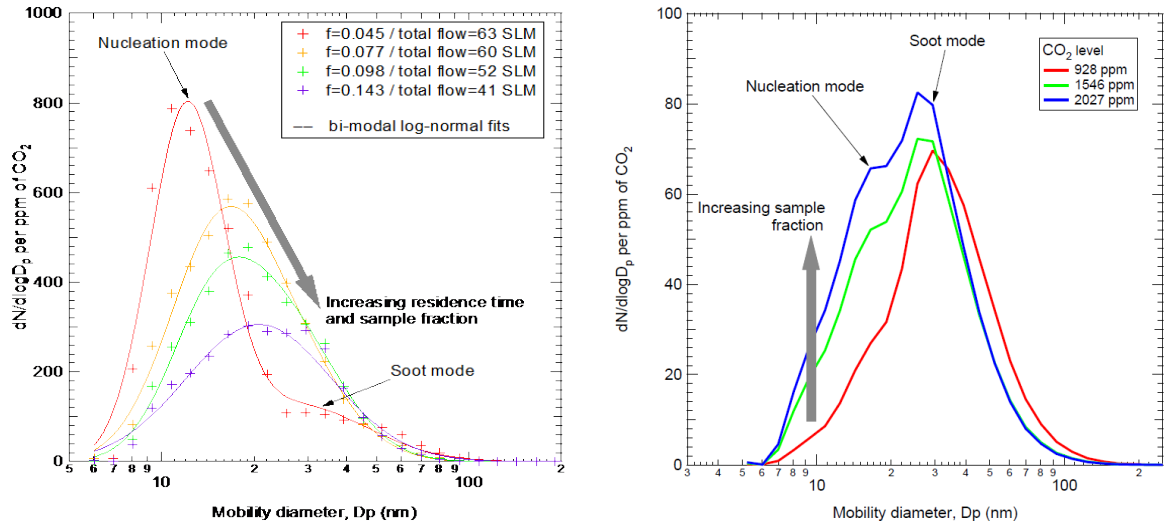

Figure 13. Particle size distribution obtained using the CDP during the CE-5 combustor rig and MDW-10 tests

3.3 ADVANTAGES AND LIMITATIONS OF THE TECHNOLOGY

Although a standard practice for the measurement of total turbine engine PM has not been established, based on current understanding it requires sampling the engine exhaust at a sufficient distance downstream from the engine to allow the volatile species to cool/dilute in the plume and nucleate into particles that can be characterized. This approach requires additional probes and sample lines, and is not practical for characterizing engines in most test facilities, which direct the exhaust vertically through high exhaust stacks. Moreover, this practice is not desired as the measured PM concentrations can fluctuate significantly due to the ambient sampling conditions (e.g. temperatures, wind direction, humidity) during the tests. The approach in this demonstration has the advantage of significantly simplifying the total PM sampling by conditioning the sample with ambient air in a controlled manner near the engine to obtain a sample similar to one found far field (20-30 m) from the engine. The limitations with the dilution devices include: lack of sufficient condensation of volatile compounds or condensation of volatiles on the surface of devices. Control of the formation of volatile PM is difficult as it is a strong function of the concentration and composition of the volatile species and environmental conditions (e.g., overall dilution, humidity, etc.). The secondary dilution flows were varied to assess their impacts on volatile condensation. Real-time particle number and size distribution measurements will be used to determine the degree of volatile specie condensation and thus, volatile particle formation. Condensation and loss of particles to the wall are reduced by heating the DC to 75°C with currently installed heat blankets and increasing the diluent concentration. In the demonstration and validation of the condensation devices, a potential risk area (or limitation) is the collection of reliable/repeatable PM emissions data at the downstream plume sample location since atmospheric conditions greatly influence PM characteristics. Risk was reduced by increasing test times (when possible) to gather statistically significant data for proper analysis.

For the non-volatile characterization, the VPS has the advantage over commercial VPR units in its simple operation, lower cost and potential to analyze the removed volatile species. The limitation may be in the potential of fouling of the metallic membrane and reduced separation efficiency with time. This will be highly dependent on the dilution ratios used and quality of the engine exhaust (i.e., soot output). Regular cleaning of the membrane will alleviate this problem. The lifetime of a membrane has been proven to be reasonably long (a few thousands of hours) based on previous work.

4. PERFORMANCE OBJECTIVES

The performance objectives, success criteria (as defined at project start) and brief summary of the results for the demonstrations are provided in Table 1 and subsequent text.

Table 1. Project Performance Objectives

Performance Objective	Data Requirements	Success Criteria	Results
Demonstrate volatile species condensation (volatile PM formation) in the DC and CDP. Significant increase in PM compared to probe-tip dilution.	Particle size distributions for samples collected at engine exit, 30 m and at DC and CDP.	Clear evidence of volatile particle formation in DC and CDP compared to tip dilution. 10X increase in 5-20 nm particle number.	• *Met 1st criteria.* Evidence of volatile PM formation. • *Did not meet 2nd criteria*. Only 2-5X increase in 5-20 nm size particles.
Demonstrate similar PM chemical characteristics for samples collected at the DC, CDP and 30 m locations.	Particle chemistry and gaseous organics using AMS and PTR-MS.	Composition of PM from DC or CDP and plume sample within ±25% in absolute or normalized terms.	*Criteria met.* Same % organics in plume and condensation devices.
Demonstrate that ambient air diluted samples in the DC and CDP produce similar total PM characteristics as at the 30 m sampling location	Particle size distributions, total mass and total particle concentrations	±40% of the particle number ±30% mass ±25% of mean diameter	*Criteria only met for some conditions. Not consistent.*
Demonstrate that N_2 diluted samples in the DC and CDP produce similar non-volatile PM characteristics as non-volatile sample	Particle size distributions and total particle concentrations	±25% of the particle number ±15% of mean diameter	Limited evaluations performed. *Criteria met for some conditions.*
Demonstrate efficient performance of the VPS to remove tetracontane particles	Particle size distributions and total particle concentrations	> 99 % vaporization of 15 nm tetracontane particles, with an inlet concentration of >10,000 cm^{-3}.	*Criteria met.*
Demonstrate efficient performance of the VPS to remove volatile species from engine PM	Particle size distributions and total particle concentrations	Qualitative data. Significant reduction in 15nm and smaller particles and increase on mean particle size	*Criteria met.* Removed both volatile and non-volatile engine PM. Recommend further evaluations at lower temperatures.

- The PM sample conditioned using the DC and CDP shall clearly show formation of nuclei size (7 – 23 nm) particles compared to particles collected at the engine exit plane. At least an order of magnitude (10X) increased concentration in nuclei size particles is typical in plume measurements relative to exit plane tip-diluted samples, and this is therefore used as criteria in this demonstration.
- The chemical composition and/or concentration of organics in the PM samples collected in the plume and the condensation devices were determined using Aerosol Mass Spectrometry (AMS) and Proton Transfer Reaction-Mass Spectrometry (PTR-MS). A valid characteristic measured using these techniques of the PM collected at plume and CDP or DC shall be between 25%.
- Particle size, total PM mass and number measured in the plume and condensation devices shall be compared to assess the performance of the devices. Data agreement between plume and condensation devices shall be equal or lower to those presented in Table 1 to be considered successful.
- Previous tests show very good agreement between the particle number of the DC diluted with nitrogen and a probe-tip diluted sample (see Figure 7). Therefore, the DC diluted with nitrogen may be used to characterize turbine engine non-volatile PM. Particle size distributions, mean particle diameter and particle numbers for nitrogen-diluted DC and the non-volatile PM techniques shall be compared to assess validity of using the DC diluted with nitrogen for non-volatile PM characterization.
- VPS performance is validated by measuring concentration of tetracontane (C_{40}) particles with and without VPS to verify 99% vaporization of 15 nm size particles. Similar to criteria used to evaluate performance of volatile particle removers (VPR) used in diesel engine non-volatile PM emissions measurements.
- VPS performance will also be assessed using PM from turbine engine exhaust. Comparison of nuclei-size PM concentration and mean particle mean diameter with and without the VPS will be completed. Significant reductions in nuclei-size particles (which results in increase mean particle size) are used as success criteria.

5. SITES/PLATFORM DESCRIPTION

5.1 TEST PLATFORMS/FACILITIES

Two turbine engines representing newer and legacy technologies were used in this demonstration program. Reasons for selecting these platforms include:

- They provide a wide range of PM concentrations, mass and size distributions for demonstration of the devices near the high and low extremes of turbine engine PM.
- The platforms represent two different engine types, i.e., turbofan and turboshaft, to demonstrate the devices at vastly different exhaust velocities and temperatures.
- The F117-PW-100 turbofan engine (referred hereafter as PW-F117) is a military variant of a commonly used commercial turbine engine.
- Demonstration in our in-house T63 engine provides unmatched scheduling and testing flexibility and allows testing with alternative fuels to deliberately influence PM exhaust.
- Demonstrations at WPAFB, Ohio reduce travel and overall costs for all teams, and are logistically more supportable than at any other location.

5.1.1 T63 Turboshaft Engine at WPAFB, OH

Tests on a T63 turboshaft helicopter engine (Figure 14) were conducted to increase understanding into the formation, composition and measurement of volatile species/PM and to characterize and demonstrate the performance of the condensation devices and VPS in a controlled environment. This engine provided the opportunity to vary fuel chemical composition (e.g., sulfur and aromatic content) to influence the concentration of volatile PM precursors. The engine is located in the Engine Environment Research Facility (EERF) in the Aerospace Systems Directorate at WPAFB.

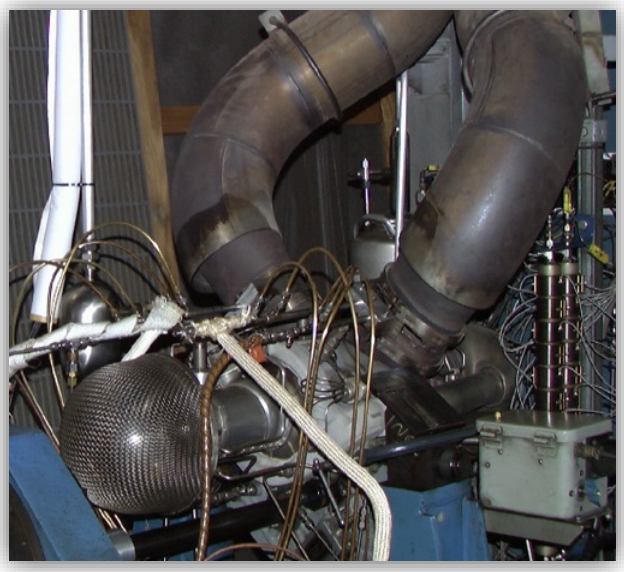

Figure 14. Demonstration platform: Allison T63 turboshaft engine at WPAFB, OH

5.1.2 PW-F117 Turbofan Engine at WPAFB, OH

The second demonstration was on a C-17 aircraft engine. The PW-F117 engine is the military variant of the Pratt & Whitney PW2000 commercial engine, which powers the Boeing 757-200 aircraft. The test site was at the 445th Air Lift Wing at WPAFB.

Figure 15. Demonstration platform: C-17 PW- F117 engines at WPAFB, OH

5.2 PRESENT OPERATIONS

Currently, PM emissions from aircraft turbine engines are evaluated by the engine manufacturer by measuring smoke number (SAE ARP 1179) during the engine certification process. Due to the cleaner burning engines and lack of compliance-type quantitative information, the smoke number is inadequate for measuring PM2.5 emissions from new turbine engines. Therefore, more advanced techniques are needed to assess the aircraft PM environmental burden.

5.3 SITE-RELATED PERMITS AND REGULATIONS

The demonstration team consulted with safety and environmental officials to comply with all EPA and/or base required site-related permits and regulations during the demonstration activities.

6. TEST DESIGN

Test engines were operated at several power settings to demonstrate operation of the dilution devices and VPS under a wide range PM levels. The engines were sampled at steady state, and tested sufficiently long to ensure statistical significance of the data. Samples were extracted with multiple probes at the engine exit plane (<1 m) and far field (20 m - plume). Raw samples in the DC and CDP were diluted to dilution ratios measured at the plume. Comparison of PM characteristics (number and size) of sample diluted at probe tip (or using an ejector diluter and secondary dilution), and the sample from the DC, CDP were conducted. The test plans for the T63 and PW-F117 engine demonstrations are provided in Table 2.

Table 2. Test Matrix for the Demonstrations on T63 and PW-F117 Engines

Engine	**Engine Condition**	**Fuel**	**Sampling Device or Location**	**Dilution Ratio at Devices**
T63	• Idle • Cruise	• JP-8 • JP-8+aromatics (25% total) • JP-8+Sulfur (3000 ppm total)	• Probe tip-diluted (engine exit) • DC (engine exit) • CDP(engine exit) • Plume	• Same as Plume • 2X Plume
PW-F117	• Idle • 20% rated thrust • 33% rated thrust	F-24 (Jet A + military additives)	• Ejector-diluted (engine exit) • DC (engine exit) • CDP (engine exit) • Plume	Same as Plume

The suite of PM and gaseous emissions instrumentation for these evaluations is shown in Table 3, and a description of several follows in sections 5.01 through 5.04. PM was sampled and characterized at both the engine exit plane (non-volatile) and far field and at the exit of the VPS and condensation devices. A primary goal of this effort is to improve the understanding of processes which affect volatile PM formation and develop viable techniques for measurement of total and volatile PM emissions from turbine engine aircraft.

The AFRL/UDRI team performed PM and gaseous emissions measurements at the engine exit plane, plume and condensation devices. Ambient air dry bulb temperature, relative humidity and wind speed were recorded to monitor potential impacts of the environmental conditions on particle characteristics.

ORNL performed non-volatile PM measurements using a modified-PMP volatile particle remover (VPR) system to compare to and assess the VPS performance. The PMP system consists of a two-stage micro-dilution system designed to vaporize the liquid-phase particles leaving only the solids (non-volatile) to be analyzed by the instruments. The first-stage and second stage dilution ratios are nominally 5:1 and 6:1 respectively, producing an overall dilution ratio of approximately 30:1. The ORNL system is similar to the commercial PMP system; however, it uses a lower dilution ratio to provide a greater number of particles for statistically significant SMPS number-size distributions. ORNL modified the commercial PMP sampling system to allow quantitation of particles as small as 10 nm (versus 23 nm for the diesel system), which required a

CPC with a smaller diameter cutoff point. ORNL compared data from the modified-PMP system to those of the VPS. In addition, ORNL assessed the VPS efficiency in removing volatile particles by using a modified PMP validation approach. The modified PMP approach consisted of supplying the VPS with tetracontane aerosols, and counting particles at the inlet and exit of the VPS. Per the diesel PMP, the VPR validation requires >99% tetracontane particles smaller than 30 nm to be vaporized (3). Since turbine engine PM are smaller than diesel PM, the VPS will be validated to >99% elimination of particles smaller than 15 nm.

Table 3. Instrumentation, Measurements and Sampling Locations

Instrument / Method	Measurement	Sampling Location	T63 Engine	PW-F117 Engine
Condensation Particle Counter (Several models)	Particle Number	1 m (probe tip or two-stage dilution), DC, CDP, VPS, VPR, plume	x	x
Scanning Mobility Particle Sizer (TSI 3936)	Particle Size Distribution (D=4.0 - 570 nm)	1 m (probe tip or two-stage dilution), DC, CDP, VPS, VPR, plume	x	x
Multi-Angle Absorption Photometer (Thermo 5012) (T63 only)	Black Carbon Mass	DC, CDP, plume	x	-
Laser Induced Incandescence	Black Carbon Mass	DC CDP, plume	-	x
Aerosol Mass Spectrometer	PM chemical speciation (organics, sulfate, nitrates)	DC, CDP, plume	x	x
Proton-Transfer Reaction Mass Spectrometer	Volatile organic species	DC, CDP, plume	-	x
FTIR Analyzer (MKS 2030)	CO_2, CO, NO_x, SO_x	1 m (Raw Sample), DC, CDP, plume	x	x
NDIR Analyzer (CA 602P)	Diluted Sample CO_2	1 m (probe tip or two-stage dilution), DC, CDP, VPS, VPR, plume	x	x
Sunset Model 3 Semi-continuous ECOC Carbon Analyzer	Elemental & Organic Carbon	DC,CDP, plume	x	-
Gravimetric Analysis	Time-Integrated Total PM	DC, CDP, plume	x	-
Ion Chromatography	Time-Integrated SO_4	DC, CDP, plume	x	-
Pulsed Fluorescence Analysis	SO_2	DC, CDP, plume	x	x
Micro-soot Sensor (AVL Model 488)	Black Carbon	DC, CDP, plume	-	x
Engine Exhaust Particle Sizer (EEPS TSI 3090)	Particle Size Distribution	DC, CDP, plume	-	x
FID Analyzer (CA 600)	Total Hydrocarbons	DC, CDP, plume	x	x

The U.S. EPA National Risk Management Research Laboratory (NRMRL) team performed characterization measurements of the volatile and non-volatile PM as well as the gas-phase precursors in the condensation devices for comparison to those observed at the plume sampling location. The instruments/techniques used quantified: total PM mass; non-volatile soot; volatile organic PM; and volatile sulfur PM contained in the engine exhaust aerosol as well as gas-phase SO_2 and total hydrocarbons (THC).

ARI in collaboration with Montana State University (MSU), performed measurements of particulates and gaseous species for the plume and diluted samples from the condensation devices. Chemical composition of volatile PM and gaseous organic species were measured using mass spectroscopic techniques. Total particle number and light extinction were measured with optical techniques.

6.0.1 AFRL/UDRI PM and Gaseous Emissions Characterization

The AFRL/UDRI team used several commercially available instruments to characterize PM and gaseous emissions from the condensation devices, plume and engine exit probe. TSI Model 3936 Scanning Mobility Particle Sizer (SMPS) with a nano-differential mobility analyzer (nDMA) and a TSI Model 3776 Condensation Particle Counter (CPC) were used to obtain the particle size distribution from 5 to 150 nm. A TSI Model 3775 and TSI Model 3020A CPC were used to measure particle number (particles per unit volume) for the condensation devices/plume and engine exit samples, respectively. The emission indices (unit per kg-fuel) were calculated based on the measured PM, the engine fuel-to-air (f/a) ratio and the sample pressure and temperature at the instrument. The engine f/a ratios were calculated based primarily on the exhaust CO_2 and fuel properties. Major and minor gaseous species were quantified using an MKS Multi Gas 2030 Fourier Transform Infrared (FTIR) based analyzer. Gaseous emissions were sampled with undiluted probes and transported through heated lines kept at 150°C which is within the range of the SAE ARP 1256 [34]. A non-disperse infrared analyzer (NDIR) measured the CO_2 for the samples from the particle instruments to correct for dilution.

6.0.2 EPA Elemental and Black Carbon Total Mass Measurement

EPA collected PM samples from diluted engine exhaust from the DC, CDP or plume for elemental and organic carbon (EC/OC) and sulfur product analysis. The EPA mobile laboratory consisted of two different instrument configurations depending on the demonstration and its requirements. The two configurations are illustrated in Figure 16.

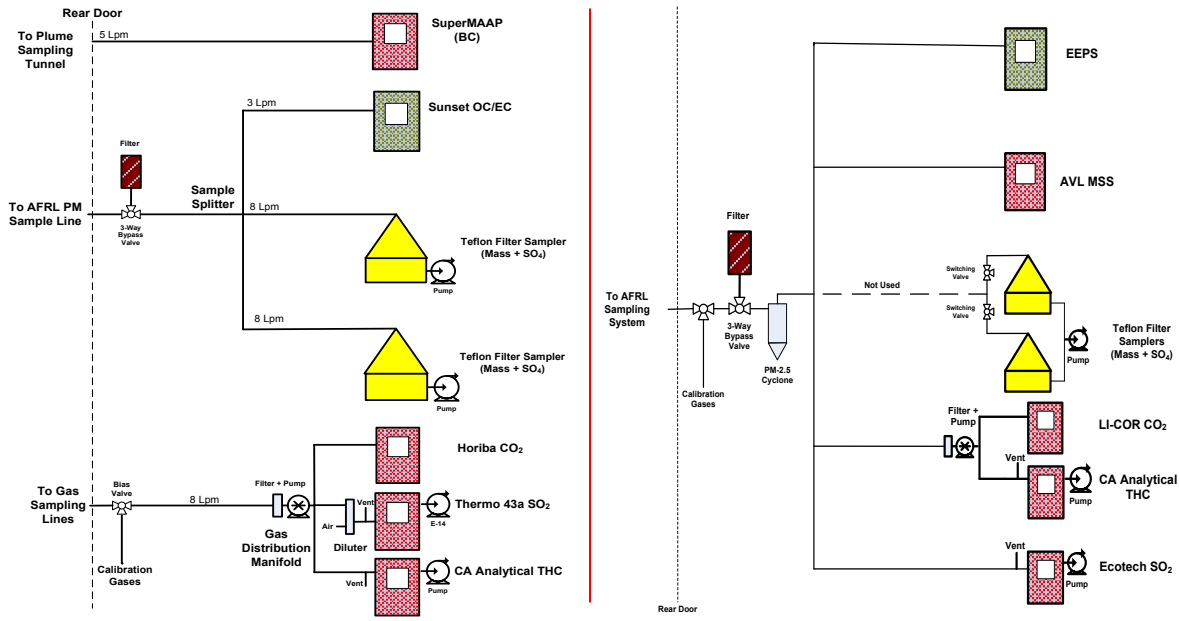

(a) (b)

Figure 16. EPA instrumentation and equipment setup for demonstrations on (a) T63 engine and (b) C-17 aircraft engine

As shown, for the T63 demonstration separate samples were provided to a modified (added sample and bypass valves) MAAP (SuperMAAP), filter samplers and ECOC analyzer, and gas analysis system (i.e., Continuous Emission Monitor [CEM] bench). For the gas phase measurements, switching between the various sampling points was accomplished by the use of hand valves.

Filter sampling for the T63 engine demonstration was conducted using either of two multi-filter samplers shown schematically in Figure 17. The sample entered the system through a stainless steel line connected to the 4-way sample splitter shown in Figure 16. Upon entering the unit, the sample could either be by-passed or sent through a 47-mm Teflon filter installed in a stainless steel filter holder. Control of the sample flow was achieved by means of a series of automated valves controlled by a computer running the DASYLAB software package. The flow through the filters was measured by a calibrated mass flow meter with the output signal logged by the DASYLAB software. Sampling system leak tests were performed prior to transporting the sampling system to the test site to assure that the system was leak free. Background filter samples were collected during periods when the engine was not running. Note that for the C-17 demonstration, filter sampling was attempted but abandoned due to very low concentration of sulfur in the fuel (20 ppm) and limited engine run time to collect sufficient sample mass for analysis.

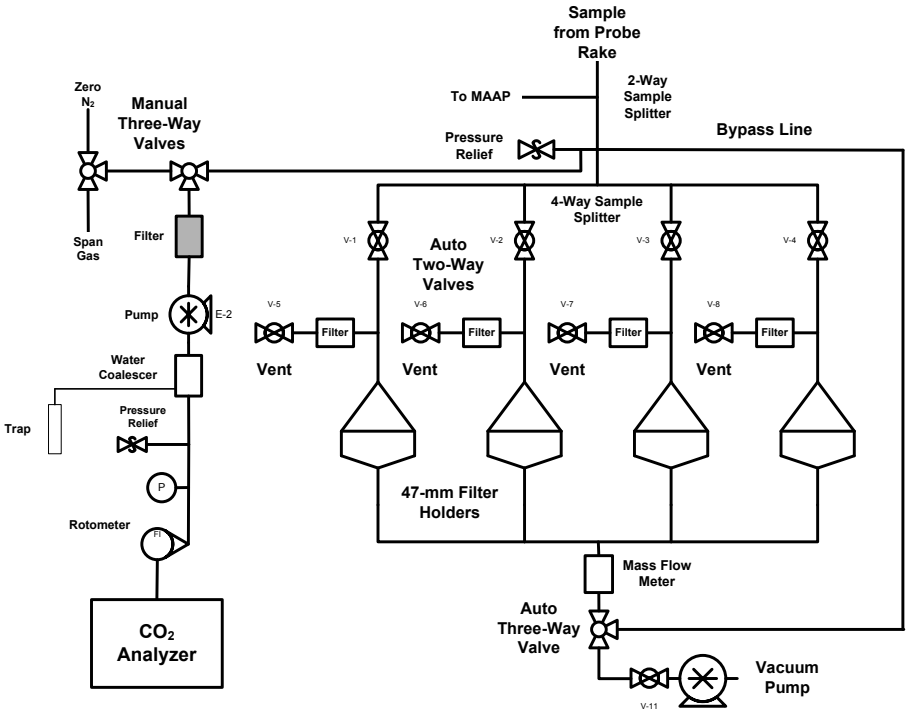

Figure 17. Diagram of multi-filter sampler connected to 4-way splitter in Figure 16

Time-integrated sampling was conducted during T63 engine testing using pre-weighed Teflon filters and subsequently analyzed by EPA for total mass and PM sulfate content. All sampling media was prepared in the EPA's Fine Particle Characterization Laboratory (FPCL) before leaving for the field. Prior to and after sampling, the Teflon filters were stored inside plastic petri dishes inside a -50 °C freezer. During transport and in the field laboratory, all sampling media were stored in a small freezer operated at a nominal temperature of -15 °C. This portable freezer was also used as the primary shipping container for the sampling media to and from the sampling site (the unit was operated on auxiliary DC power supplied by the truck engine). Sample collection was performed using the DASYLAB software package described previously. The necessary valve sequence and delays are programmed into the software thus freeing up the operator to focus on the start and stop time at each experimental condition. In addition, the time at which the sample stream or bypass flow was activated was also logged by the computer for later analysis. Proper operation of the software was verified before deploying to the field.

After the demonstration, all sampling media were stored at -50 °C in the FPCL until analysis. Note that samples maintained at this temperature in sealed containers may be safely stored for long periods of time prior to analysis without degradation. Substrates were weighed before and after the field sampling campaign to determine the total mass of PM collected. Teflon filter samples were weighed using an ATI Cahn C-44 microbalance located in a climate-controlled clean room. The method requires that the filter samples be conditioned before weighing by exposure for a minimum of 24 hours to air maintained at 20-23 °C and a relative humidity of 30-40%.

After gravimetric analysis, Teflon filters were extracted for inorganic ion analysis by placing each filter in a 11-mL vial with 10 mL of deionized water. The sample was sonicated for 30 minutes and then analyzed by Ion Chromatography (IC) within one week of extraction using a Thermo Scientific ICS-2100 Ion Chromatograph with a sample loop of 25 µL. An external calibration curve was developed using quantitation standards as described in the applicable MOP for this type of analysis.

Black carbon (BC) mass emissions were measured from the T63 engine plume using a modified Thermo Scientific Model 5012 Multi Angle Absorption Photometer (MAAP). The off-the-shelf instrument, designed to measure BC mass concentrations from ambient air, was modified by EPA to allow its use for source measurements through the addition of externally mounted hardware and custom Labview software.

Elemental carbon (EC) mass concentration data were obtained for the T63 engine using a Sunset Semi-Continuous ECOC Analyzer as specified by the NIOSH Method 5040. BC mass concentrations for the PW-F117 engine were measured using an AVL Model 483 Microsoot Sensor. A TSI Engine Exhaust Particle Sizer was used to measure particle size distributions in all the emissions samples for the PW-F117 engine.

All instruments were operated using their respective Standard Operating Procedure (SOP) or Miscellaneous Operating Procedure (MOP) with the data logged using a multi-computer network. The output from each analyzer was time synchronized each morning using a clock card installed in the master computer which is set daily using a portable atomic clock.

6.0.3 ARI Compact Time-of-Flight Aerosol Mass Spectrometer (C-ToF-AMS)

A compact time-of-flight aerosol mass spectrometer (C-ToF-AMS) instrument was used by ARI to characterize semi-volatile PM emissions. Figure 18 shows a schematic of the AMS instrument. The diluted engine exhaust sample is drawn into the instrument at a flow rate of ~1.4 cm^3/s through a 100 µm diameter critical orifice, and then into an aerodynamic lens based on the design of Liu *et al.* [35] and Zhang *et al.* [36, 37]. The lens focuses the particles into a narrow beam, which then enters into a vacuum chamber while most of the gas is pumped away. Fluid dynamics simulations of the lens system as well as laboratory experiments have shown 100% transmission efficiency of spherical particles in the range of 60–600 nm at sea level sampling pressure [38]. Upon gas expansion into the vacuum chamber, the particles acquire a size-dependent terminal velocity. The particle beam is modulated by a chopper wheel that rotates at a frequency of 128 Hz. The duty cycle of the chopper (percentage during which the chopper is open to allow for actual sampling) is approximately 50% due to the application of an efficient multiple chopper apparatus. Particle aerodynamic size can be determined from the measured particle time of flight after calibration with particles of known sizes, densities, and shapes, such as Polystyrene Latex (PSL) spheres (Duke Scientific, Palo Alto, California). After a flight distance of 39.5 cm, the particle beam reaches a heated, roughened molybdenum surface under high vacuum (~10^{-4} Pa). Then non-refractory species in/on the particles such as nitrates, sulfates and organics are vaporized at about 600°C. Highly volatile species in/on the particles like water may be lost during the particle time of flight. The vaporized species are then ionized into molecular fragments by the impact of energetic electrons (70 eV) emitted from a pair of heated tungsten wires. The ion fragments formed are analyzed by a time-of-flight mass spectrometer (Tofwerk, Thun, Switzerland). The detection

range of C-ToF-AMS for ion fragments is 14-400 in m/z and its resolution power is about 500. For this resolution the ion fragments of hydrocarbons and oxygenated hydrocarbons with the same unit mass like $C_4H_9^+$ and $C_3H_5O^+$ cannot be distinguished by this instrument.

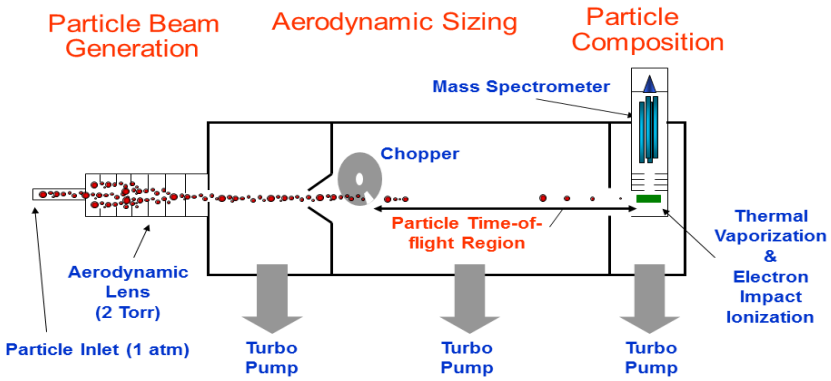

Figure 18. Schematic of the C-ToF-AMS instrument

Particle size distribution in vacuum aerodynamic diameter (D_{va}) is also determined by the C-ToF-AMS via measurements on particle time-of-flight, in which the starting time is provided by the opening time of a rotating beam chopper and the arrival time by the chemical detection. A calibration function between particle time-of-flight and particle size of ammonium nitrate was performed and used to calculate particle size for the measurements. The C-ToF-AMS therefore offers the detailed information upon both particle size distributions in mass and semi-volatile chemical compositions of PM emissions by monitoring size-dependent characteristic mass spectrum of non-refractory PM.

6.0.4 ARI Engine Soot Compliance Monitor (ESCOM)

ARI deployed a newly developed instrument specifically for aviation PM measurement called the Engine Soot Compliance Monitor (ESCOM). The ESCOM instrument consists of three commercially available devices: a LiCor 802A CO_2/H_2O NDIR-based gas analyzer, a Mixing Condensation Particle Counter (MCPC) and a Cavity Attenuated Phase Shift (CAPS) PM extinction monitor (CAPS PM_{ex}) for the determination of emission indices of soot particles in number and mass. During the ESCOM operation, the CO_2 concentration in the diluted exhaust sample was monitored by the LiCor 802A CO_2/H_2O gas analyzer (LI-COR Environmental); particle concentration was measured with the Mixing Condensation Particle Counter (MCPC, Model 1720, Brechtel); and black carbon soot mass was monitored by the CAPS PMex instrument, which is patented and manufactured by ARI. Since the upper measurement limit of the MCPC is only 100,000 particles/cc, which is more than one order of magnitude lower than the normally particle concentration from aircraft engine exhausts, a capillary diluter with a dilution ratio of 38:1 was used to reduce the sample concentration into the dynamic range of the MCPC device. The total flow rate of the ESCOM instrument is 2.8 liter per minute (lpm) and all the three devices were set at a data acquisition rate of once per second. The CAPS PM_{ex} device is based on cavity attenuated phase shift technique and is capable of determining particle light extinction, which is mostly due to absorption for aviation soot. The CAPS technique [39-40], similar in nature to cavity ring-down spectroscopy, relies on the use of a sample cell employing high reflectivity mirrors

(R>99.99%). A schematic of the CAPS PM_{ex} monitor is shown in Figure 19. Square-wave modulated red light (~635 nm) from a high-power light emitting diode (LED) is directed through one mirror and into the sample cell. The distortion in the square wave caused by the effective optical path length within the cavity (~ 1 km) is measured as a phase shift in the signal by a photodiode located behind the second mirror. The presence of particles in the cell causes a change in the phase shift ($\vartheta - \vartheta_0$) which is related to the total extinction (the sum of scattering and absorption), ε_{part} by the following relationship:

$$\cot \vartheta - \cot \vartheta_0 = \frac{c}{2\pi f} \varepsilon_{part} \tag{3}$$

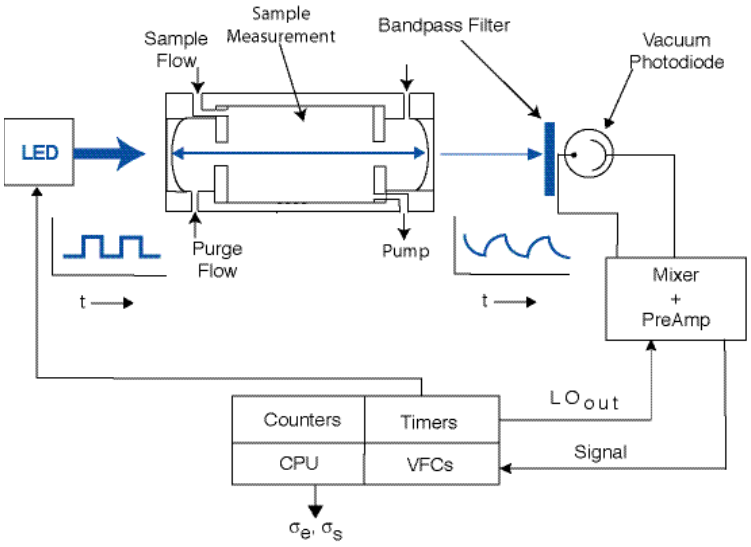

Figure 19. Schematic of CAPS PM_{ex} for measurement of black carbon soot mass

where ϑ_0 is the phase shift measured in the absence of particles, c is the speed of light and f is the modulation frequency. The CAPS PM_{ex} extinction monitor has a detection level of 1 Mm^{-1} with a time response of 10 seconds using a flow of only 0.85 liter per minute (lpm). Complete details of this extinction monitor and its performance are presented elsewhere [41,42]. Detection limit of the CAPS PM_{ex} device is 0.3 μgm^{-3} (2σ) in 1s data acquisition.

6.0.5 ARI Sulfate PM Measurement

Sponsored by a NASA SBIR program, ARI developed a new type of particle characterization instrument to quantify the mass emissions of sulfate PM, based on SO_2 detection using ARI's "Quantum Cascade Laser (QCL) Tunable Infrared Laser Direct Absorption Spectrometer (TILDAS)" technology. In this instrument, the sulfate particle-laden sample goes through an acid gas denuder where gas-phase SO_2 is removed, and then the sample is passed through a high-temperature (950°C) oven where the particle sulfates are reduced to gas-phase SO_2. The SO_2 concentration liberated from the PM sulfates is detected with the QCL-TILDAS instrument. Figure 20 shows the schematic (a) and a photograph (b) of the sulfate conversion module (without QCL).

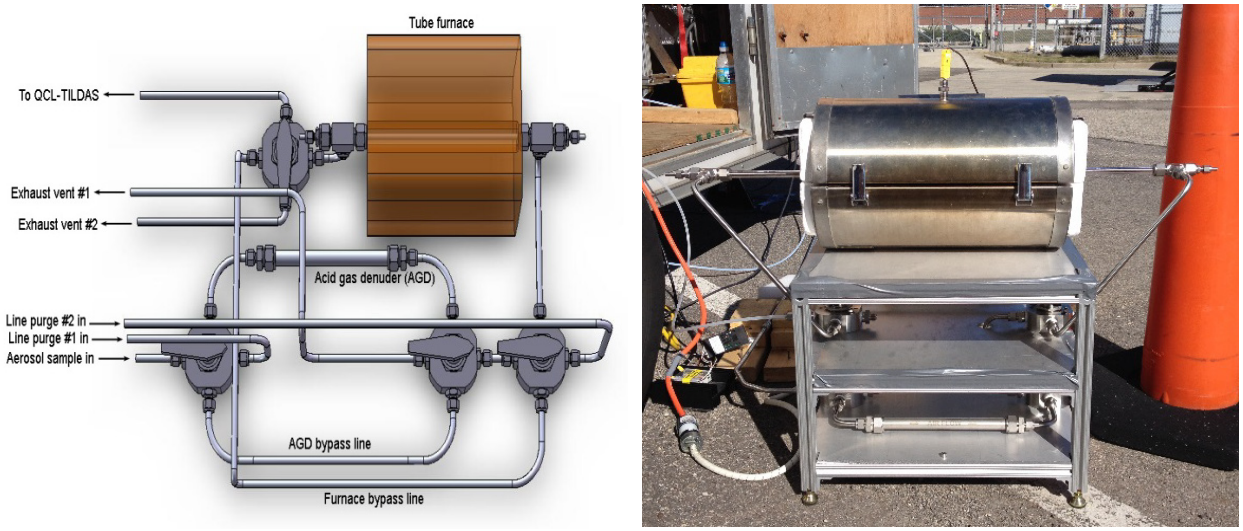

(a) (b)

Figure 20. Schematic (a) and picture (b) of the sulfate conversion module to measure PM sulfates

6.0.6 MSU Measurement of Selected Gas Phase Organics via PTR-MS (C-17 only)

A proton transfer reaction mass spectrometer (PTR-MS) was deployed by Montana State University (MSU) for the measurement of selected gas phase organics from the PW-F117 engine. The PTR-MS is a chemical ionization mass spectrometry technique based on H_3O^+, which is capable of measuring compounds having a proton affinity greater than that of water [43,44]. The permanent components of air (N_2, O_2, Ar, CO_2 etc.) and the alkanes all have proton affinities less than water [45] and are not detected. Most non-alkane organic components except ethylene and acetylene have proton affinities greater than water and will react with H_3O^+ via a proton transfer reaction. A schematic of the PTR-MS is provided in Figure 21. H_3O^+ reagent ions are produced in an external hollow cathode ion source by ionization of water vapor. The H_3O^+ reagent ions and a small amount of O_2^+ and NO^+ (impurity ions produced from the back diffusion of air into the hollow cathode) are electrostatically injected into the drift tube reaction region where they interact with the ambient sample. These reagent ions are pulled through the ambient sample at reduced pressure (~ 2 mbar) under the influence of an applied electric field where they will transfer a proton to any component having a proton affinity greater than that of water. A fraction of the reagent ions and product ions formed are sampled through a small aperture at the end of drift tube and mass analyzed using a quadrupole mass spectrometer operated in the ion counting mode.

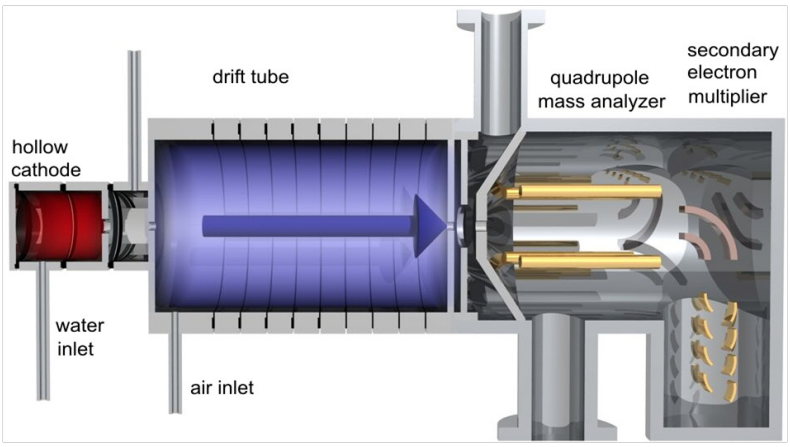

Figure 21. Schematic of the proton transfer reaction mass spectrometer (PTR-MS)

Proton transfer is considered to be a soft ionization method which in many cases produces only the protonated molecule (MH^+) and is detected at 1 atomic mass unit (amu) higher than its molecular weight. Some molecules fragment upon ionization. Ions possessing oxygen can form hydrates. These fragmentation and hydration reactions can complicate the interpretation of the PTR-MS mass spectrum. Even in the absence of these complicating reactions, interpretation of the PTR-MS mass spectrum requires a detailed knowledge of the composition of the sample being interrogated, because ion mass is not necessarily a unique indicator of compound identity. This instrument has been employed in numerous aviation engine exhaust studies and a detailed description can be found in Knighton et al [46].

The PTR-MS sampled through a short section (< 1m) of standard 3.175 mm OD Teflon line. The flow rate through this tube was approximately 200 sccm and was controlled via pressure controller and a fine metering valve. The flow path into the instrument was controlled by a series of 3-way valves. In the 'background mode' the gas flow was directed into heated platinum catalyst tube to remove any VOCs without affecting the sample humidity prior to its introduction into the instrument. In the 'measurement mode' the sample flowed through the valves and then to sample inlet of the instrument. Sample concentrations are derived from the difference in the response between the measurement and background responses. Because the background response is expected to only drift slightly between background measurements, the background signal is linearly interpolated between the measurements.

6.0.7 Calculation of Pollutant Emission Indices

Fuel-specific emission indices (EIs) were calculated using the measured PM and gaseous emissions concentrations. For PM, the mass emission index, expressed in pollutant mass per kg of fuel burned, EI_m *(g/kg-fuel)*, was calculated based on the SAE AIR 6241 guidelines using the following equation:

$$EI_m \text{ (g/kg-fuel)} = (PM_{mass\_STP} * DF * 10^6 * 22.4)/(CO_{2\_raw} * [M_c + \alpha M_h]) \quad (4)$$

where:
- PM_{mass_STP} = total PM and sulfate mass concentration (g/m^3)
- DF = dilution factor (= dilution ratio + 1) (dimensionless)
- CO_{2_raw} = CO_2 concentration at engine exit (ppmv)

M_c	= atomic weight of carbon = 12.011
α	= H/C (hydrogen-to-carbon) ratio in the fuel (dimensionless)
M_h	= atomic weight of hydrogen = 1.008
STP	= standard temperature and pressure (0 °C and 1013.25 mBar)

To calculate the dilution factor (DF) in the condensation devices or plume, the following expressions were used:

$$DF = ([CO_{2\_raw} - CO_{2\_dil}]/[CO_{2\_dil} - CO_{2\_amb}] + 1)$$ for 100% ambient air dilution

$$DF = (CO_{2\_raw}/CO_{2\_dil})$$ for dilution with 100% N_2

where:	CO_{2_dil}	= CO_2 concentration measured after dilution (ppmv)
	CO_{2_amb}	= ambient background CO_2 concentration (ppmv)

Note that these EIs for PM were not corrected for sampling system losses and as such, should not be used to estimate the PM emissions factors for these engines.

For the demonstration on the C-17, the sample in the DC used N_2 as the motive gas and ambient air for secondary dilution, which complicates the calculation of the DF by gas measurement. For this DF calculation, it is necessary to know the sample flow gas flow rate. The sample flow rate was estimated based on correlations with the motive flow rate and ejector sample and motive inlet pressures developed in the laboratory and validated in-field prior to the test measurements.

Similar EI calculations were performed for the other pollutants by substituting the average mass concentration from the instrument into the EI_m equation. For calculation of the particle number EI (EI_n), the constant in the numerator was 10^{12} instead of 10^6 and the number concentration (PM_{num_STP}) expressed in particles/cm^3 was substituted for PM_{mass_STP}.

6.1 T63 Engine Demonstration Setup

The emissions sampling system for the T63 engine demonstration is shown in Figure 22. Three sampling probes (two raw sample probes and one diluted at probe tip) were installed at the exit of the engine exhaust extension pipe to collect samples for distribution to several systems or instruments. Both raw sample lines were heated to 150°C consistent with the SAE ARP1256 guidelines for gaseous emissions [34]. Raw sample was provided to a carbon sampler to collect samples for organic and elemental carbon analysis or to a MAAP for black carbon mass concentration measurement. A second raw line provided sample for gaseous emissions measurements and to the DC or CDP. The line lengths between instruments and sample location for the devices and plume were similar to ensure equivalent particle losses for valid comparisons of PM emissions. The plume was sampled with a 3.8 cm diameter probe port installed at the same height and at 4 m from the engine exhaust tube. Pictures of the sampling system and mobile laboratories outside of the T63 engine test cell are shown in Figure 23 and 24.

All research groups were provided diluted samples from either from the DC, CDP, or the plume probe. AFRL also analyzed the tip-diluted sample representing the "non-volatile" PM emissions. Instrumentation employed by each group was provided in Table 3 and shown in Figure 22.

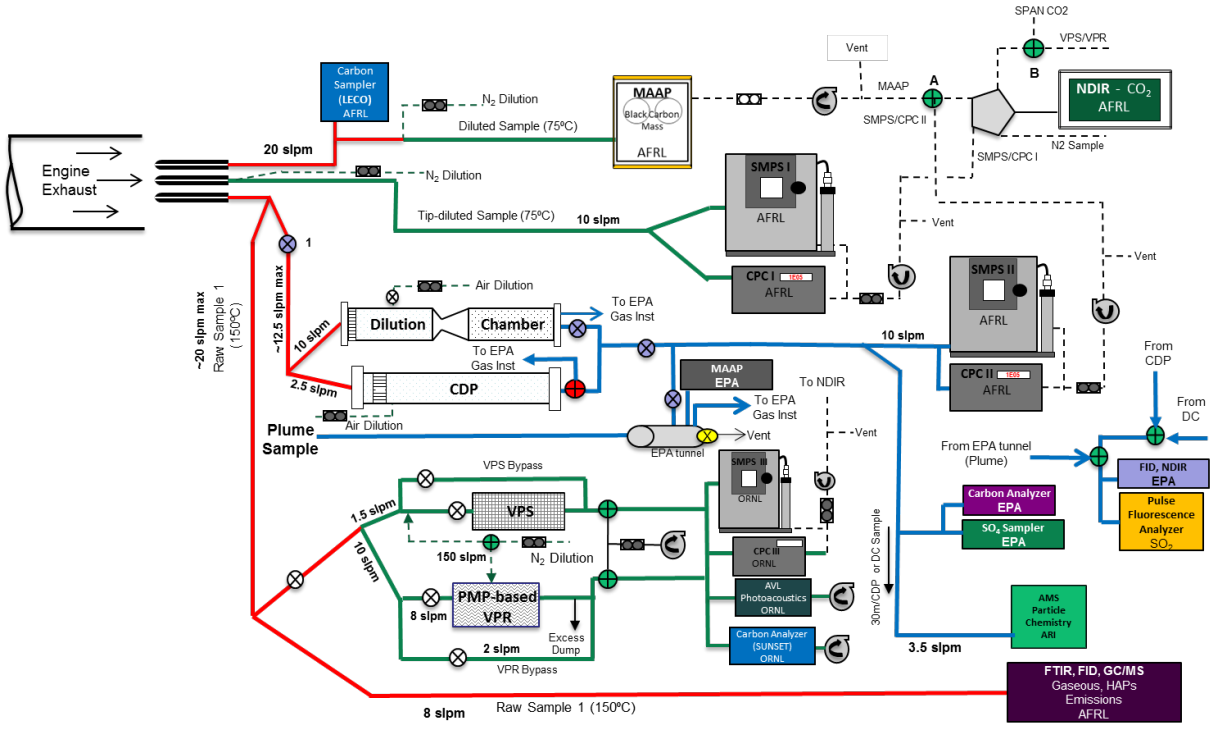

Figure 22. Sampling system diagram for T63 emissions demonstration

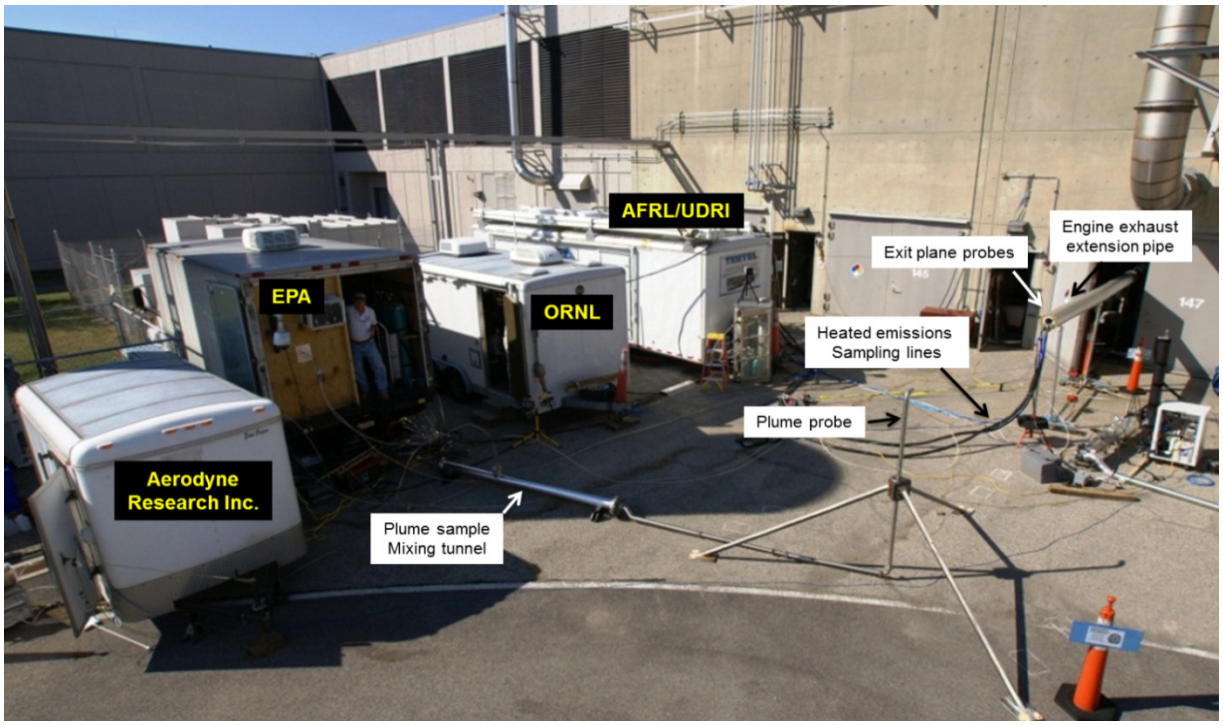

Figure 23. Sampling system and emissions laboratories setup at T63 emissions demonstration

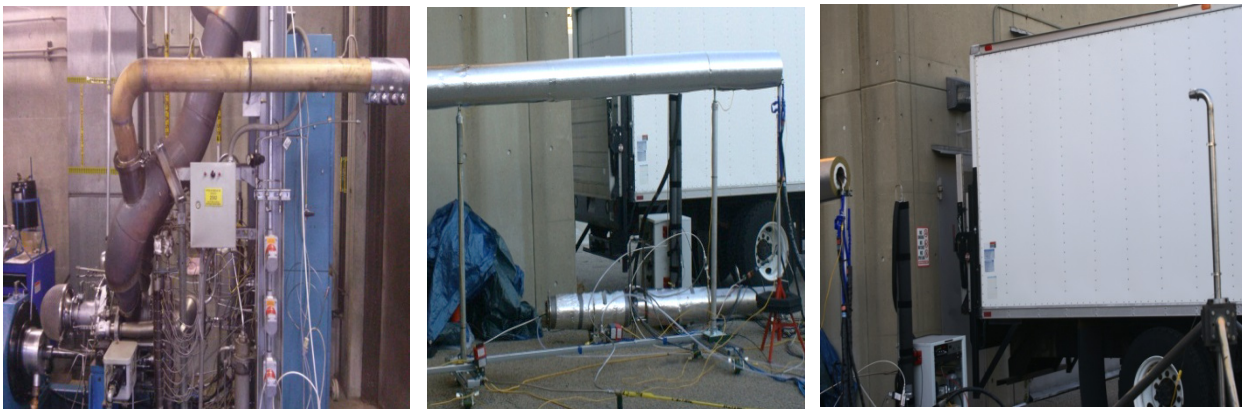

Figure 24. T63 engine exhaust extension pipe and sampling probes setup

6.2 C-17 (PW-F117 Engine) Demonstration Setup

A schematic of the emissions sampling system used in the C-17 aircraft engine demonstration is shown in Figure 25. The system consisted of four ganged gas probes which collected engine exhaust raw sample for distribution to the condensation devices, VPS and instruments. The raw sample was transferred to a heated box (shaded blue) where it was split to provide sample to the condensation devices, the gas analyzer and to ORNL for the VPS evaluation. A portion of the raw sample was diluted with heated nitrogen in a Dekati ejector-diluter and transferred through unheated electrically conductive tubes (both stainless steel and carbon-loaded, electrically grounded PTFE) to a second stage nitrogen dilution before entering the instruments. A catalytic stripper was available to remove volatile species downstream of the secondary dilution; however, it was not used due to complexities with the device and lack of sufficient test time to properly address. Although there may be some volatile PM formed in the lines, these were considered minimal compared to those formed in the plume and condensation devices. This two-stage nitrogen-diluted sample was used to represent the non-volatile PM to compare to the total PM from the plume and condensation devices. The remaining raw sample was distributed to the VPS and to the condensation devices. Two plume probes, installed at 10 and 20 m from the engine exit plane, where used to sample the plume at the two locations. Plume samples were transferred to the instruments via 5.1 cm stainless steel tubing and drawn into the sampling system with a blower installed inside a 15.2 cm diameter, 310 cm long mixing tunnel. Initial tests showed that only engine fan (bypass) air was sampled through the 10 m probe due to its relatively close proximity to the engine, thus, only the 20 m probe was used for plume measurements. Samples from the DC, CDP and plume were evaluated individually and isolated from the instruments using remotely actuated ball valves. Figures 26 - 28 depict the emissions system and mobile laboratories for the C-17 demonstration. Figure 26 (right panel) shows the water-cooled probe rake with multiple probes (only four used in this demonstration). The sampling probes consisted of 1.52 mm diameter ports and were separated 3.18 mm center-to-center in the rake. The probes were installed ~42 cm from the engine exit plane, with the top probe was positioned at the center of the engine. The rake was mounted on a heavy duty steel structure restrained with three tanks of water (~3,400 kg total weight) to prevent movement during engine operation. The plume probes had 19.0 mm diameter ports and where placed at approximately 3 m height from the ground (engine center was at 5 m) to collect well-mixed engine core/fan diluted samples.

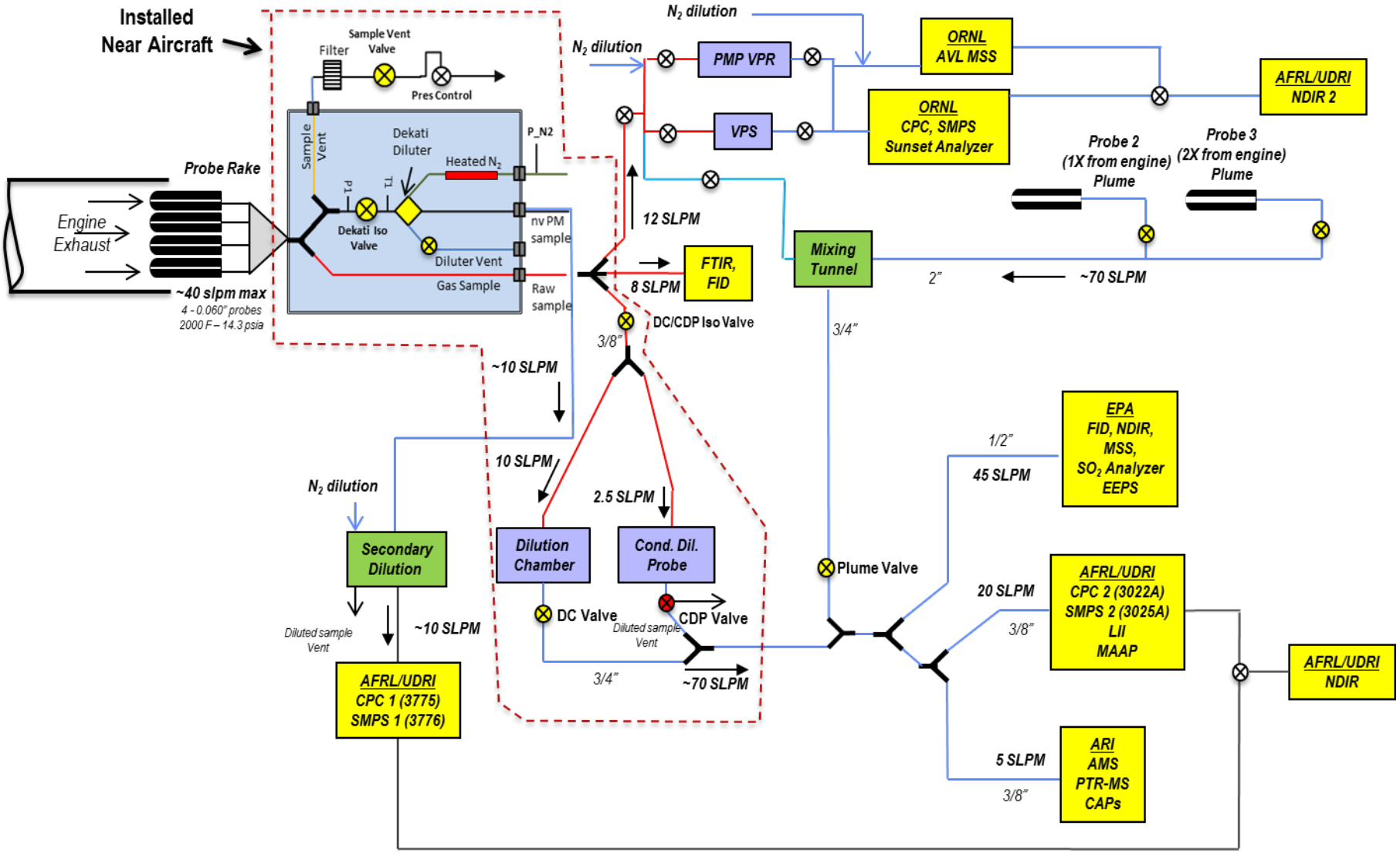

Figure 25. Schematic of sampling system for measurement of non-volatile and total PM emissions used during demonstration on C-17

Figure 26. Emissions sampling probes at engine exit, 10m and 20 m, and probe rake for engine exit plane emission sampling

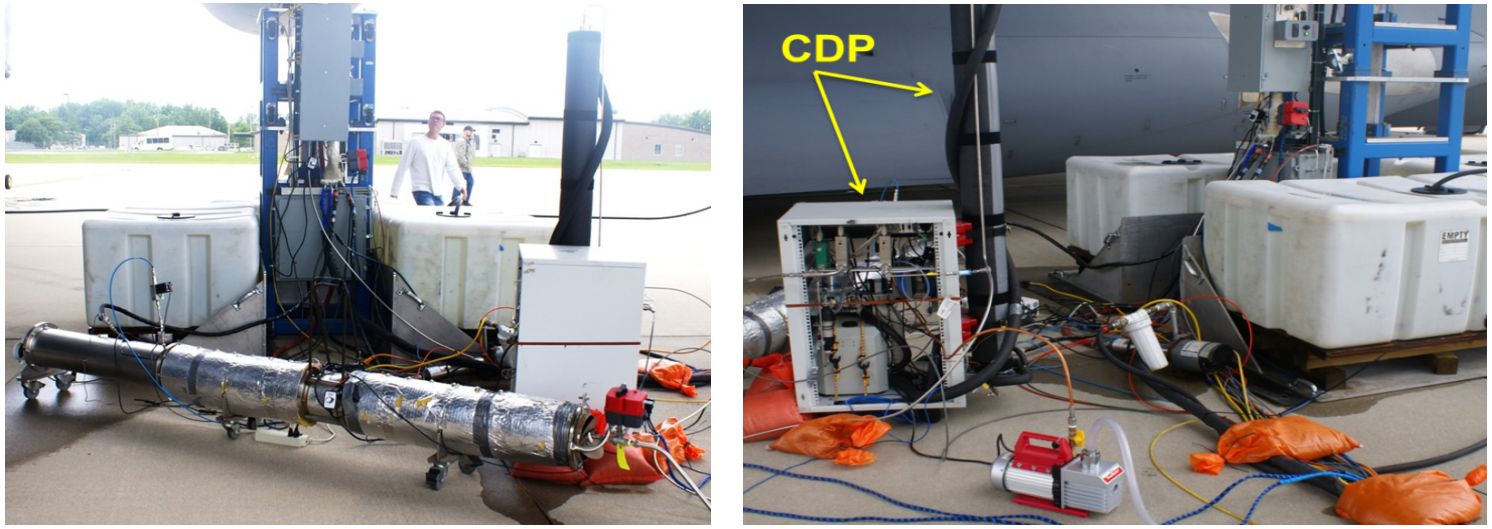

Figure 27. DC and CDP installed near engine during C-17 demonstration

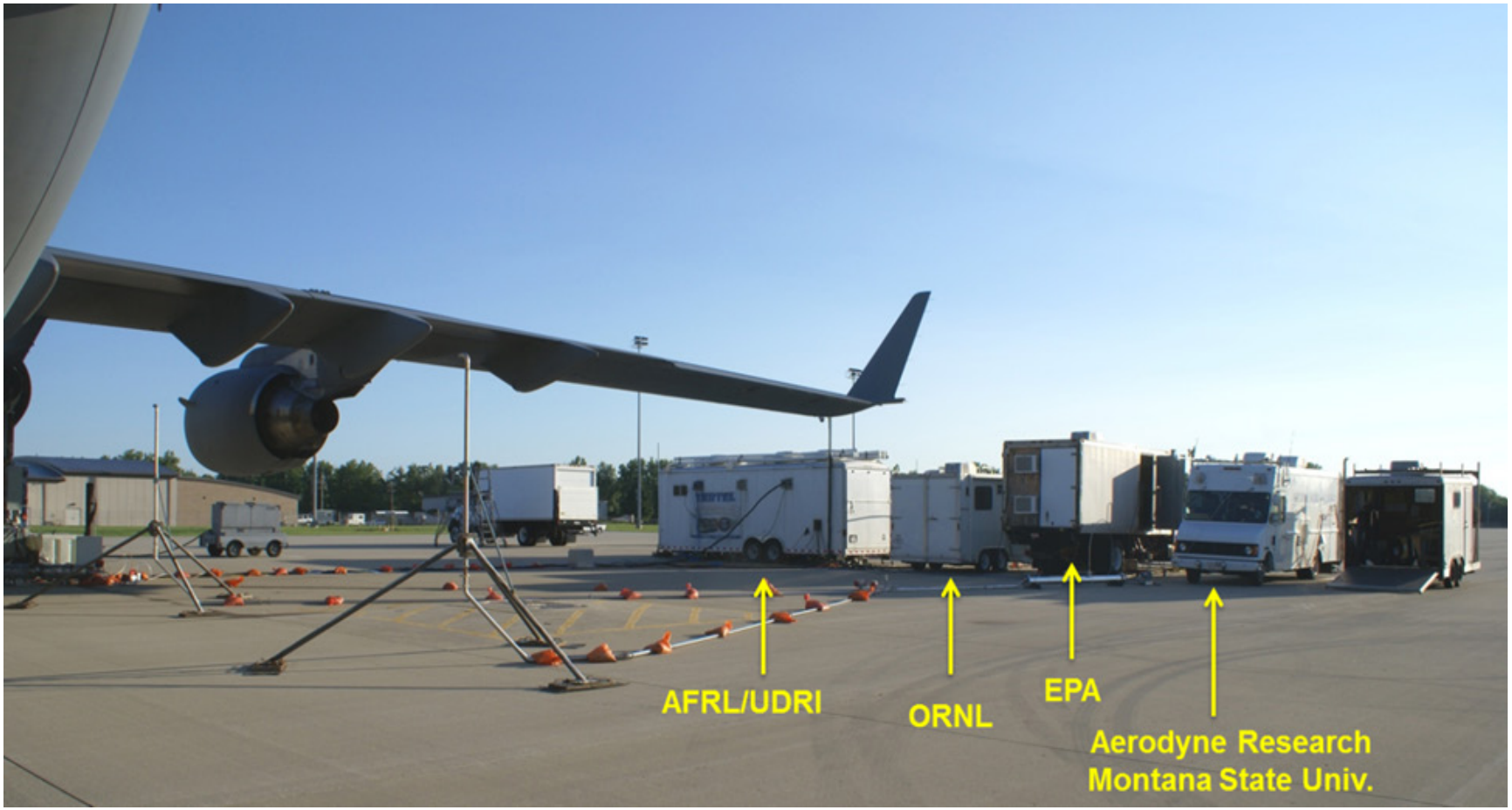

Figure 28. Emissions mobile laboratories and plume probe setup at C-17 aircraft engine emissions demonstration

7. PERFORMANCE ASSESSMENT

Particle number, size distribution, mass, and chemical composition were measured for samples extracted at the engine exit plane, at the exit of the dilution devices and at the far field location. General metrics or indicators of effective performance of the dilution devices and the VPS are listed in Table 4.

Table 4. Systems Performance Criteria

Demonstration Device	**Measurement**	**Metric (compared to designated non-volatile PM)**
Vapor Particle Separator (VPS)	• Non-volatile Particle Number (PN)	• PN (±15%)
	• Non-volatile Particle Size	• Similar size (±15% of mean diam.)
	• PM chemical composition • EC/OC NIOSH 5040	• OC reduction (>70%)
	• Modified PMP validation	• Evaporation of >99% tetracontane 15 nm particles
Dilution Chamber (DC) and Condensation Dilution Probe (CDP) Total PM	• Particle Number	• Increased PN (10X)
	• Particle Size Distribution	• Evidence of nuclei PM formation (10X in 5-20 nm range)
	• Particle Mass	• Increased mass (>30% depends on fuel composition and volatile PM)
	• Non-volatile chemical composition	• Increased organics in non-volatile fraction (>30% depends on fuel composition and volatile PM)
	• EC/OC NIOSH 5040	• Increased organic fraction(>30% depends on fuel composition and volatile PM)
Dilution Chamber (DC) Non-volatile PM	• Particle Number • Particle Size • Particle Mass	• Similar PN (±25%) • Similar size (±15% of mean diam.) • Similar Particle Mass (±25%)

Specific details for each demonstration and data collected by the individual teams are discussed in the following subsections. Performance assessments of the condensation devices and VPS relative to the success criteria described in Table 1 are discussed.

7.1 Demonstration on T63 Engine

Engine test conditions for the demonstration of the devices on the T63 engine were shown in Table 2. Raw samples were taken at the engine exit (extension pipe) and transferred through heated sampling lines at 150°C to the DC, CDP and gas emissions instrumentation. The dilution ratios in the condensation devices were controlled to match and double the sample dilution measured in the plume probe. Doubling the dilution ratio was performed to investigate if volatile PM were promoted with increased dilution. As previously noted, the plume probe was installed relatively close to the engine exhaust extension tube exit to obtain a strong PM signal while sufficiently far to promote volatile PM nucleation. Infrared images of the engine exhaust plume at the exit tube and near the plume probe are shown in Figure 29 for both engine conditions. As shown, the plume thermal signatures for each condition were very strong near the exit tube, but weak near the plume probe due to the rapid mixing of engine gases and air, and the low velocity exhaust from the turboshaft engine. It is noteworthy that the low momentum of the exhaust gases combined with the erratic ambient air recirculation flows near the exhaust pipe (due to its proximity to the facility structure and architecture) produced very complex flows at the plume, which deviates from the characteristics of turbofan exhaust flows. Thus, it is recognized that these exhaust flows or plumes are not representative of typical turbine engines exhaust, but provide insight into the gas-to-particle transformations in the plume and comparisons with those processes in the condensation devices.

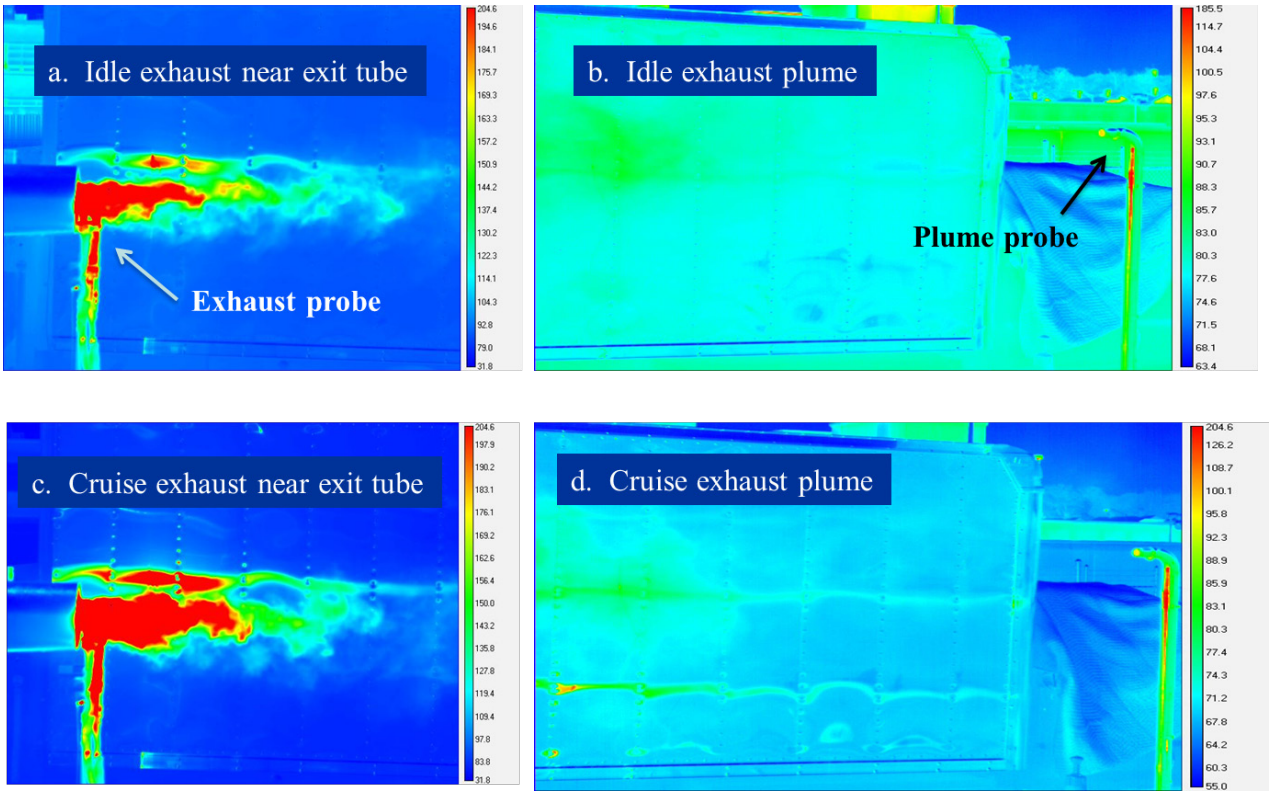

Figure 29. Infrared thermal images of T63 engine exhaust at the engine exhaust exit and at plume probe at idle (a, b) and cruise (c, d) conditions.

After entering the probe, the plume sample was drawn into a mixing tunnel (to enhance mixing of ambient air and engine exhaust) where the sample was drawn into the instruments via internal or external pumps. Three fuels with varying concentrations of aromatics and sulfur were used during the demonstration to vary the concentration of volatile PM formed. The fuels used included: a conventional low sulfur and aromatic JP-8 (40 ppmw and 11% by w respectively), the JP-8 doped with a blend of aromatics to increase concentration to 25% by vol and the JP-8 doped with an organosulfur compound, *tetrahydrothiophene* (C_4H_8S), to increase its sulfur content to the maximum (although very unlikely) sulfur content in jet fuel of 3000 ppmw.

7.1.1 PM Characterization for Plume, DC and CDP Samples - AFRL/UDRI

7.1.1.1 Comparison of T63 engine PM Concentration and Size between Plume, DC, CDP and Probe-tip Diluted Samples

Displayed in Figure 30 are the particle number emission indices (EI_n) data for the plume and probe-tip (non-volatile) diluted samples. As anticipated, the particle concentrations (mostly nvPM) increased with the aromatic-doped fuel at both engine conditions regardless of sampling technique. As observed, the EI_n in the plume were significantly higher than at the exit plane especially at idle and with the high sulfur fuel due to the higher concentration of organics (i.e., unburned hydrocarbons) and sulfates respectively. Factors of 4.25 and 11.5 times more particles were observed in the plume than at the engine exit at idle for the baseline JP-8 and JP-8+sulfur fuels respectively. Smaller relative increases were observed for cruise due to the lower concentration of organics and increased exhaust velocities which reduced residence times for the formation of volatile PM. Of note is the negligible impact of fuel sulfur content on engine EI_n for samples diluted at the probe-tip, therefore demonstrating that volatile PM produced by sulfur species are suppressed when samples are rapidly diluted near the sampling point.

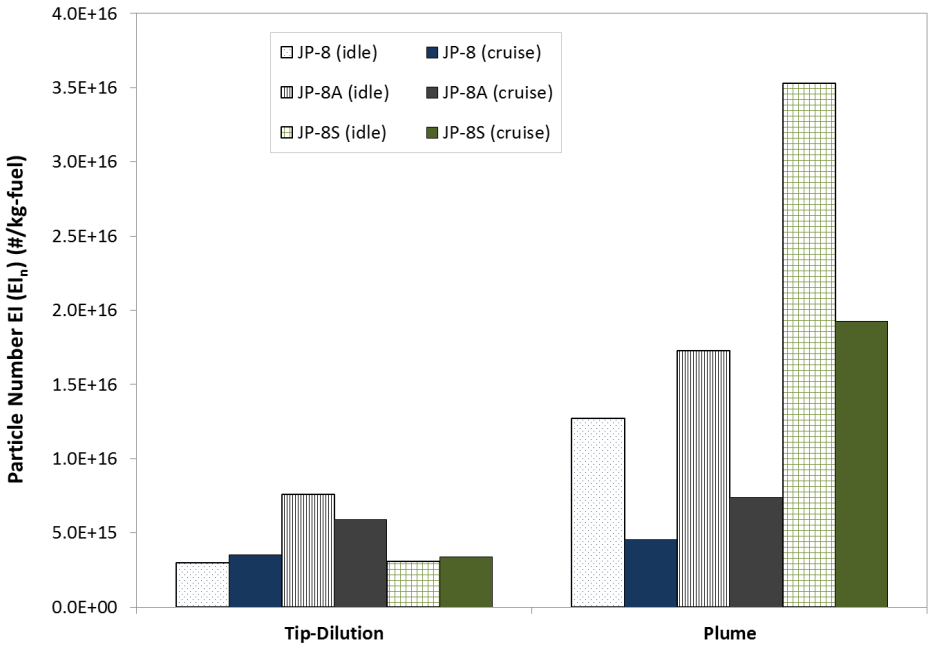

Figure 30. Particle Number Emission Indices for probe tip and plume diluted T63 engine PM

Differences between EI_n for the tip-diluted (nvPM), CDP and DC samples relative to the plume for both engine conditions are shown in Figure 31. All samples at idle conditioned through the CDP and DC yielded significantly lower EI_n than the plume samples. For the sulfur-doped fuel, the EI_n differences were approximately 90% lower as the result of a high yield of volatile PM formation from sulfates in the plume, which evidently were not formed in the condensation devices. Doubling the dilution ratios in the CDP and DC to those found in the plume did not encourage further nucleation of volatile PM. For the high sulfur fuel at cruise, similar differences in EI_n between plume and condensation devices were observed. For JP-8 and JP-8+ aromatic fuels, the EI_n for the cruise condition for the DC were within the 40% success criteria (~20%), however, these EI_n were almost identical to the nvPM samples which suggest that there were very few organics available for the formation of volatile PM (unburned hydrocarbons at cruise < 85 ppm). The relatively low particle concentrations from the CDP may be due to: 1) higher relative PM losses in the device; 2) coagulation of particles; or 3) quenching volatile PM, preventing nuclei formation.

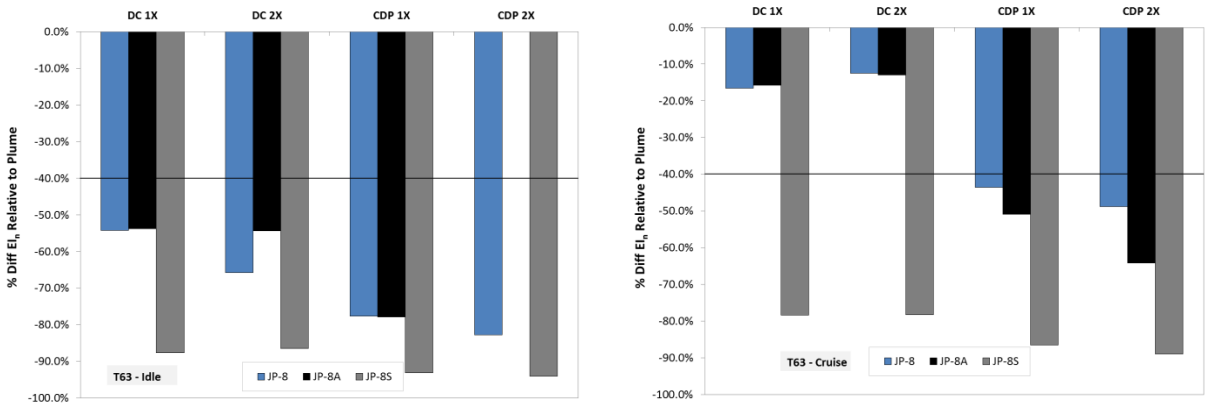

Figure 31. Percent differences in EI_n between PM at DC and CDP relative to plume samples fromT63 engine

Particle size distributions (PSD) were measured for samples at the engine exit plane, plume and condensation devices to assess the degree of particle nucleation and for comparisons between each other. Figure 20 displays the PSD for the T63 engine at idle. Consistent with observations discussed previously, dramatic increases in particle number were observed in the plume for both JP-8 and JP-8S fuels relative to probe tip-diluted samples (both JP-8 and JP-8S were statistically the same). The CDP and DC are shown to promote volatile PM formation as compared to the tip-diluted sample. Nuclei size particles (assumed to be 7-23 nm) increased by a factor of at least four in the DC for both engine conditions. However, as discussed, these increases were significantly lower than those observed in the plume. It is noteworthy that natural dilution in the plume and dilution in the condensation devices increased particle concentrations not only in the nucleation zone but throughout the full range of sizes measured, therefore suggesting that many of these volatile species nucleate into new particles (perhaps in the 7-23 nm range), but also are adsorbed on to non-volatile PM resulting in particles with larger sizes up to near 100 nm. As such, the criteria selected based on only the nuclei size particles may not have been the most appropriate. Nonetheless, based on these data, the success criteria for the condensation devices (10X increase in PM nuclei size concentrations relative to probe-tip dilution) were not achieved.

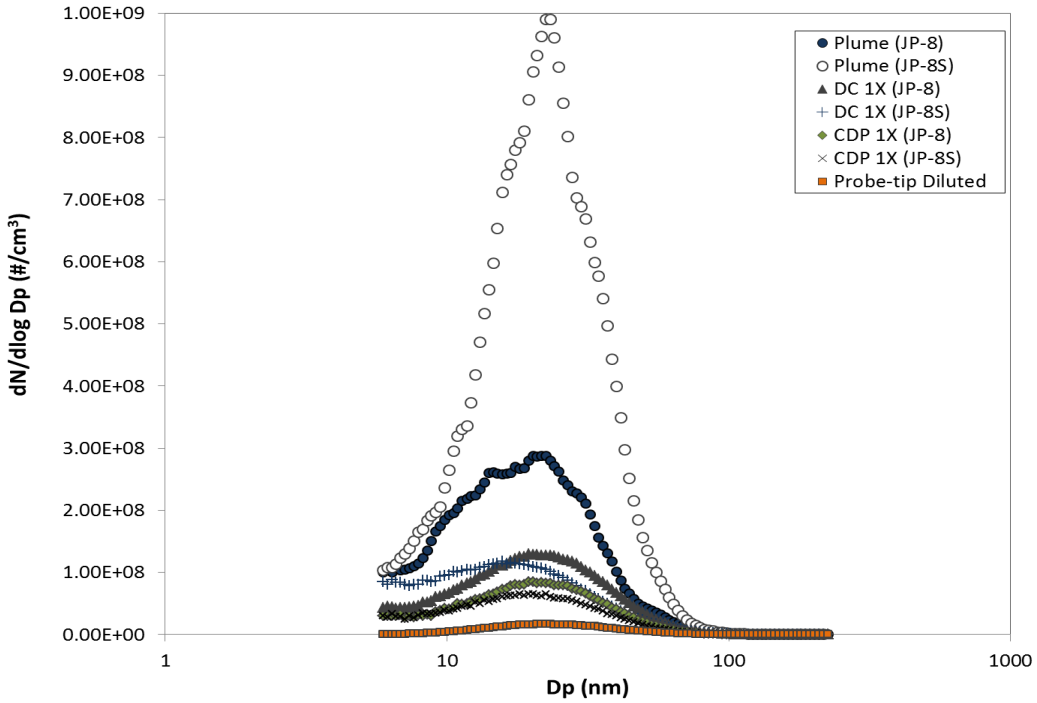

Figure 32. Particle size distributions for T63 engine at idle for the engine exit plane, plume, DC and CDP

7.1.1.2 Comparison of Nitrogen Dilution DC and Probe-tip Dilution Samples

The DC was evaluated to use for nvPM sampling by diluting with nitrogen (rather than ambient air) in the secondary dilution path. Particle size data show similar size distributions and mean particle diameters for the tip-diluted and DC nitrogen-diluted samples; however, the concentrations were significantly lower for the latter. Figure 33 shows the comparison of EI_n and black carbon mass concentration between the two samples. The PM mass concentration measurements using the MAAP show excellent agreement between the two sampling techniques for both engine power settings. The EI_n comparison; however, show lower (~30-45%) particle concentrations in the DC than for tip-diluted samples. The success criterion of ±25% of the tip-diluted sample EI_n was therefore not met. The agreement in PM mass data, but not in particle concentration may be due to loss of very small (i.e., low mass) particles in the DC, which are not reflected in the mass measurement. Since the DC EI_n are relatively close to the success criteria, further studies with different splits of dilution nitrogen between primary (ejector) and secondary dilution are warranted as these may reduce small particle losses.

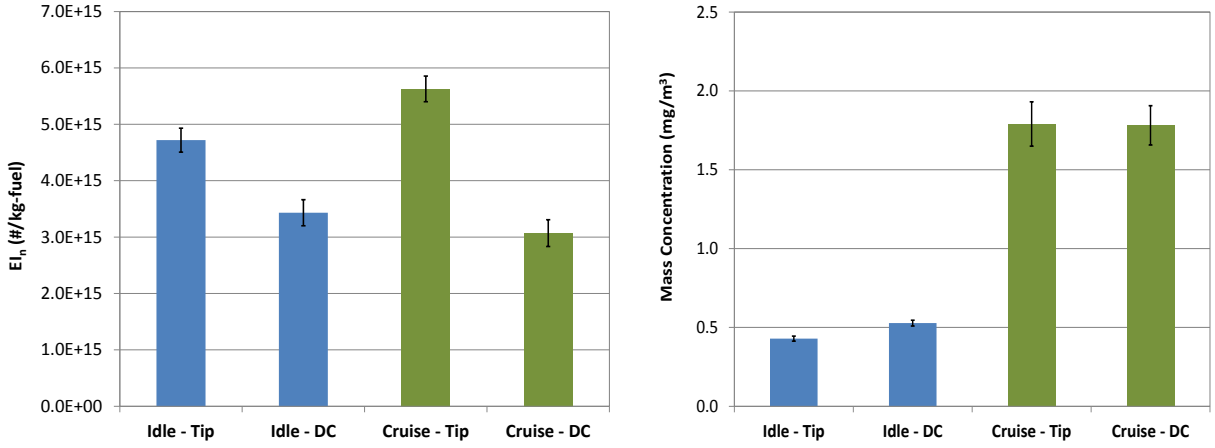

Figure 33. Comparison of EI_n and particle mass concentration between tip-diluted and DC nitrogen-diluted sample for the T63 engine (operated on JP-8) PM exhaust

7.1.2 Volatile PM Characterization – ARI

7.1.2.1 PM Volatile Mass and Size Measurements

As mentioned previously, to demonstrate volatile PM formation and volatile species condensation on soot particles from aircraft engine exhaust, the composition of the JP-8 fuel used was varied by adding either aromatic or sulfur-containing compounds. In the first case, aromatic compounds were added to the fuel to increase the fuel aromatic content from 11% to 25%, which is the specification maximum for jet fuel. In the second case, *tetrahydrothiophene* was added to the base fuel to increase its sulfur concentration to 3000 ppm (specification maximum of jet fuel), compared to the initial sulfur content of 200 ppm. Given the S(IV) to S(VI) conversion rate of 0.1-1% from jet engine combustion, this increase in sulfur content would significantly enhance the emission of sulfuric acid, which is considered one of the most important species for nuclei formation in the engine exhaust.

In this study, particle size distributions in vacuum aerodynamic diameter (D_{va}) were obtained via the C-ToF-AMS particle time-of-flight (PToF) measurements on non-refractory components. There were two volatile components detected in the C-ToF-AMS PToF measurements on the T63 engine exhaust: sulfate and organic (also referred to as organic carbon (OC)). From the obtained particle size distributions, the mass of sulfate and organic PM were determined by integrating over both soot and nucleation/growth modes via fitting to log-normal functions for each mode, as shown in Figures 34 and 35. The particle mode that peaks at 70 nm is the nuclei/growth mode, which is formed by volatile species that nucleate to form new particles and larger aerosols by coagulation/growth during cooling and dilution of the engine exhaust. The mode at 94 nm is the soot mode, of which the sulfate and organic volatile components can be detected by the C-ToF-AMS, while the refractory black carbon (BC) cannot be observed because the melting point of the BC (3500°C) is much higher than the vaporizer temperature of the AMS (~600°C). The figures were generated by fitting each of the size-resolved sulfate and organic mass concentrations with three log-normal curves (dash lines) and fixing the peak locations at 70 nm for nucleation/growth mode, 94 nm for soot mode, and 220 nm for ambient mode. The ambient mode is the result of the interaction of the plume with the existing ambient particles.

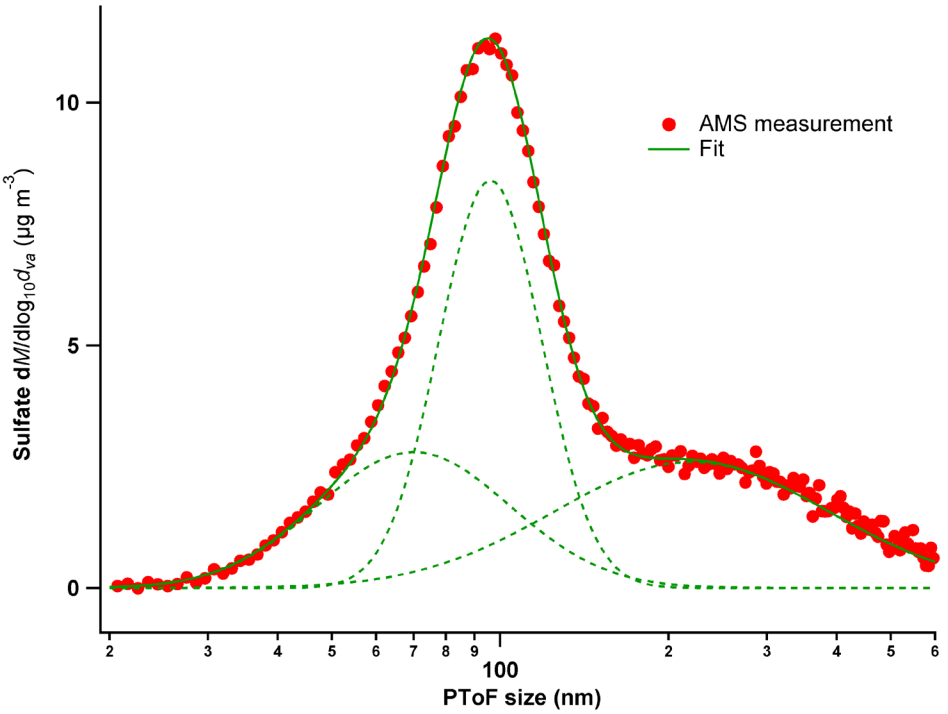

Figure 34. Particle size distribution of PM sulfate at idle with the high sulfur fuel

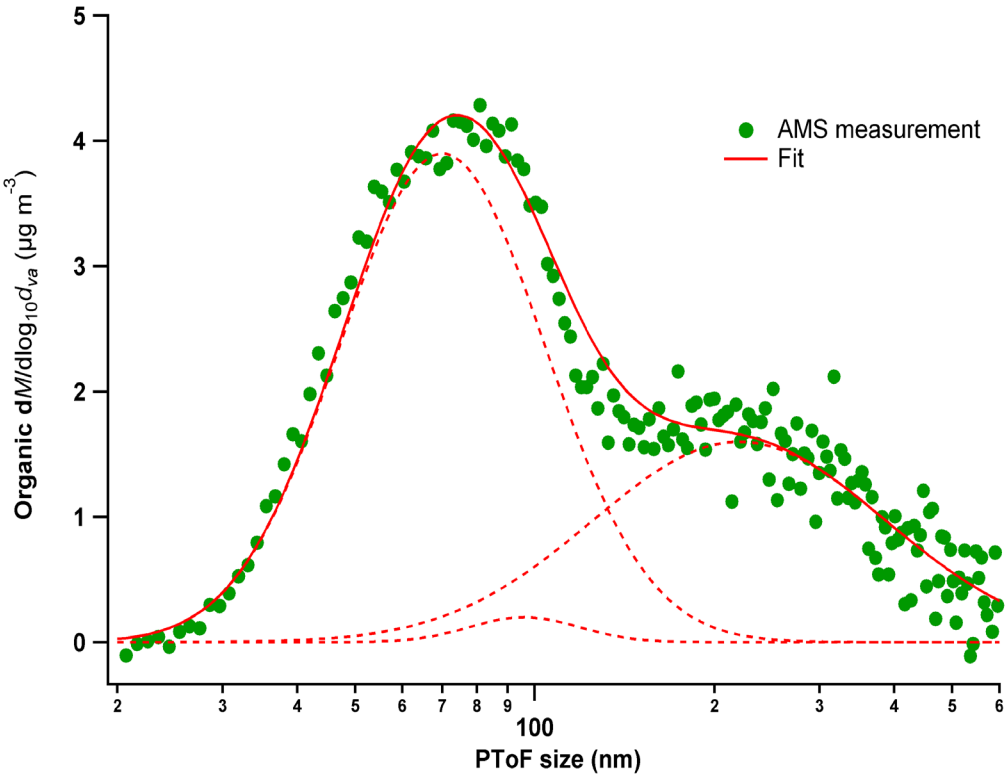

Figure 35. Particle size distribution of PM organic at idle with the high sulfur fuel

After determination of sulfate and organic volatile PM mass, their composition in each particle mode was calculated by dividing the mass of each component by the sum of PM organic and sulfate mass. This method eliminates interferences from ambient particles, which are not negligible as shown in the figures. This analysis also provides a more valid comparison between the plume and DC samples, which are both affected by ambient particles, with the CDP sample, which was diluted with particle-free nitrogen gas. The volatile PM composition in percentage for the T63 engine exhaust as determined from the C-ToF-AMS, are listed in Table 5. It is observed from the AMS measurements that at all engine powers and sampling conditions, there was a significant increase in PM sulfate emissions with the addition of sulfur to the fuel. For instance, in the engine exhaust plumes at cruise power condition, PM sulfate counts for 4% of the total volatile PM mass emissions with the baseline fuel, while it increased to 82% with the high sulfur fuel. Organic PM emission indices are shown for each engine condition and sampling method in Figure 36. As shown, at T63 engine cruise, adding sulfur increased the sulfate PM EI from 0.34 mg/kg_fuel to 59 mg/kg_fuel, a 173-fold increase. For the same power condition, adding aromatics only increased the volatile PM emission indices from 4.4 mg/kg fuel to 15.7 mg/kg fuel, a factor of 3.6. Interestingly, the high sulfur fuel also increased the detected organic PM EI, especially at idle. This is due to the higher sulfate concentration that generates increased nucleation particles, which efficiently scavenge organic species. Compared to the organic PM emissions from the T63 engine burning baseline fuel, the sulfate PM emissions were in many cases below detection limit and/or paricle size cut-off of the C-ToF-AMS instrument, due to the low sulfur concentration in the conventional JP-8 fuel.

Table 5. Volatile PM Composition

Fuel	**Power**	**Composition (%)**					
		Organic			**Sulfate**		
		Plume	DC1X	CDP1X	Plume	DC1X	CDP1X
JP-8	Idle	100	100 (0.91)	100 (0.93)	0	0	0
	Cruise	96	100 (0.93)	90 (0.98)	4	0	10
JP-8S	Idle	32	— (0.87)	— (0.90)	68	—	—
	Cruise	18	58 (0.86)	73 (0.96)	82	42	27
JP-8A	Idle	100	100 (0.97)	100 (0.84)	0	0	0
	Cruise	100	93 (0.98)	95 (0.98)	0	7	5

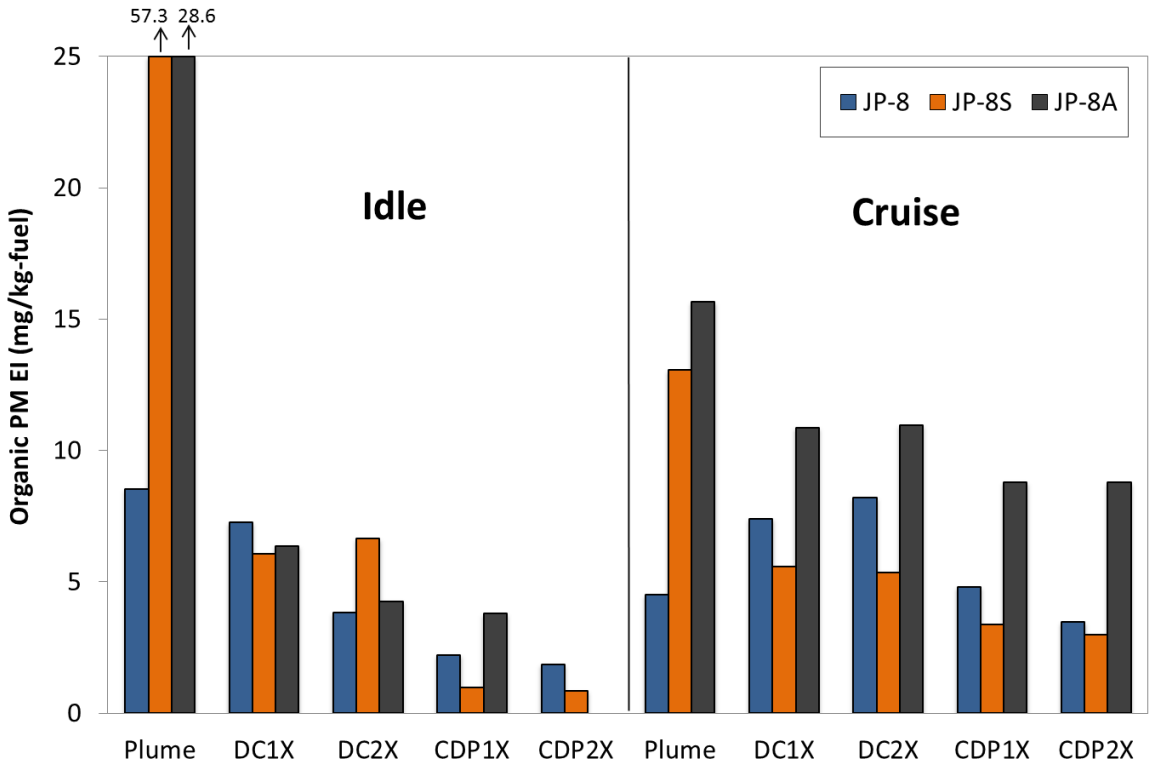

Figure 16. Organic PM EIs for different engine powers and probes

The CAPS PM_{ex} instrument measures particle light extinction at 635 nm. Although light extinction is not directly related to particle mass, since the aviation soot particle size is normally much smaller compared to the radiation wavelength (60 nm vs 635 nm in this case), the contribution of light scattering to the total extinction is usually small. Thus, the particle extinction measurement from the CAPS PM_{ex} in this study becomes a particle absorption measurement, which is linearly proportional to particle mass according to the Beer-Lambert law. In this study, we used the mass absorption coefficient of 6.5 m^2/g to calculate black carbon (BC) mass concentrations from the CAPS PM_{ex} measurements.

In addition to BC mass EIs, variation in OC/BC ratio was another critical parameter to assess in this demonstration. In Figure 37, significant differences in OC/BC at engine idle and cruise power except for the aromatic-enhanced fuel are demonstrated. At idle, the OC/BC ratios were 0.12 to 0.55, showing the significant contribution of organic PM to the total PM mass, while at cruise power, OC/BC ratios were normally less than 0.05. For the aromatic-enhanced fuel (JP-8A), the aromatics dramatically increased soot formation during engine combustion, but provided less influence on the volatile organic emissions. Thus the OC/BC ratios were noticeably reduced compared to the conventional JP-8 fuel. Throughout the measurements, the plume sample typically measured higher OC/BC ratios than the DC and CDP. This is partly attributed to uncharacterized flow pattern in the plume, and differences in exhaust sample residence times and mixing with air in the plume, compared to processes in the DC and CDP. This effect was more pronounced at idle power.

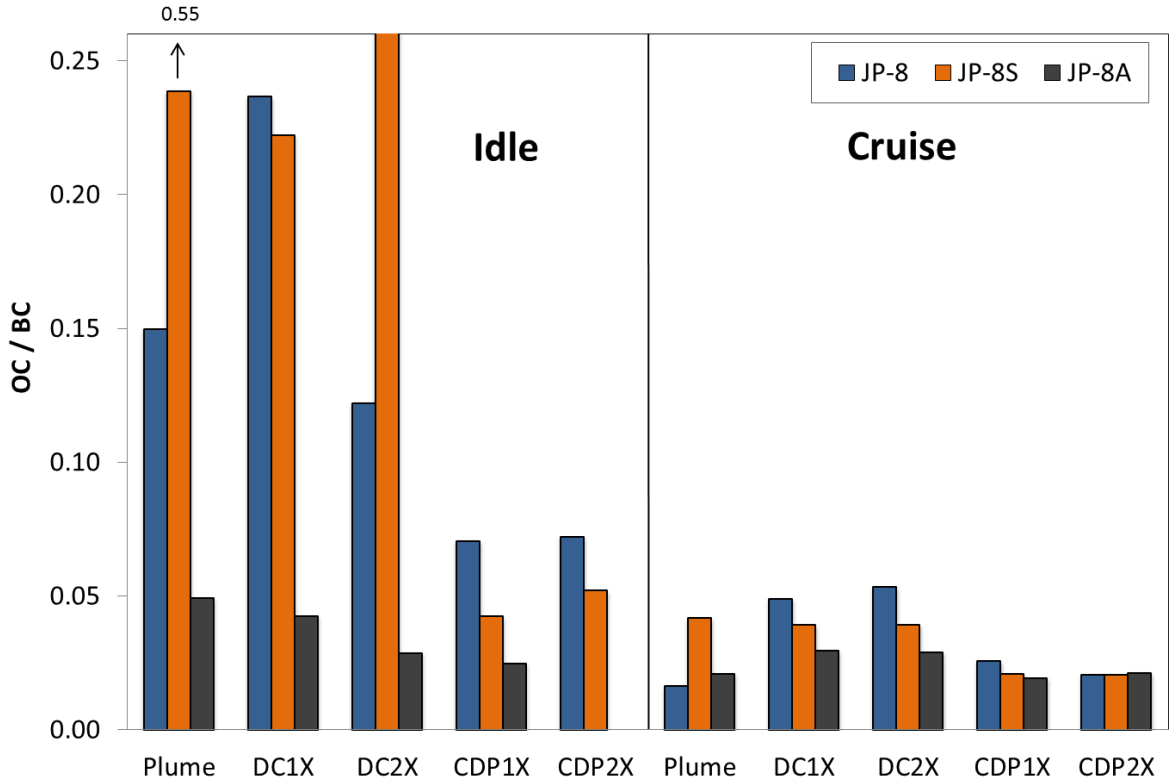

Figure 37. OC/BC ratios for different engine powers and probes

7.1.3 PM and Gaseous Emissions Characterization from Plume, DC and CDP – EPA

7.1.3.1 Gaseous Pollutants

Gaseous emissions data grouped by pollutant, fuel type, and power level are shown in Figures 38, 39, and 40. The SO_2 data for tests with the JP-8S fuel were plotted separately due to the higher EI relative the other two fuels. The theoretically calculated EIs of SO_2 were 80 mg/kg for JP-8 and JP-8A, and 6 g/kg for JP-8S. Measured SO_2 concentrations were generally in trace (ppbv) levels for the JP-8 and JP-8A fuels which contained very little sulfur. Since SO_2 is a reactive gas which is soluble in water, it is often difficult to measure accurately in such trace quantities, which contributes to high data scatter. It was observed that the DC generally produced higher SO_2 EIs than the plume and CDP for all fuel types at idle. The largest difference observed between the plume and the DC was for JP-8A fuel which was a factor of ~ 2. For JP-8S at idle, however, the DC EI values were comparable to those from the plume. For SO_2 at cruise power, the DC produced EIs relatively close to those observed at the first plume sampling point, at least for the JP-8S and JP-8A fuels. For the JP-8S fuel, again all SO_2 EIs at cruise were comparable.

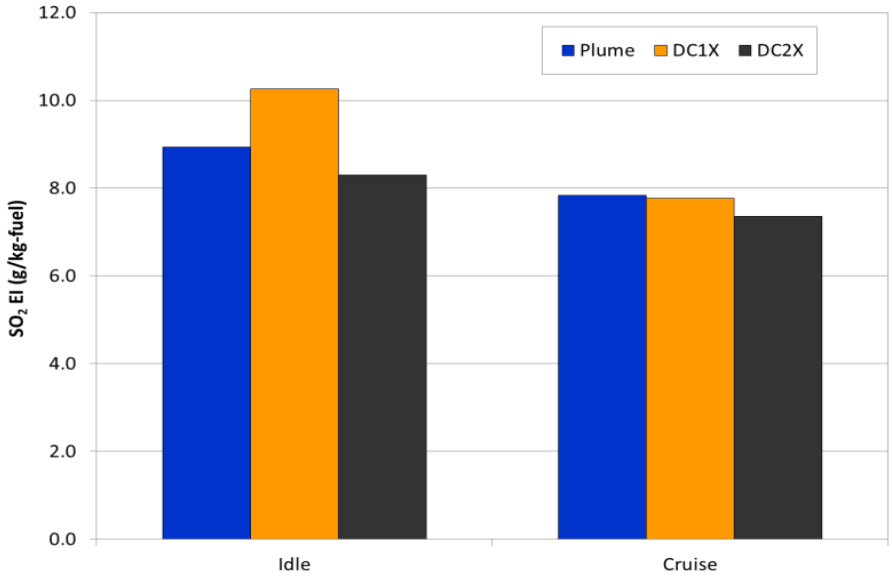

Figure 38. T63 Engine SO_2 emission indices for sulfur-doped JP-8 (JP-8S) fuel

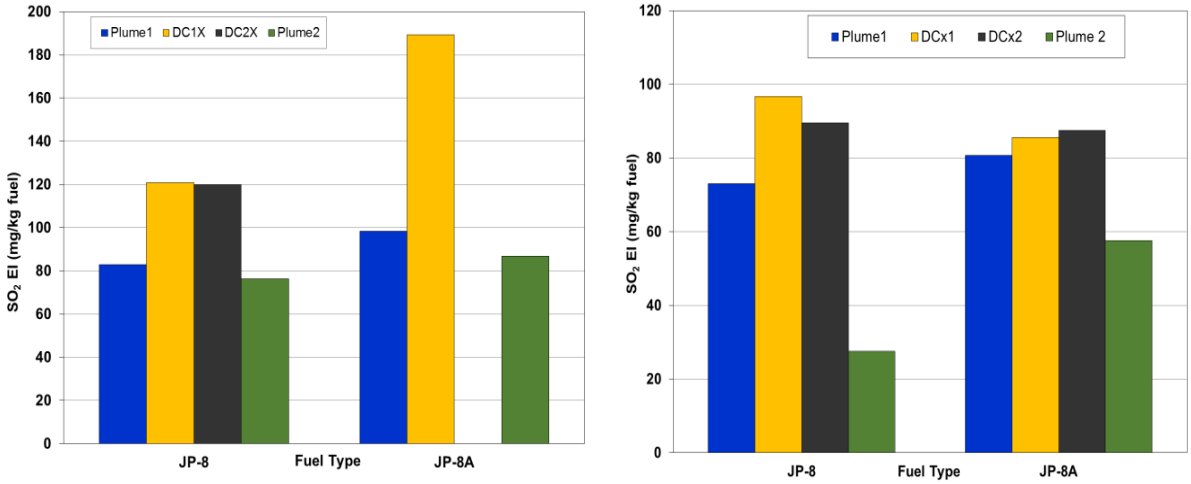

Figure 39. SO_2 emission indices by fuel type for idle and cruise power.

The total hydrocarbon (THC) emissions data are plotted in Figure 40. For THC at idle, both condensation devices appear to provide EIs in the same general range as the plume measurements with two notable exceptions for the DC. For cruise, however, the results were more scattered. The best agreement between the two dilution systems and the plume at cruise was for JP-8 with the DC2X operating condition consistently showing EIs 25-50% higher for all fuel types. The CDP EIs for the JP-8S and JP-8A fuels were also found to be exceptionally low for the JP-8S and JP-8A fuels compared to the plume with differences over a factor of 30 existing between the CDP and plume for JP-8A.

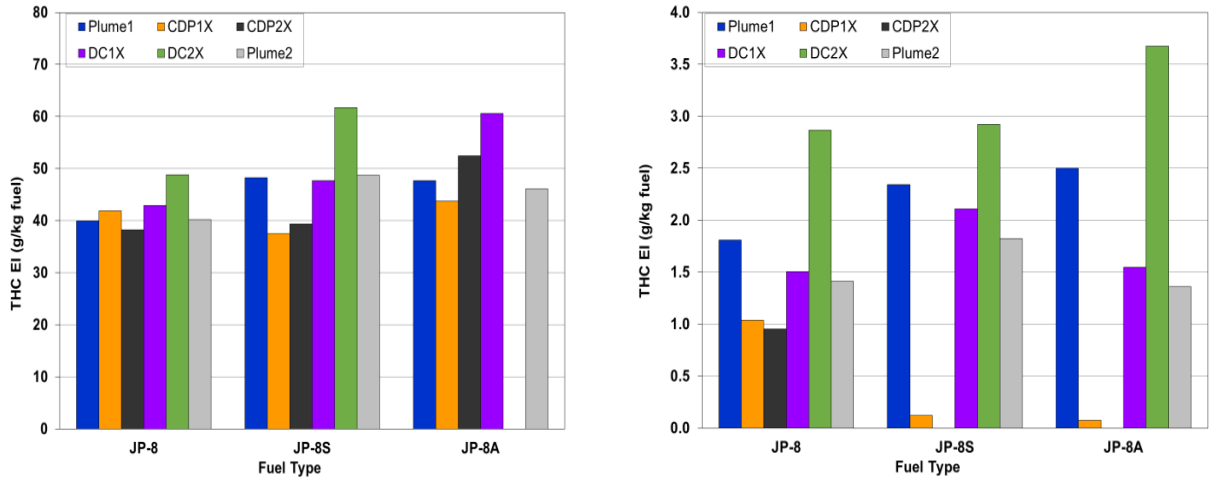

Figure 40. THC emission indices at idle (a) and cruise (b) by fuel type

7.1.3.2 Black and Elemental Carbon Measurements

Black carbon (BC) mass concentrations were measured in the plume using the SuperMAAP. BC EIs were only calculated for test points where concurrent sampling and CO_2 measurements were made. Excellent agreement was obtained between the BC measurements made at the two idle and cruise points for each fuel type. BC EI were approximately 60 and 261 mg/kg fuel for idle and cruise conditions respectively for both JP-8 and JP-8S fuels. As expected, fuel sulfur content did not impact BC emissions. Also as anticipated, significant increases in BC EI (4.6X and 2.3X for idle and cruise respectively) were observed for the JP-8A fuel relative to JP-8 and JP-8S. Unfortunately, BC measurements in the CDP and DC were not acquired due to the relatively small diameter sample lines from these devices and inadequate flow to the SuperMAAP instrument.

Elemental carbon (EC) mass concentration data were obtained using a Sunset Semi-Continuous ECOC Analyzer. This analyzer collects a soot sample on a small quartz filter and then undergoes a rather lengthy oven temperature ramp process using multiple carrier gases as described in the NIOSH 5040 method [47]. Due to the long analysis period, only the 1X dilution condition was sampled for both the DC and CDP with their analysis cycle conducted during the 2X dilution tests. Organic carbon (OC) was also obtained by this method, but could not be corrected for gas phase artifacts which required a second instrument and additional sample flow both of which were not available during the study.

The EC emission indices are shown in Figure 41 for both idle and cruise power conditions. At idle power, scatter in the data was significant with the best agreement observed for the JP-8 fuel where the two dilution systems provided EIs that were within ±50% of the plume EI. For the other two fuels, the DC and CDP both produced much lower EIs as compared to the plume.

For the tests at cruise power, the EC EIs for the DC and CDP were found to be consistent with each other but lower than those for plume. This is especially the case for JP-8 and JP-8S fuel which were within about 55-80% of the plume EIs. The largest spread in EC EI was observed between the DC/CDP and the plume for the JP-8S fuel.

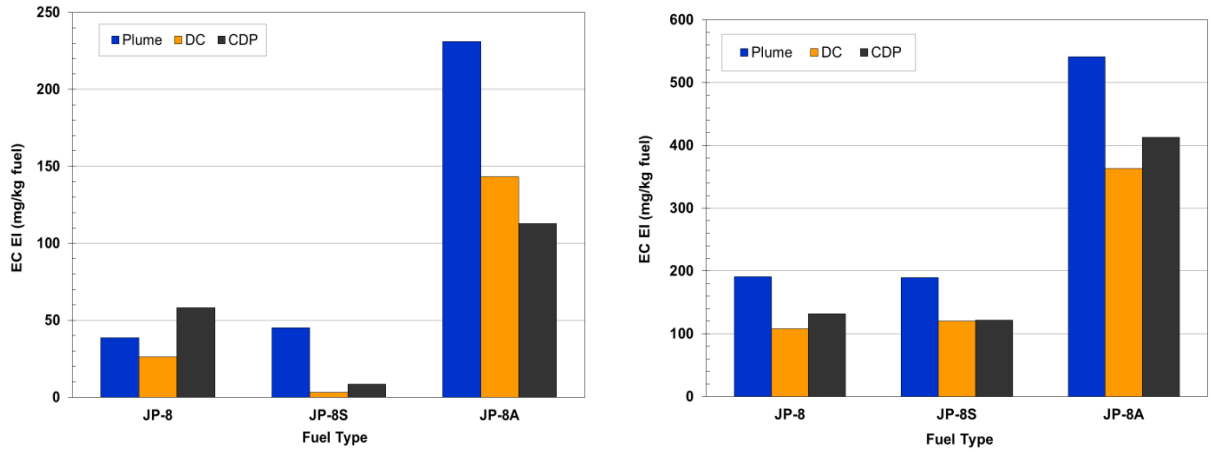

(a) (b)

Figure 41. Elemental carbon (NIOSH 5040) EIs at idle (a) and cruise (b) by fuel type

Comparisons between the SuperMAAP BC and the NIOSH EC for samples collected in the plume are shown in Figure 42. As illustrated, excellent agreement was obtained between the two methods.

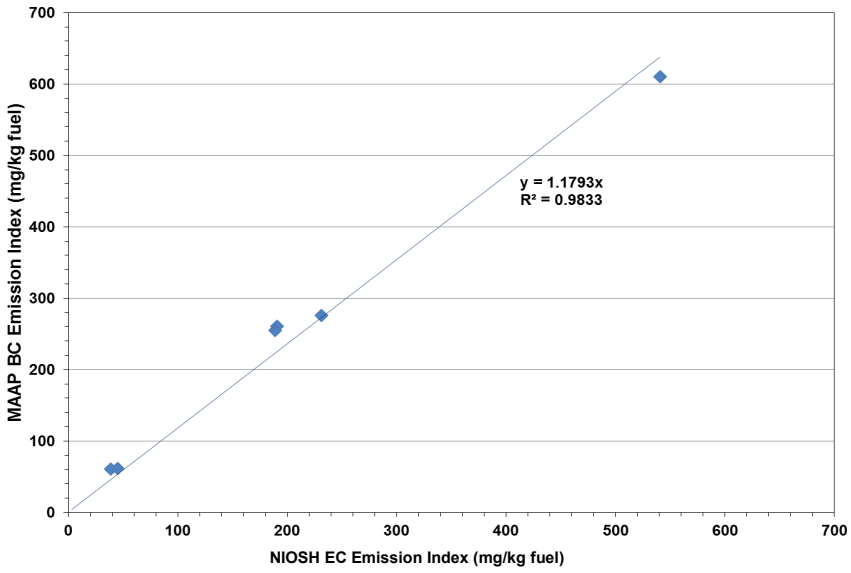

Figure 42. Comparison of NIOSH 5040 EC to SuperMAAP BC determined in the plume

7.1.3.3 Total Mass and Sulfate Measurements

Filter samples were collected at all test points and conditions during the T63 demonstration. Upon recovery of the filters, it was discovered that both multi-filter samplers had been contaminated by small gravel probably from the ground around test site. The small pieces of gravel were easily removed without compromising the filters but unfortunately this contamination created very high mass loadings and low sulfate values during analysis. For this reason, no filter data can be reported here. When the multi-filter samplers were eventually disassembled after

completion of the program, gravel was found throughout both systems and a rigorous cleaning had to be implemented to remove the contamination found.

7.1.4 VPS Performance Assessment - ORNL

Tests were conducted to evaluate the performance of the VPS in comparison to the PMP VPR (evaporation-condensation) with T63 engine exhaust. Figures 43 and 44 show the lognormal fit of the averaged particle size distribution (PSD) for T63 engine particles after conditioning through the VPS and PMP devices at different power conditions with JP-8 fuel. The peak size shift of the PSD for the VPS is not dramatic, but the one for the PMP VPR (Figure 43b) shows an 8 nm left shift toward smaller size. Both VPS and PMP were able to reduce the number concentration of particles produced at idle and cruise conditions for engine operation with all fuels. When particles of mobility diameter smaller than or equal to 15 nm were counted and compared to the incoming particles, the removal efficiency for both PMP and VPS in all engine conditions were statistically 100% (Figure 45).

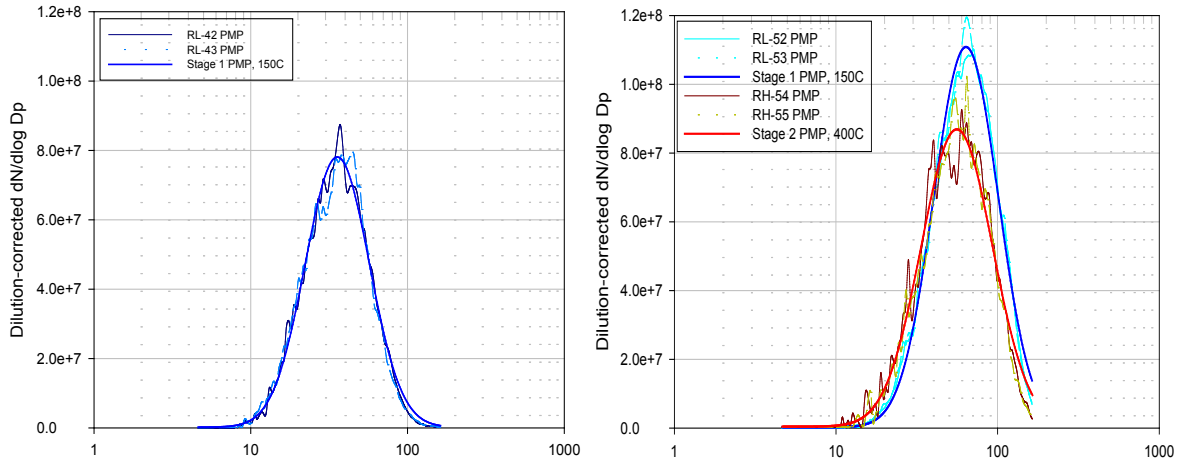

(a) (b)

Figure 43. Lognormal fit of averaged particle size distribution for the T63 engine at: (a) idle and (b) cruise conditions measured after conditioning with the PMP VPR

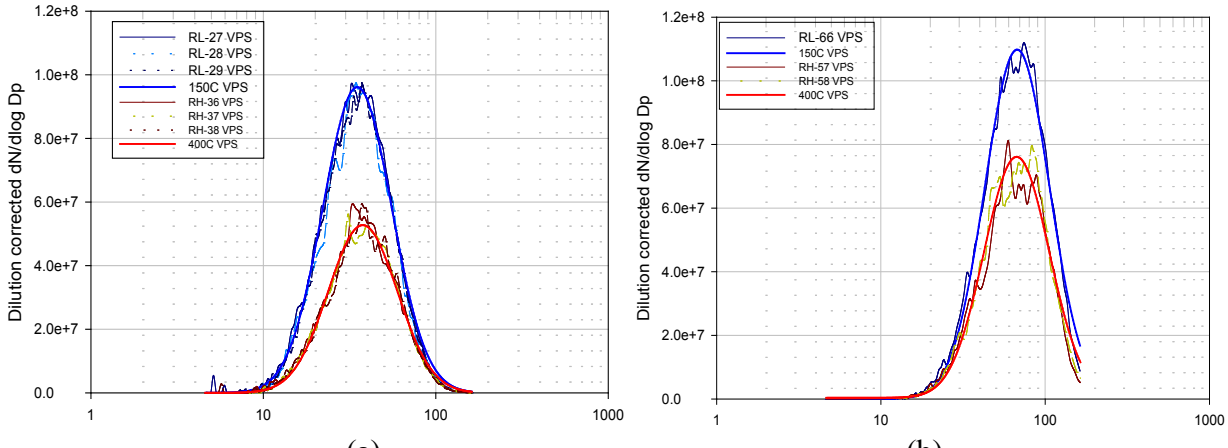

(a) (b)

Figure 44. Lognormal fit of averaged particle size distribution for the T63 engine at: (a) idle and (b) cruise conditions measured after conditioning with the VPS

The results suggest that VPS met the program criteria and performed successfully in removing virtually all turbine engine particles smaller than 15 nm, which aerosol population is generally considered to be volatile. However, data to prove that all particles smaller than 15 nm are volatile are lacking. Verifying that particles are non-volatile can be performed by microscopic imaging, spectroscopic, and nano-indentation tests. The thermographic test used in this program is a method of validating the particles are volatile but it is not definitive.

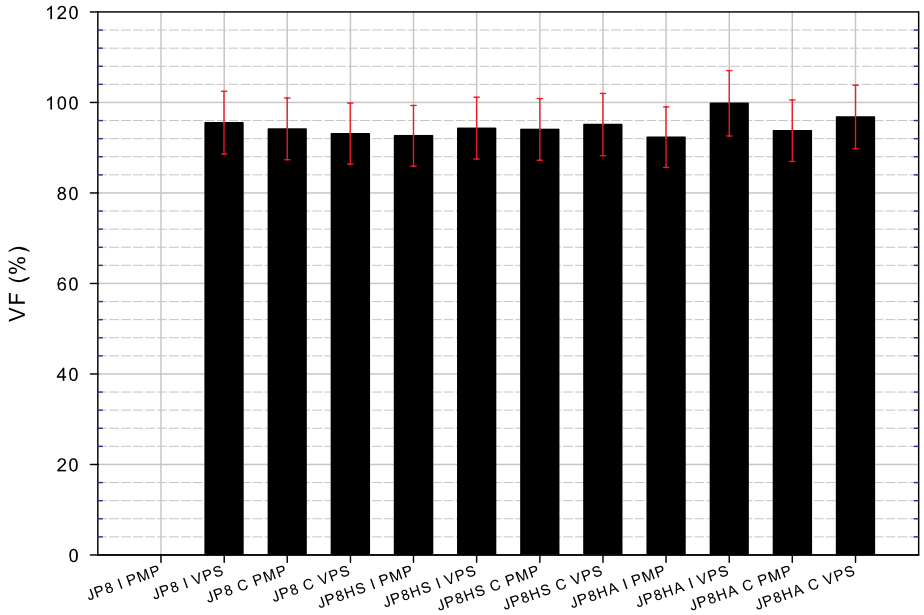

Figure 45. Percentage of particles smaller than 15 nm removed by VPS and PMP VPR at studied T63 engine conditions

7.2 Demonstration on C-17 (PW-F117) Engine

Test conditions for the demonstration of the devices on the C-17 aircraft (PW-F117 engine) were shown in Table 2. The demonstration was conducted with one fuel, a Jet A plus military additives. The fuel was an average jet fuel in terms of physical and chemical properties with very low sulfur (20 ppmw). Low engine power settings were selected for the demonstration as these are the most prone to high volatile PM formation due to the higher concentration of organics (unburned hydrocarbons) in the exhaust. Raw samples collected from the engine exit through four gas probes were transferred through heated sampling lines at 150°C to the Dekati ejector ("non-volatile" PM), DC, CDP and gas emissions instrumentation. The total dilution ratio (DR) (ejector plus secondary) for the non-volatile PM sample was between 6:1 – 20:1 for most cases. For the volatile PM samples, the DR in the condensation devices were controlled to match the sample dilution measured in the plume (20 m) probe. These varied based on engine power as follows: DR=~32:1 at idle, DR= ~25:1 for 20% max thrust and DR= ~21:1 for 33% max thrust. The DR in the CDP was varied by controlling the total nitrogen dilution flow, while in the DC the secondary dilution (air) was adjusted while maintaining constant nitrogen flow to the ejector.

Due to the limited aircraft availability (445th Airlift Wing reserve unit mission commitments), this demonstration was limited to one full day of testing. Although a second test day was planned, adverse weather (i.e., strong winds, rain, thunderstorms) limited the demonstration to only a few hours on day two. Unfortunately, this severely constrained the number of tests and variables considered, which hindered our ability to fully demonstrate the devices. Potential sample leaks through a sampling system fitting for tests at engine idle, very likely affected the magnitude of the measured PM parameters; however, it is believed that it did not impact the trends of the data and conclusions of the demonstration. Test results of the shortened demonstration are discussed in the following sections.

7.2.1 Emissions Measurements at Plume, DC, CDP and Engine Exit - AFRL/UDRI

7.2.1.1 Gaseous Emissions

In order to have a valid comparison between the PM characteristics at the plume and the condensation devices, a representative engine core sample must be collected at the engine exit plane. Figure 46 displays the CO and NO_x emission indices (EI) for the demonstration engine at similar conditions compared to data from the ICAO Databank for the commercial variant (PW2040) and a separate field campaign. As shown, there is very good agreement between the data sets, which increases confidence that that the probes were capturing a representative core sample without diluting with the fan/bypass air. The present tests showed that even at the idle setting, the unburned hydrocarbons were extremely low (<65 ppm). The low organic volatiles combined with the atypical low sulfur fuel, produced very low concentration of volatile species, which reduced the potential for volatile PM formation. Nonetheless, as discussed in the next sections, sufficient volatile PM was produced for assessment of the condensation devices.

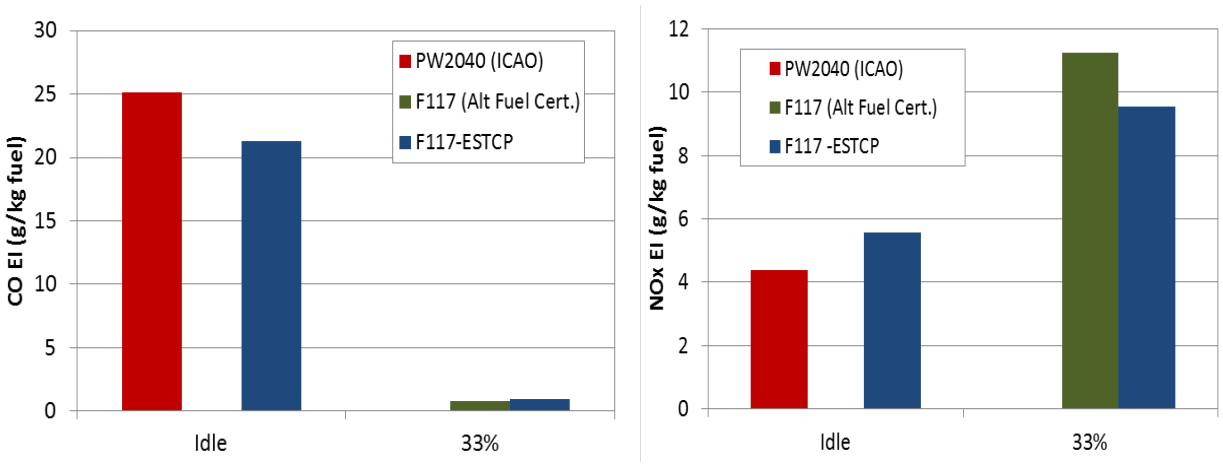

Figure 46. Comparison of CO and NO_x emissions between PW-F117 engines and commercial variant engine (data from ICAO Databank) at idle and 33% max thrust

7.2.1.2 Comparison of PM Concentration and Size between Plume, DC and CDP

Particle size distributions for idle and 33% max engine thrust conditions are shown in Figure 47. At idle, the plume sample shows significant increases in particle concentrations compared to tip-diluted samples. A shift in the size distribution to smaller mean particle sizes is also observed. This is evidence of formation of volatile particles in the plume. Comparisons of the DC to the tip-diluted sample, also shows increases in particle number and shift to smaller particles but at a much lesser degree. These results are consistent with those observed in the T63 demonstration, which also showed increases in particle concentrations with the DC, but significantly lower than in the plume. The CDP conditioned sample had slightly fewer particles than the tip-diluted sample and slight shift to smaller diameters. This could be related to increased particle losses in the CDP.

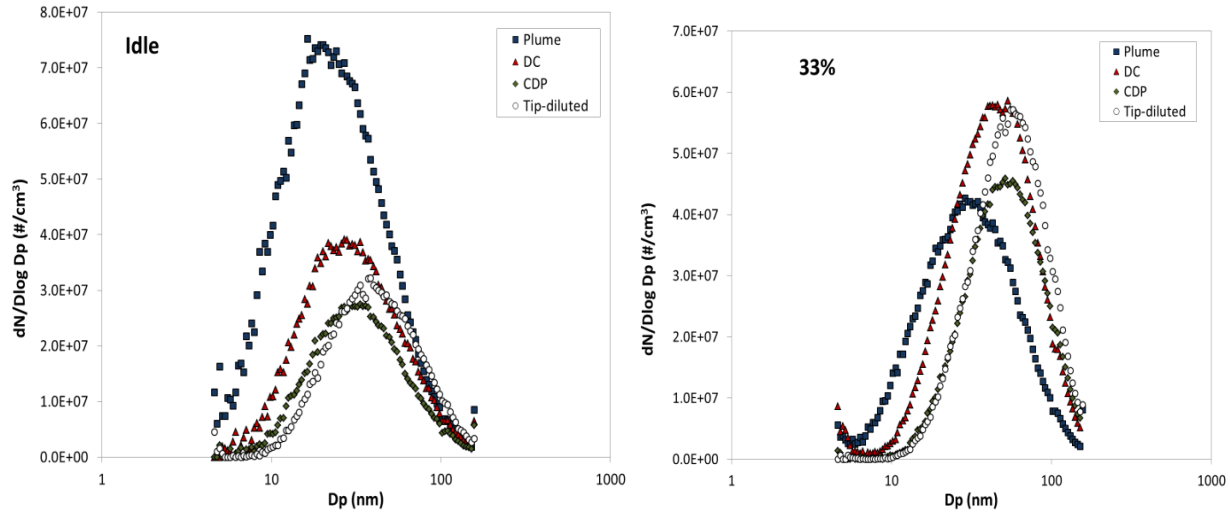

Figure 47. Particle size distribution for PW-F117 engine PM exhaust at idle and 33% max thrust operation sampled at engine exit with tip-diluted probe, through DC, CDP and at plume.

At the 33% condition, the particle distribution shifted to smaller sizes for the plume compared to the tip-diluted sample, however, the concentrations were significantly lower particularly for the larger soot particles. This behavior was consistent for repeated tests, but not fully understood. The DC and tip-diluted sample size distributions were very similar, which could be due to the lower concentration of volatile species present to form volatile PM. However, it is not clear why there were larger PM concentrations for the DC compared to the plume. Particles from the CDP had geometric mean diameter similar to the tip-diluted sample, but again, at lower concentrations.

Figure 48 shows the concentration of nuclei particles (7-23 nm diameter) for the four sampling techniques employed during the demonstration. Assuming that the nuclei size particles are mostly volatile PM, the formation of these in the plume is evident especially at engine idle. Increased engine power operation reduced the concentration of organic species (volatile PM precursors) and the difference between volatile and non-volatile (tip-diluted) PM. It is observed that the DC also promoted the formation of volatile PM with increases 4.3X at idle compared to those observed with tip-dilution; however, consistent with the T63 demonstration, the concentration of particles was significantly lower than those formed in the plume (13X). Even lower concentrations were observed with the CDP. **Therefore, although there is evidence of volatile PM formation, neither condensation device met the success criteria of an order of magnitude increase in the volatile PM concentrations relative to tip-dilution as stated in Table 1.**

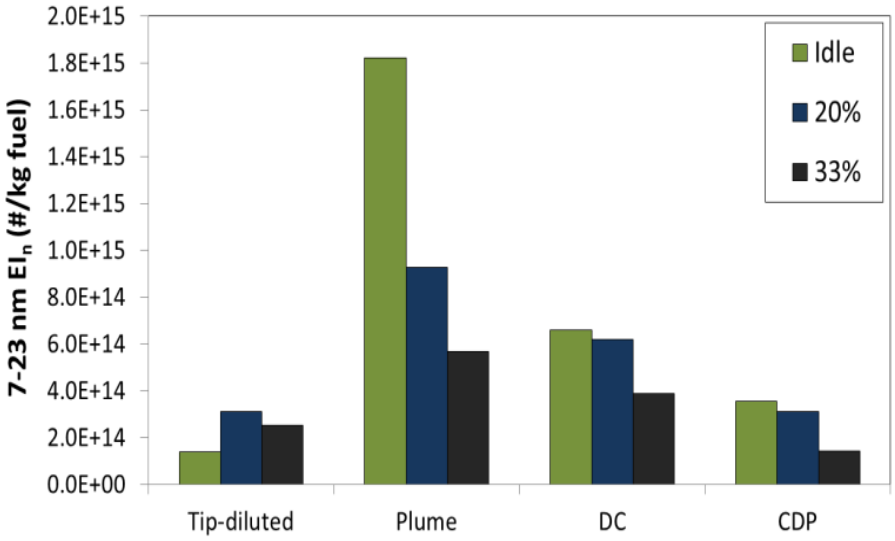

Figure 48. Particle Number EI for "volatile" PM based on nuclei size particles measured with the SMPS

Figure 49 shows the mean particle diameter data for samples using the four sampling techniques. As expected, the mean particle size decreased in the plume and condensation devices relative to tip-diluted samples due to the formation of new nuclei size particles. The mean diameter at idle for the DC was within 26% of that of the plume, which is slightly above the 25% success criteria. The mean diameter for the 20% and 33% max thrust conditions and for the CDP also exceeded the set criteria.

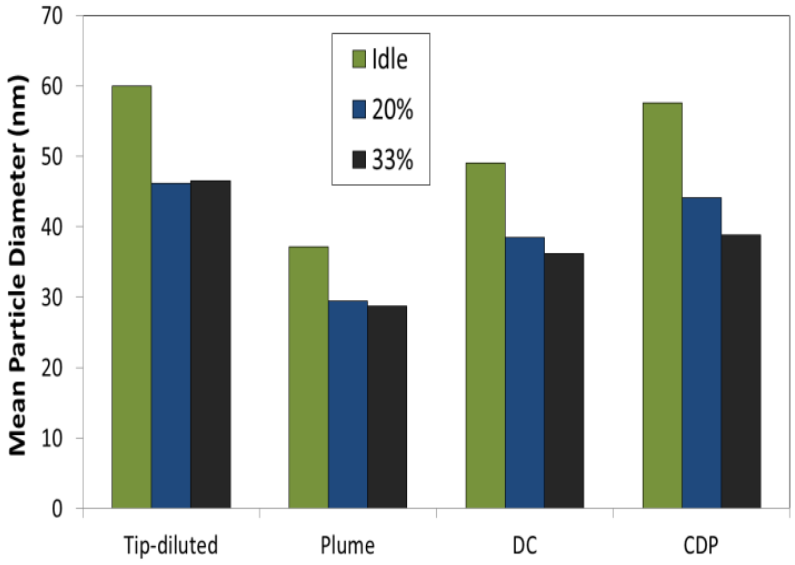

Figure 49. Mean particle diameter for PW-F117 engine PM exhaust sampled with tip-diluted probe, through DC, CDP and plume

BC was measure using a Laser Induced Incandescence (LII) instrument. Data for the BC LII mass measurements at the plume and condensation devices are shown in Figure 50. Excellent agreement in BC PM mass was observed for the DC at the two lower power conditions; however, consistent with particle number data, the DC produce much higher PM than the plume at 33% max thrust power. Unfortunately, time constraints limited the data collected for the CDP. Agreement of BC data was expected as the volatile PM should not impact the non-volatile BC PM mass as measured with the LII.

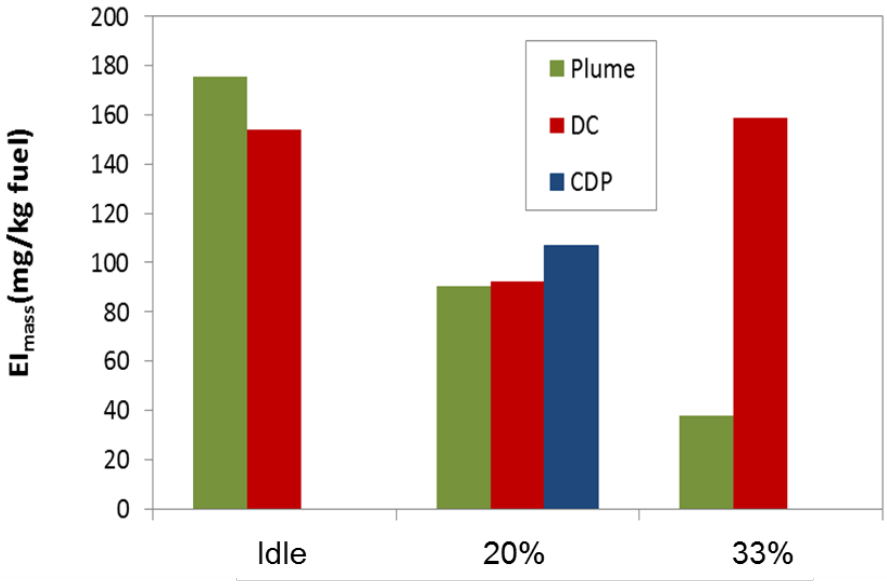

Figure 50. PM Mass EI for PW-F117 engine PM exhaust sampled through DC, CDP and plume measured with LII

7.2.2 Volatile PM Chemical and Physical Characterization - ARI

ARI characterized volatile PM with a C-ToF-AMS, which measures mass spectrum from non-refractory PM composition and determines mass concentration and particle size distribution in vacuum aerodynamic diameter (D_{va}); and an ESCOM device, which simultaneously detects CO_2 concentration, particle count, and light extinction.

Based on the C-ToF-AMS and ESCOM measurements, emission indices of volatile PM mass, particle number, and BC mass were calculated using equations described in section 5.0.5. Results from the MCPC and CO_2 gas analyzer led to the determination of particle number emission index, EI_n. The EI_n represents particle emissions contributed by both the newly formed volatile particles (nucleation/growth mode) in the engine exhaust or condensation devices and the black carbon soot particles (soot mode) from engine combustion. As shown in Figure 51, the determined EI_n at the three power conditions and sampling techniques are similar, all around $1x10^{15}$ particle/kg fuel. For instance, for the plume probe the EI_n was 1.1×10^{15} particle/ kg_fuel at idle, 0.7×10^{15} particle/ kg_fuel at 20% thrust, and 0.9×10^{15} particle/ kg_fuel at 33% thrust. On the other hand, EI_n from both DC and CDP increased with engine power by about 140% from idle to 33% thrust, as demonstrated in Figure 51. It was determined from the C-ToF-AMS measurements that there is significant contribution of engine lubrication oil to volatile PM emissions when sampling from the plume. Unlike the mass spectra of n-alkanes such as n-decane, the mass spectra of lubricant oils show significantly different fragment patterns at the mass range above m/z = 57, which have been used to identify and quantify them from engine exhaust plumes. It was determined that more than 90% of the PM organics from the plume at idle, 20%, and 33% thrust was lubrication oil, which is also identified as Mobile II lubrication oil [48,49].

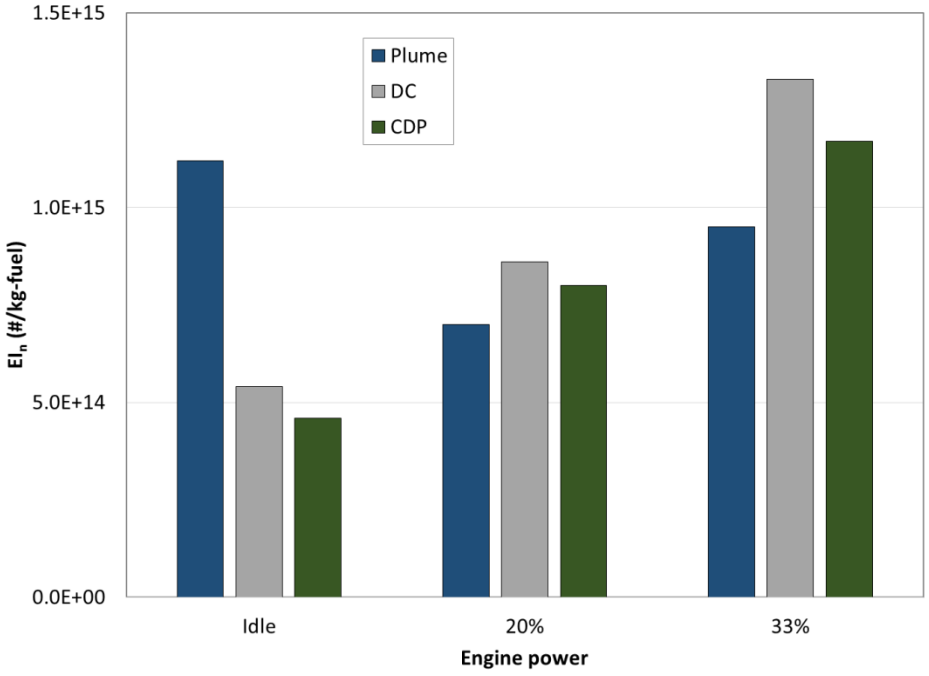

Figure 21. PW-F117 engine particle number emission index measured using the ESCOM for the tested power settings and sampling methods

After correcting the contribution from lubrication oil, it was observed that organic PM composition accounted for a very small portion of total PM mass, as demonstrated in Figure 52 indicating that this engine produced very low hydrocarbon emissions even at the idle setting. This is consistent with the gaseous measurements by AFRL/UDRI. As to the PM organic emissions, shown in Figure 53, the organic PM EI at engine idle condition was 2.46 mg/kg_fuel for the plume sample, 2.60 mg/kg_fuel for DC and 1.80 mg/kg_fuel for CDP. These values represent a difference of +6% and -27%, respectively relative to the plume sample, which are close to the instrument experimental uncertainty. Therefore, the organic PM EI appeared insensitive to the sampling methods used in this study. In addition, the engine PM organic emissions were found to vary only modestly with engine power in this study. For instance, organic PM EI from the probe was 2.46 mg/kg_fuel at idle, 1.51 mg/kg_fuel at 20% thrust, and 3.50 mg/kg-fuel at 33% thrust. Both DC and CDP showed modestly higher values than the plume at higher engine power conditions.

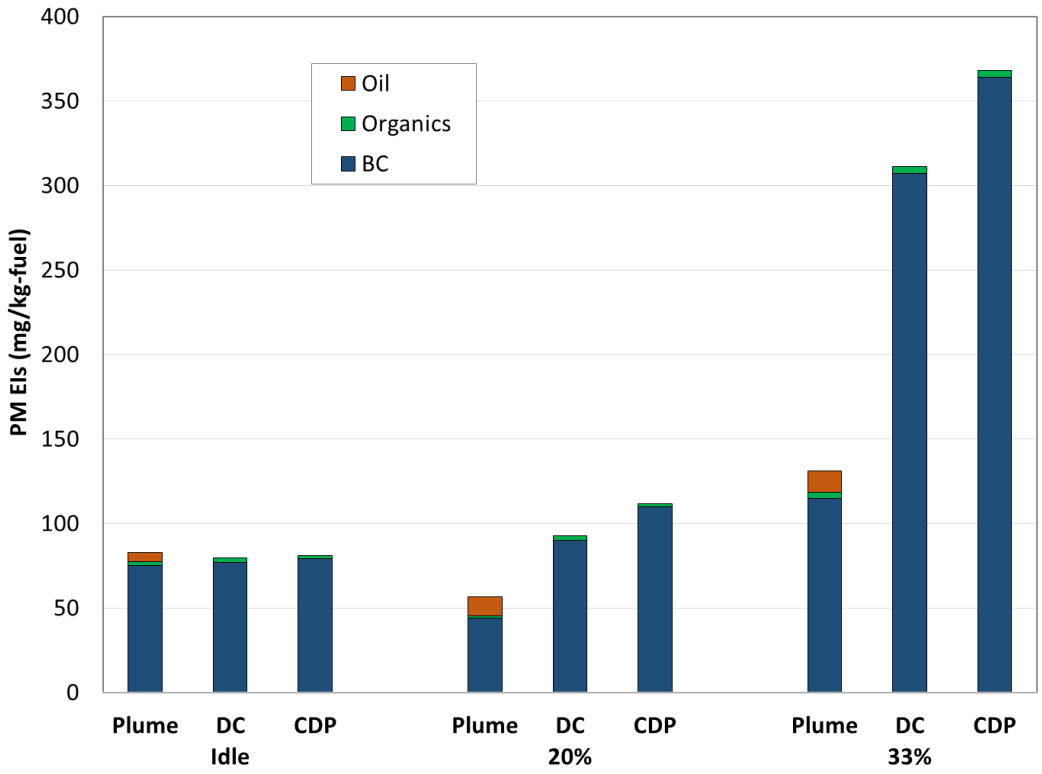

Figure 52. Contributions from lubrication oil, organics, and black carbon to total PM mass emission index

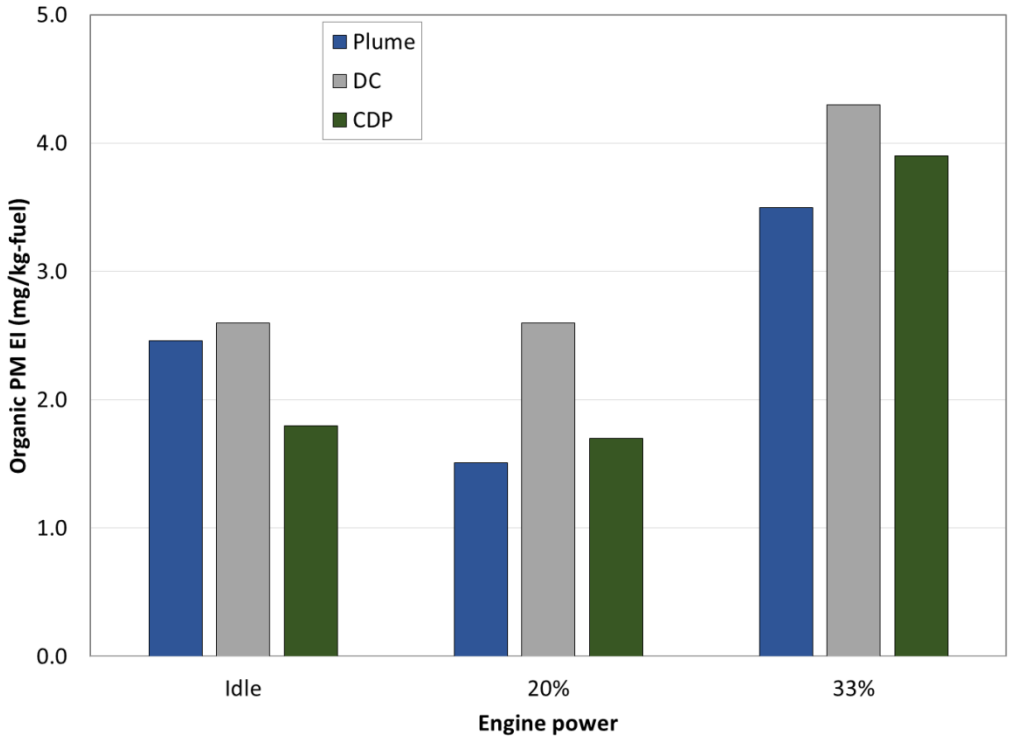

Figure 53. PM organic emission index after correction on lubrication oil contribution

7.2.3 Gas Phase Organics Measurements – MSU

A proton transfer reaction mass spectrometer (PTR-MS) instrument, as described previously, was used by MSU for the measurement of selected gas phase organics from the plume and condensation devices, which included: formaldehyde, methanol, acetaldehyde, the sum of acetone + propanal + glyoxal, benzene, toluene, C_2-benzenes, C_3-benzenes and naphthalene. Isomeric and isobaric compounds which cannot be separated by the quadrupole mass spectrometer are reported as sums. The C_2-benzenes represent the sum of three xylene isomers, ethyl benzene and benzaldehyde, whereas the C_3-benzenes represent the sum of C_9H_{12} and C_8H_8O isomers. Figures 54 and 55 show plots of compound EIs a function of engine power for the three different sampling techniques. The error bars reflect the variability in the measured concentrations, which reflects changes due to dilution, source variations as well as instrumental variability. Thus, the error bars do not necessarily reflect the true uncertainty but are useful when comparing data collected for different compounds on the same probe.

Figures 54 and 55 show comparisons of compound EIs a function of engine power for the three different sample probes: 20-meter plume probe, DC and CDP. Several features stand out in these figures.

- The EIs are the greatest at the lowest engine power condition (idle).
- At idle, the EIs measured on the 20-meter plume probe are significantly higher than those observed for the DC or CDP probes.
- Except for methanol and the sum of acetone + propanal + glyoxal, the EIs measured on the DC and CDP probes appear to be similar across all of the test conditions.

As anticipated the emission indices for all the components shown in Figures 54 and 55 exhibit an inverse power dependence [50, 51] where they are highest at the lowest power condition (idle) with significantly lower values at the higher engine powers. Several of the components, methanol and the sum of acetone + propanal + glyoxal, appear to have a different power dependence, but this is an artifact in the measurement. Acetone and methanol both have significant concentrations in the ambient air and their presence in the DC and the 20-meter plume probes affects the reported emissions. While it is recognized that this ambient influence must be removed to have a measure of the true emission from engine, no correction was made due to the large ambient variability observed during the testing event. It is assumed that EIs for methanol and the

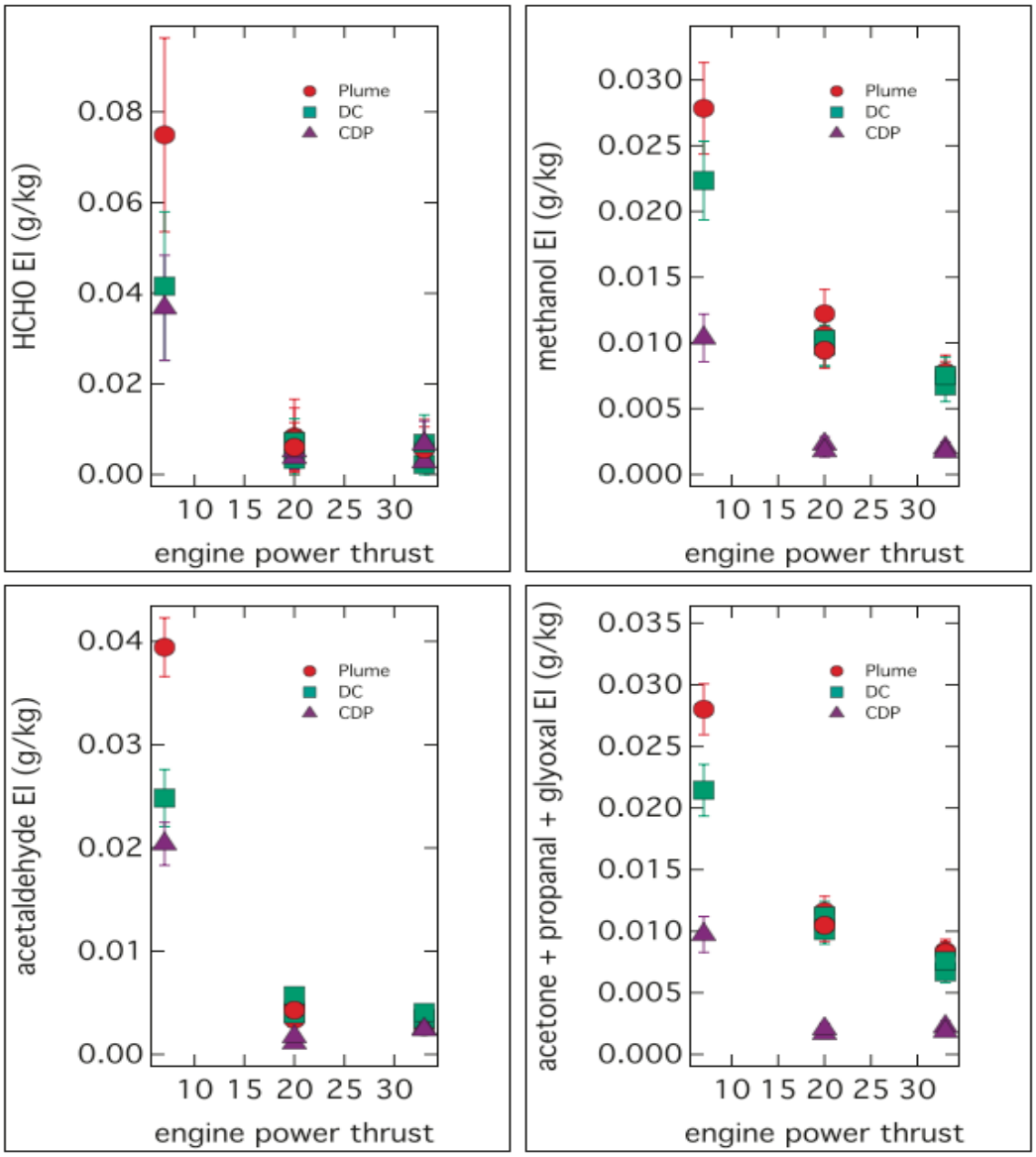

Figure 54. Gas phase component emission index as a function engine power and sampling methodology

sum of acetone + propanal + glyoxal are better represented by the data determined on the CDP (since ambient air is not used for conditioning in this device). For the 20-meter plume probe and the DC, a first-order correction can be made for the ambient contribution by subtracting the EI measured at the highest power, where essentially all of methanol or acetone originates from the dilution air, from the EIs measured at idle and 20% rated thrust. It is more challenging to reconcile why the EIs measured at idle on the 20 m plume probe are elevated with

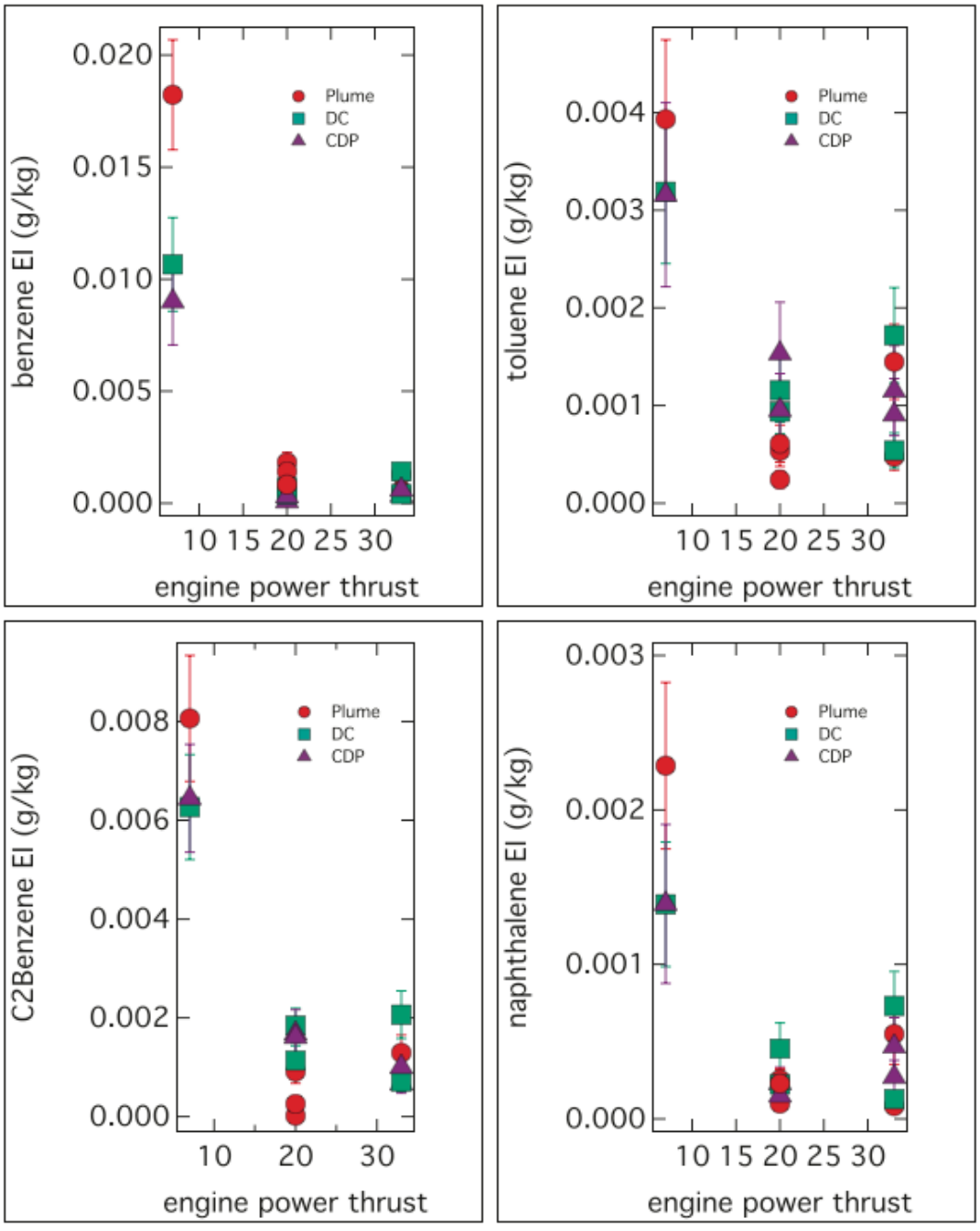

Figure 55. Aromatics emission index as a function engine power and sampling methodology

respect to those taken on the DC and CDP probes. It is noted that this difference in the samples appears to be restricted to this single test point. The simplest explanation for this observation is that there was a leak in the sample line that delivered the engine exhaust to the condensation devices. This leak would allow the exhaust to be diluted prior to entering the devices leading to lower apparent EIs.

A main objective of the project was to examine to what extent, if any, the gas phase organic composition varied between the different sampling approaches. Based on this very limited set of measurements, aside from the ambient effects described above, it appears that the high volatility gas phase organic composition is approximately uniform across all the three sampling techniques. An important result, not immediately apparent from data presented in Figures 54 and 55, is that the C-17 engine has very low high volatility gas phase organic emissions as compared to the CFM56-2C1 engine studied at AAFEX2 [50]. This is highlighted in Table 6, which shows the measurements reported here for the CDP (corrected for dilution) with the EIs determined under similar low power conditions and standard temperature (288K) as for the CFM56 engine burning JP-8 fuel.

Table 6. Comparison of EIs for the Idle Emissions of PW- F117 (sampled from CDP) and CFM56 Engines [Reference 50]

Compound	EI (g/kg fuel) PW-F117 (This study)	EI (g/kg fuel) CMF56-2C1 (AAFEX2)
Formaldehyde	0.037	1.15
Methanol	0.01	0.18
Acetaldehyde	0.021	0.45
Acetone + Propanal + Glyoxal	0.01	0.22
Benzene	0.009	0.17
Toluene	0.003	0.085
C_2-benzenes	0.0065	0.16

While the data in Table 6 should not be directly compared from an engine performance perspective, it is noteworthy to recognize that the gas phase organic concentrations were significantly lower (by over a factor of 10) than for previous studies on the CFM56 engine. While the exhaust gas concentrations of PW-F117 and CFM56 engines– under the conditions studied – are substantially different, the trend in composition is remarkably similar as is illustrated in Figure 56 where the compound EIs found in Table 6 for the two engines are plotted versus each other. Only formaldehyde appears to significantly different. However, this difference is not considered important given that challenges of measuring of formaldehyde with the PTR-MS and that it represents a single data point.

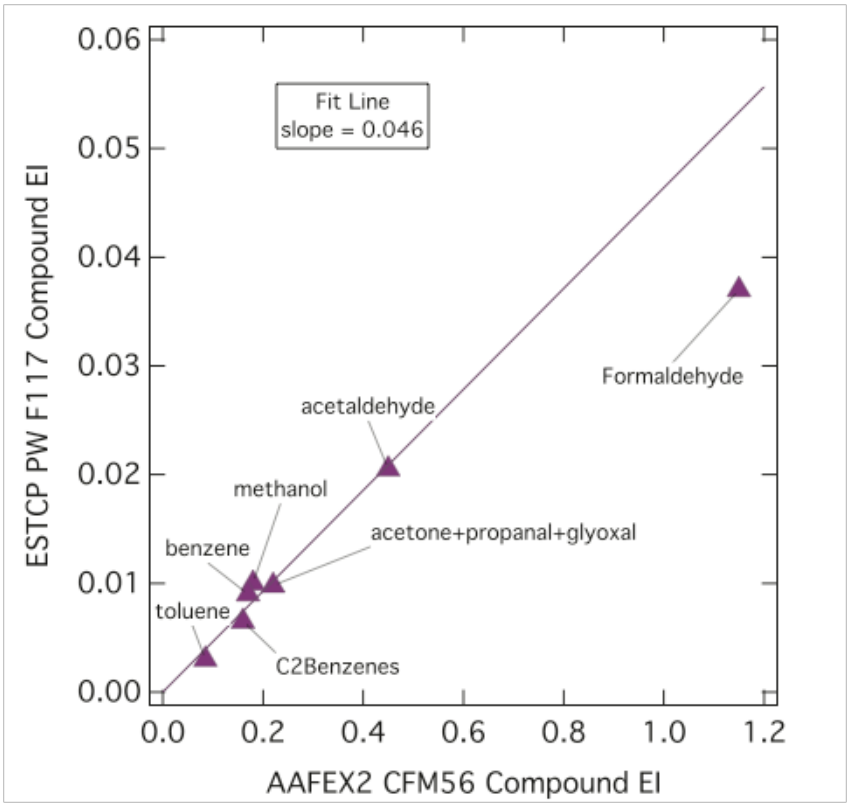

Figure 56. Plot of organic compound EIs for PW-F117 versus for CFM56 engine from a previous campaign

7.2.4 PM and Gaseous Emissions Characterization from Plume, DC and CDP – EPA

7.2.4.1 Gaseous Pollutants

The calculated EIs for THC and SO_2 are shown in Figure 57 for all power conditions. As the reference value, the theoretical SO_2 EI for fuel with a 20 ppm sulfur content is 40 mg/kg. As was the case for the demonstration on the T63 engine, the SO_2 EIs for the CDP are not provided. Also, THC EIs for the CDP are not provided since only negative THC values (below sensitivity limits) were measured during this demonstration.

As shown in Figure 57, the DC THC EIs were generally lower than those found in the plume except at idle. The most consistent agreement was observed at 20% thrust where the DC EI was within about 30% of the two plume values. In the case of the SO_2 EIs, DC and CDP data were only available at 20 and 33% thrust. For these power conditions, the DC SO_2 EIs were either higher or lower than those of the plume depending on which plume EI is used for comparison. Like THC, the EIs obtained at 20% power appear to be most consistent with the DC providing an EI which is approximately two times higher than the two plume measurements.

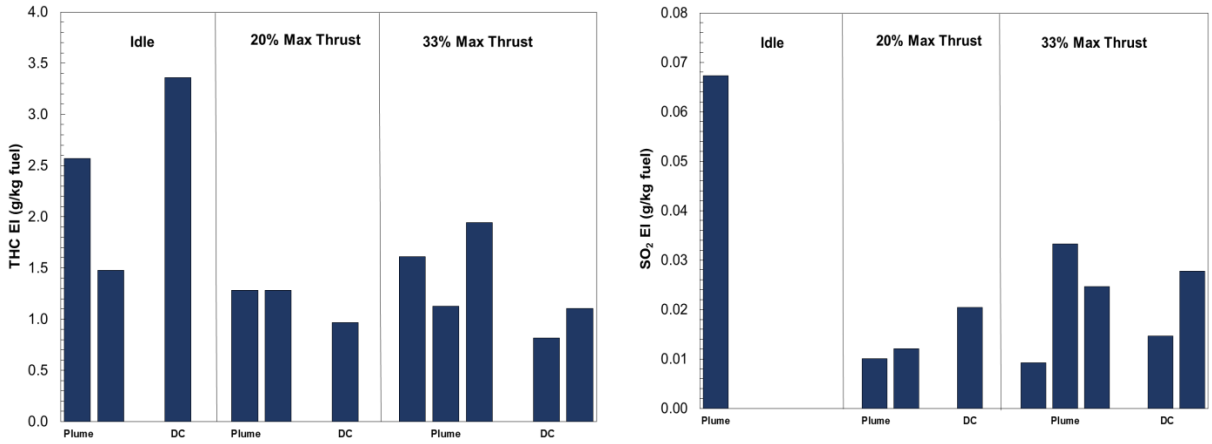

Figure 57. THC and SO_2 EIs for all F-117 engine power conditions

7.2.4.2 Black Carbon Data

The BC EIs calculated from the MSS data are shown in Figure 58 and appear to have much less scatter than the gas phase measurements. In general, the DC sample had a factor of ~ 2 to 3 higher BC EIs than those found in the plume. The CDP EIs on the other hand can either be higher or lower than the plume depending on thrust level. At 33% and 20% rated thrust, the CDP EIs were about a factor of 1.5 to 2 higher than the plume whereas at idle, the CDP BC EI was up to a factor of 2 lower than the plume.

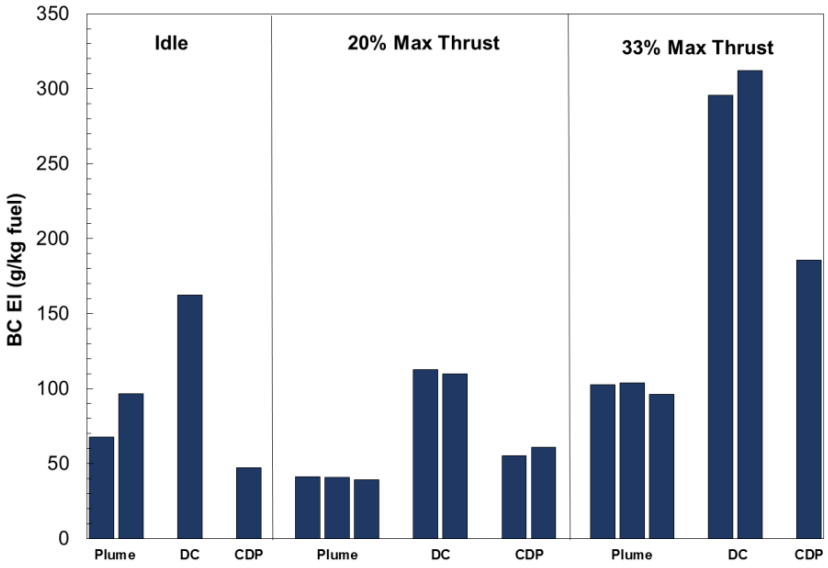

Figure 58. BC emission indices as determined by the AVL MSS at all engine power levels.

7.2.4.3 Particle Number Emissions Data

The particle number EIs calculated from the EEPS data are shown in Figure 59. At 33% max thrust, the particle number EIs from the DC were about a factor of 1.5 higher than those obtained for the plume whereas the CDP EI is about a factor of two lower. For the 20% thrust

condition, both the DC and CDP EIs compare fairly well with the plume measurements except for the first DC test point which is a factor of almost three higher than the plume. Finally, for idle, the DC EI_n is a factor of ~ 3.5 to 18 times higher than the plume depending on which plume EI used, while the CDP EI_n is only 10% of the plume average. It is clear that the lack of consistency between plume measurements makes data interpretation very challenging. These data also disagree with data from the AFRL and the ARI teams. It is uncertain why the disagreement at this condition as the trends for the other conditions are consistent with the different teams.

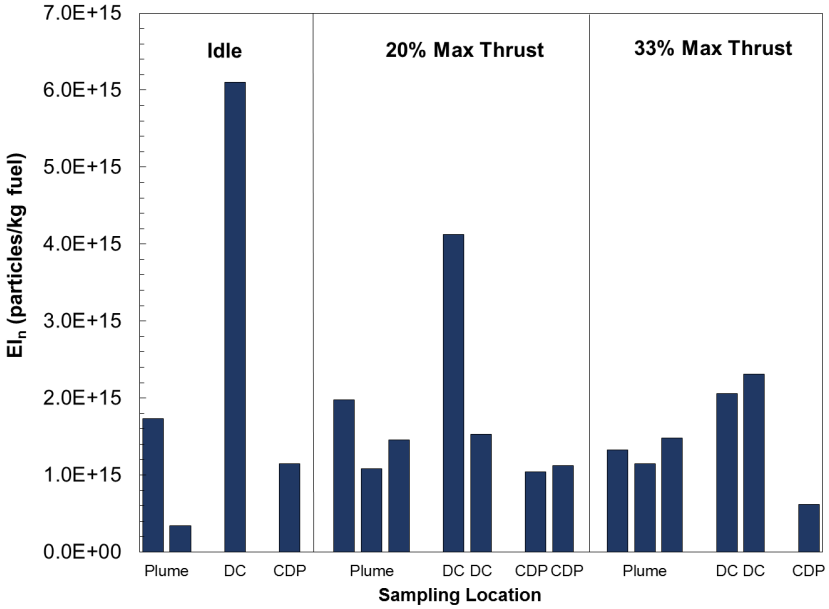

Figure 59. Particle number EIs as determined by the EEPS instrument at all thrust levels.

7.2.4.4 Particle Size Distributions

The particle size distribution (PSD) was obtained by the TSI EEPS for each engine thrust level along with the geometric mean particle diameter (GMD). These are shown in Figure 61 to 62 with all data corrected for dilution. As shown in these figures, all PSDs are lognormal and mono-modal with no nuclei mode evident. A number of differences in the PSD were observed between thrust levels as discussed below.

Regarding the PSDs obtained at 33% power, shown in Figure 60, it can be seen that the PSDs fell into three groups depending on sampling location. The PSDs for the DC exhibited the highest number and largest particle size (GMD ~ 40 nm) as compared to the plume and CDP. The three plume PSDs show a generally smaller number of particles and smaller particle sizes (GMD ~ 25-30 nm). Finally, the CDP had the lowest number of particles, the size of which were about the same as the plume PSDs (GMD ~ 31 nm). From these data it appears that the DC produces a noticeably different aerosol as compared to the plume and CDP at 33% power.

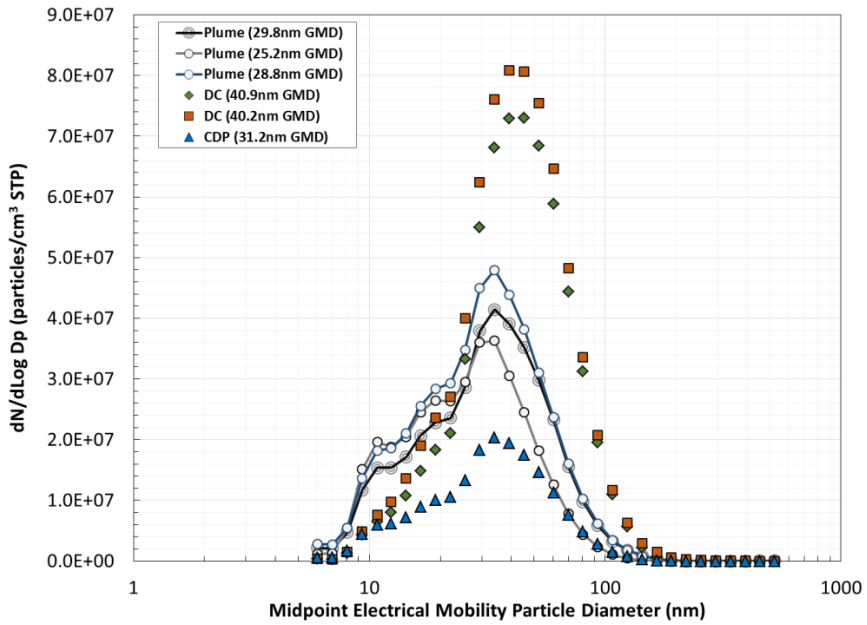

Figure 60. Particle size distributions for PW-F117 engine in plume and condensation devices at 33% max thrust condition

From Figure 61, substantially different PSDs were obtained at 20% thrust. In this case, the plume, DC, and CDP all produced similar PSDs. The only notable exception was a replicate test of the DC, which cannot be explained from the available data.

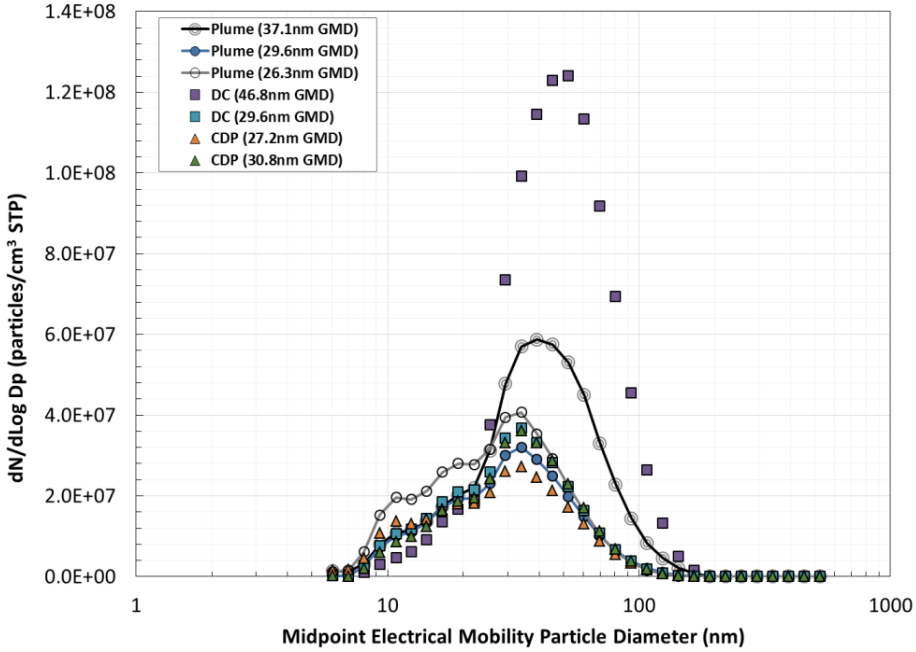

Figure 61. Particle size distributions for PW-F117 engine in plume and condensation devices at 20% max thrust condition

The PSD data shown in Figure 62 show that the DC produced a similar size distribution to that of one of the plume test points but with a greater number of particles and slightly lower GMD (25 vs. 34 nm). The CDP more closely matched the second plume test point except with a higher number of particle counts in each size bin. Also, the DC's PSD appears to be more "ragged" in the 10-20 nm range than was the case for the other two thrust levels indicating a higher level of inconsistency.

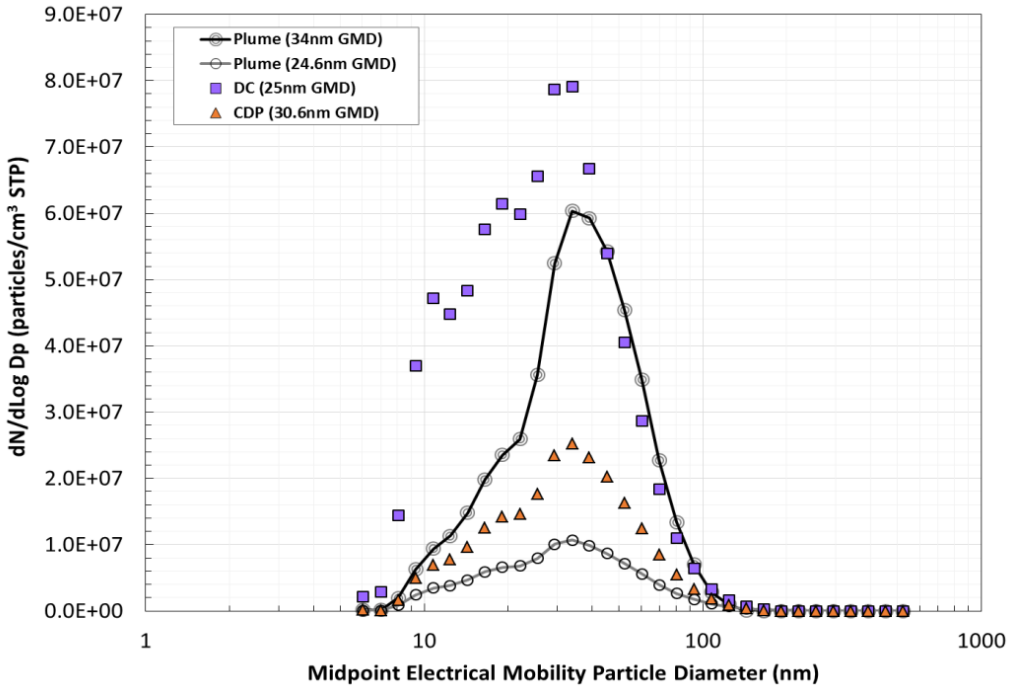

Figure 62. Particle size distributions for PW-F117 engine in plume and condensation devices at idle condition

7.2.5 VPS Performance Assessment - ORNL

The VPS performance was assessed during this demonstration using exhaust from the C-17 engine. Figure 63 shows several particle size distributions (averages of 4-6 sample scans) for the idle engine power condition. The engine PM sample data are shown in black symbols and the lognormal fit in the black curve. Since the overall particle removal performance of VPS and PMP VPR are compared, data from the last stage output (i.e., the second stage) of the PMP VPR is provided in the figure. It is noticed that the raw data showed variation beyond that of a generally smooth particle size distribution such as the lognormal-fit curve show in the figure. It was noticed that the variation in the 4-6 scans was usually greater than ±20% in this test, which is large compared to past experience. It is believed that the particle population in the sample was unstable due to large dilution or potential contamination in sampling system. Considering the adverse weather conditions during the campaign and several technical issues with valves and leaks, some data instability was expected. It was noticed that the left tail (nuclei side of the curve) of the raw-data distribution appeared to be going upward that indicates a large number of particles in the 10nm or smaller size range were present in the sample. This observation was present in all scans of the raw sample. The data variation was significant which further indicates the incoming particle

population was unstable during the idle engine power operation and the aerosol population might have contained significant number of volatile particles. If these particles were indeed volatile, the mode diameter of these particles was smaller than 10nm, which supports of the programmatic assumptions of 15nm mentioned above. Note that a lognormal fit analysis to particle size distribution using a single mode assumption was unable to fit both the primary engine particles and the volatile particle population in Figure 63. Thus, it is clear that there were two modes indeed existing in the PM data resulting from the idle engine power condition.

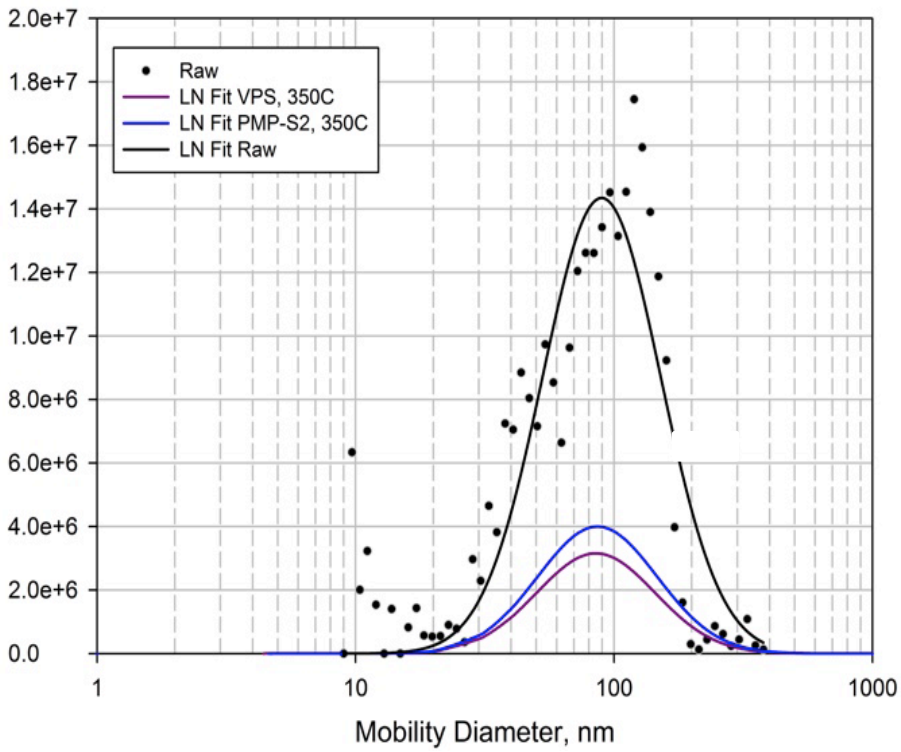

Figure 63. Particle size distribution for PW-F117 engine exhaust sample at idle after conditioning with VPS and PMP VPR (after stage 2)

Once the incoming particles were subject to thermal conditioning by either PMP VPR or VPS at 350°C, both VPS and PMP results showed a significant removal of particles. Thus, it appears that the C-17 engine volatile PM were thermographically similar to C_{40} particles, despite the latter being a complex mixture of hydrocarbons while the C_{40} particles are a single-component. For idle, the particle removal efficiency by VPS is estimated to be 82.3% for the size across all SMPS measurable size bins from 9 to 379nm, and that for PMP VPR is 75.5%. For particles smaller than or equal to 15nm, the removal efficiency for VPS was found to be 100% and 93.6% for PMP VPR. The results showed that the VPS was as effective as PMP in removing particles for the entire size range. However, only the VPS performed reasonably for the 15-nm particles with an efficiency greater than 99% as required by the performance criteria of this program.

Figure 64 shows particle size distributions for engine PM exhaust for the 33% max thrust condition. The particle number concentrations at this power were about an order of magnitude higher than for the idle condition. It is noteworthy that there was no upward tail found at the left end of the curve in Figure 65 to indicate the presence of volatile particles in contrast to that of

Figure 64. This confirms as expected that the volatile particle population was much smaller at 33% engine power compared to that at the idle condition. The particle removal efficiency by VPS is estimated to be 90.2% and that for the PMP VPR 82.7% across all SMPS measurable size bins from 9 to 379nm. For particles smaller than or equal to 15nm, the removal efficiency for VPS was at 99.91% and 99.37% for PMP VPR. The removal efficiency results show that the VPS was about as efficient as the PMP VPR across the entire size range. Both devices performed very well in the removal of 15 nm and smaller particles with an efficiency greater than 99%, therefore both devices met the performance criteria set in the program, (1) the removal of 15-nm particles and smaller ≥ 99%, and (2) the reduction of the mode diameter of the overall particle population at 350°C.

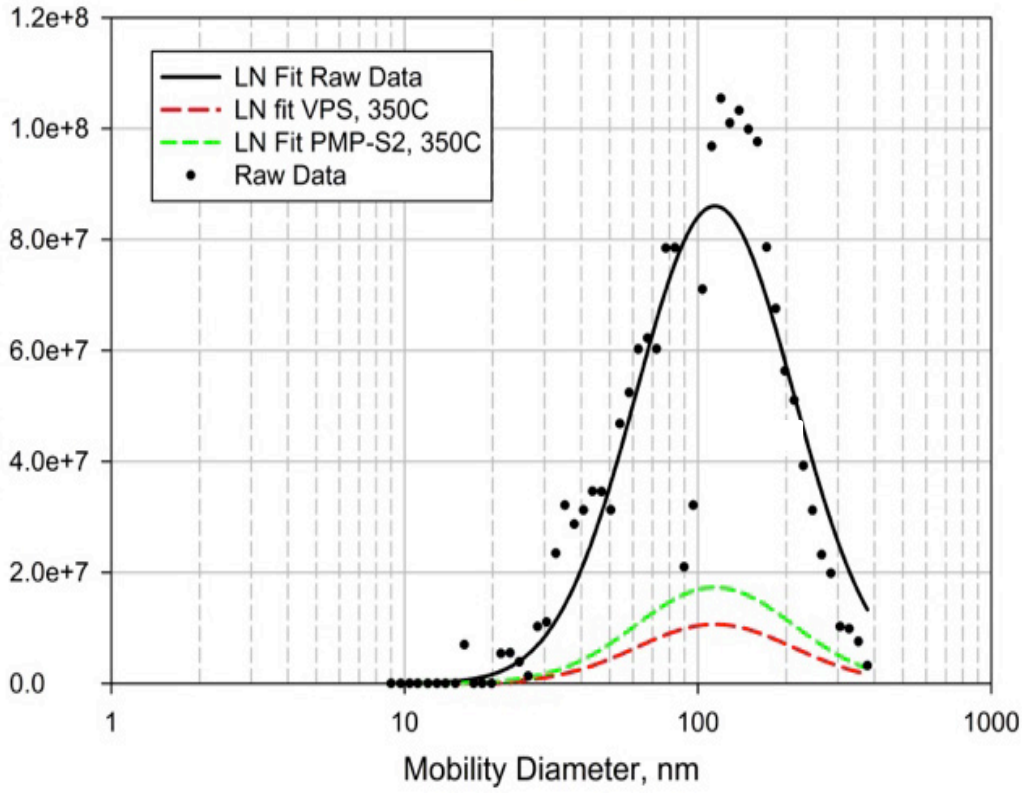

Figure 64. Particle size distribution for PW-F117 engine exhaust sample at 33% max thrust after conditioning with VPS and PMP VPR (after stage 2)

7.3.1 Technology Demonstration Performance Summary

A summary of the performance objectives, success criteria and results of the demonstrations (as discussed in the previous subsections) are listed in Table 7. The results show the potential of the condensation devices to simulate gas-to-particle processes in the atmosphere; however, due to performance inconsistencies and that not all success criteria were met, it is concluded that the devices are not ready for compliance relevant measurements. The VPS demonstrated very high potential to remove volatile species for the measurement of only non-volatile PM and should be considered for engine certification measurements after further validation against the updated VPS requirements listed in the SAE ARP 6320 [51].

Table 7. Summary of Demonstration Objectives, Success Criteria and Actual Performance

Performance Objective	Success Criteria	Criteria Met?
Demonstrate volatile species condensation (volatile PM formation) in the DC and CDP. Significant increase in PM compared to probe-tip dilution.	Clear evidence of volatile particle formation in DC and CDP compared to probe-tip dilution.	**YES**
	10X increase in 5-20 nm particle number	**NO**. Only 2-5X increase.
Demonstrate similar PM chemical characteristics for samples collected at the DC, CDP and 20 m locations.	Composition of PM from DC or CDP and 30 m sample within ±25% in absolute or normalized terms.	**YES**. Organic carbon EI_{mass} similar magnitude.
Demonstrate that ambient air diluted samples in the DC and CDP (N_2 dil) produce similar total PM characteristics as at the 20 m sampling location.	±40% of the particle number	**INCONCLUSIVE** **YES** at higher engine power. **NO** at idle.
	±30% mass	**YES** at two lower conditions.
	±25% of mean diameter	**INCONCLUSIVE** **YES -** T63 engine tests. **NO -** C-17 tests. Larger concentrations of nuclei particles at plume with significantly reduced mean diameter but not matched with DC or CDP.
Demonstrate that N_2 diluted samples in the DC and CDP produce similar non-volatile PM characteristics as probe-tip	±25% of the particle number	**INCONCLUSIVE** **YES** – T63 engine tests Not evaluated – C17
	±15% of mean diameter	**YES** – T63 engine tests Not evaluated – C17
Demonstrate efficient performance of the VPS to remove tetracontane particles	> 99 % vaporization of 15 nm tetracontane particles	**YES**
Demonstrate efficient performance of the VPS to remove volatile species from engine PM	Qualitative data. Significant reduction in 15nm and smaller particles and reduction on mean particle size	**YES.**

8. COST ASSESSMENT

Although the performance of the condensation devices did not satisfy all the demonstration goals, an initial cost assessment for implementation is provided below in case a future program can continue development and the performance goals are achieved.

8.1.1 Cost Model

The successful demonstration of the PM sample conditioning devices and VPS, in concert with already accepted PM instrumentation, provides turbine engine manufacturers a methodology for measuring non-volatile and total PM2.5 emissions factors from military weapon systems, in a controlled environment. Current (non-standard) practices to measure total PM (i.e., far field) are complex, time consuming, expensive, and provide unstable data. Since there isn't an established alternative for a total PM measurement methodology, a cost comparison between the current and demonstrated methodology is difficult. However, based on current practices, the demonstrated methodology is expected to significantly reduce testing and logistics costs by using existing gas probes and reducing the required set up and actual engine run times. The cost comparisons below are based on the present cost of current practices and the demonstrated approach.

8.1.2 Cost Analysis and Comparison

For the characterization of only non-volatile PM, the VPS will lead to significant savings in equipment costs to remove volatile species from the PM sample. The volatile particle remover (VPR) system currently considered by the SAE E31 committee for non-volatile PM sample characterization is manufactured by AVL and costs approximately $250K. The VPS in this project is estimated at a much lower $55K, and allows analysis of the volatile fraction. Table 8 shows a comparison of estimated costs between the current practices and the technologies demonstrated in this project. The long-term savings are realized in the test costs at approximately $85K less per test for the demonstrated technologies.

Table 8. Type of Cost and Cost Comparison for Current and Demonstrated Technologies

Demonstrated Technology Costs		**Current Process Costs**	
Activity	**Avg. Cost ($k)**	**Activity**	**Avg. Cost ($k)**
Equipment		**Equipment**	
- **Dilution Chamber**	50	- Volatile Particle Remover	250
- **Condensation Dilution Probe**	50	- Black Carbon Instrument	50
- **Vapor Particle Separator**	55		
- **Condensation Particle Counter**	60	- Condensation Particle Counter	60
- **Particle Sizer**	75	- Particle Sizer (2)	150
- **Particle Mass Instrument**	100	- Particle Mass Instrument (2)	200
- **Sampling System**	100	- Sampling System	150
- **Gas Emissions Instrumentation**	200	- Gas Emissions Instrumentation	200
- **Probe System**	75	- Probe Systems	85
Test Costs		**Test Costs**	
System Installation & Teardown	40	System Installation & Teardown	50
Near Field Testing	80	Near and Far Field Testing	130
Data Analysis	40	Data Analysis	65
Other (travel, supplies, misc.)	30	Other (travel, supplies, misc.)	30
Total	**955**	**Total**	**1420**

9. IMPLEMENTATION ISSUES

The demonstrations in this project showed that the two condensation devices to promote volatile PM formation in turbine engine exhaust did not meet all of the performance criteria set for the program. Although both the DC and CDP showed potential, as evidenced by the formation of PM from volatile species, these were not sufficient to fully simulate the thermo-physical processes in the atmosphere which lead to the formation of volatile PM and PM with characteristics of those found in aircraft engine plumes. However, as mentioned previously, the demonstration on the turbofan (PW-F117) engine was very limited, which precluded the adjustment of dilution parameters that could have improved PM data agreement between plume and devices. If further work is performed and improved performance can be demonstrated, the implementation issues for turbine engine OEMs are relatively minor since the sampling system from engine to device is the same as those existing for gaseous emissions and smoke number certification of engines. Additions include the dilution device, sampling lines for the sample after conditioning, and the PM characterization instruments.

The VPS met the success criteria based on its comparison to the PMP VPR performance using C_{40} and turbine engine particles. Implementation issues are minimal and perhaps simpler than the use of the VPR systems considered presently by the SAE E31 committee.

10. REFERENCES

1. C. Pope, R. Burnett, M. Thun, E. Calle, D. Krewski, K. Ito, and G. Thurston., "Lung, Cancer, Cariopulmonary Mortality and Long-term Exposure to Fine Particulate Air Pollution," *J. of American Medical Association*, 2002: 1132-1141.
2. D.B. Kittelson, M. Arnold, W. F. Watts, "Review Of Diesel Particulate Matter Sampling Methods," EPA Final Report (1999).
3. B. Giechaskiel, et al., "Evaluation of the Particle Measurement Programme (PMP) protocol to remove the vehicles' exhaust aerosol volatile phase," *Science of the Total Environment* 408 5106–5116 (2010).
4. H. Burtscher, U. Baltensperger, N. Bukowiecki, P. Cohn, C. Huglin, M. Mohr, U. Matter, S. Nyeki, V. Schmatloch, N. Streit, and E. Weingartner*, J. Aerosol Sci.* 32, 427 (2001).
5. D. B. Kittelson, W. F. Watts, J. C. Savstrom, and J. P. Johnson, *J. Aerosol Sci*. **36**, 1089 (2005).
6. G. R. Johnson, Z. Ristovski, and L. Morawska, *J. Aerosol Sci.* 35, 443 (2004).
7. P. Villani, D. Picard, N. Marchand, and P. Laj, *Aerosol Sci. Technol*. 41, 898 (2007).
8. W. J. An, R. K., Pathak, B.-H. Lee, and S. N. Pandis, *J. Aerosol Sci.* 38, 305 (2007).
9. L. Newman, *Atmos. Environ*. 12, 113 (1978).
10. W. G. Cobourn, R. B. Husar, and J. D. Husar, *Atmos. Environ*. 12, 89 (1978).
11. J. Slanina, M. P. Keuken, and C. A. M. Schoonebeek, *Anal. Chem*. 59, 2764 (1987).
12. W. T. Sturges, and R. M. Harrison, *Environ. Sci. Technol*. 22, 1305 (1988).
13. B. Wehner, S. Philippin, and A. Wiedensohler, *J. Aerosol Sci*. 33, 1087 (2002).
14. M. Fierz, M. G. C. Vernooij, and H. Burtscher, *J. Aerosol Sci.* 38, 1163 (2007).
15. D. Park, S. Kim, N. K. Choi, and J. Hwang, *J. Aerosol Sci*. 39, 1099 (2008).
16. J. A. Huffman, P. J. Ziemann, J. T. Jayne, D. R. Worsnop, and J. L. Jimenez, *Aerosol Sci. Technol*. 42, 395 (2008).
17. Z. Wu, L. Poulain, B. Wehner, A. Wiedensohler, and H. Herrmann, *J. Aerosol Sci*. 40, 603 (2009).
18. J. Swanson, and D. B. Kittelson, *J. Aerosol Sci.* 41, 1113-1122 (2010).
19. H. Burtscher, S. Kuenzel, C. Hueglin, *J. Aerosol Sci*. 26, S129 (1995).
20. M. M. Maricq, R. E. Chase, D. H. Podsiadlik, and R. Vogt, SAE Technical Paper Series, 1999-01-1461 (1999).
21. K. Vaaraslhti, A. Virtanen, J. Ristimaki, and J. Keskinen, *Environ. Sci. Technol.* 38, 4884 (2004).
22. K. K. Virtanen, J. M. Ristimaki, K. Vaaraslhti, and J. Keskinen, *Environ. Sci. Technol*. 38, 2551 (2004).
23. A. Petzold, M. Fiebig, L. Fritzsche, C. Stein, U. Schumann, C. W. Wilson, C. D. Hurley, F. Arnold, E. Katragkou, U. Baltensperger, M. Gysel, S. Nyeki, R. Hitzenberger, H.-R. Giebl, D. J. Hughes, R. Kurtenbach, P. Wiesen, P. Madden, H. Puxbaum, S. Vrchoticky, and C. Wahl, *Meteorologische Zeitschrift* 14, 465 (2005).
24. Mamakos L. Ntziachristos, and Z. Samaras, *Environ. Sci. Technol.* 40, 4739 (2006).
25. M.-D. Cheng, GT2010-22175, *Proceedings of ASME Gas Turbine Congress* (2010).
26. B. Giechaskiel, R. Chirico, P. F. DeCarlo, M. Clairotte, T. Adam, G. Martini, M. F. Heringa, R. Richter, A. S. H. Prevot, U. Baltensperger, and C. Astorga, *Sci. Total Environ.* 408, 5106 (2010).

27. T. J. Phelps, A. V. Palumbo, B. L. Bischoff, C. J. Miller, L. A. Fagan, M. S. McNeilly, and R. R. Judkins, *J. Microbial Methods* 74, 10 (2008).
28. J. Peck, et al., "Measurement of volatile particulate matter emissions from aircraft engines using a simulated plume aging system," *J. Eng. Gas Turbines Power*, 134(6), 061503 (2012).
29. E. Corporan, M.J. DeWitt, C.D. Klingshirn, D. Anneken, "Alternative Fuels Tests on a C-17 Aircraft: Emissions Characteristics," USAF AFRL Technical Report, AFRL-RZ-WP-TR-2011-2004 (2011).
30. C.C. Wey, B.E. Anderson, C. Wey, R.C. Miake-Lye, P. Whitefield and R. Howard, "Overview on the aircraft particle emissions experiment," *J. Propul. Power*, 23, 898–905. (2007).
31. D. Bulzan, et al., "Gaseous and Particulate Emissions Results of the NASA Alternative Aviation Fuel Experiment (AAFEX)," *Proceedings of the ASME Turbo Expo*, GT 2010-23524 (2010).
32. M. -D. Cheng, E. Corporan, M. J. DeWitt, and B. Landgraf *, J. Aerosol and Air Qual. Res*. 9, 237 (2009).
33. M.-D. Cheng, E. Corporan, M. J. DeWitt, C. W. Spicer, M. W. Holdren, K. Cowen, B. D. Harris, R. Shores, R. Hashmonay, and R. Kagann, *J. Air Waste Manage. Assoc*. 58, 787 (2008).
34. SAE 1971, "Procedure for the Continuous Sampling and Measurement of Gaseous Emissions from Aircraft Turbine Engines," SAE: Warrendale, PA, SAE Aerospace Recommended Practice ARP 1256 (1971).
35. P. Liu, P.J. Ziemann, D.B. Kittelson, and P.H. McMurry, "Generating Particle Beams of Controlled Dimensions and Divergence: I. Theory of Particle Motion in Aerodynamic Lenses and Nozzle Expansions", *Aerosol Sci. Technol*. 22:293–313 (1995).
36. X.F. Zhang, K.A. Smith, D.R. Worsnop, J. Jimenez, J.T. Jayne and C.E. Kolb, "A Numerical Characterization of Particle Beam Collimation by an Aerodynamic Lens-Nozzle System: Part I. An Individual Lens or Nozzle", *Aerosol Sci. Technol*. 36(5): 617–631 (2002).
37. X.F. Zhang, K.A. Smith, and D.R. Worsnop, "Characterization of Particle Beam Collimation: Part II Integrated Aerodynamic Lens-Nozzle System", *Aerosol Sci. Technol.* 38(6): 619–638 (2004).
38. J.T. Jayne, et al., Development of an Aerosol Mass Spectrometer for Size and Composition Analysis of Submicron Particles, *Aerosol Sci. Technol.* 33:49–70 (2000).
39. P. Kebabian, and A. Freedman "System and Method for Trace Species Detection Using Cavity Attenuated Phase Shift Spectroscopy with an Incoherent Light Source," U.S. Patent No. 7301639 (2007).
40. P. Kebabian, W. Robinson, and A. Freedman, "Optical Extinction Monitor Using CW Cavity Enhanced Detection," *Rev. Sci. Instrum.,* 78: 063102 (2007).
41. P. Massoli, P. Kebabian, T. Onasch, F. Hills and A. Freedman "Aerosol Light Extinction Measurements by Cavity Attenuated Phase Shift Spectroscopy (CAPS): Laboratory Validation and Field Deployment of a Compact Aerosol Extinction Monitor," *Aerosol Sci. Technol.,* 44:428–435 (2010).
42. Z. Yu, et al., "Direct Measurement of Aircraft Engine Soot Emissions Using a Cavity-Attenuated Phase Shift (CAPS)-Based Extinction Monitor," *Aerosol Sci. Technol.*, 45:1319-1325 (2011).

43. J. de Gouw, C. Warneke, “Measurements of volatile organic compounds in the earth’s atmosphere using proton-transfer-reaction mass spectrometry,” *Mass Spectrometry Reviews,* 26 223-257 (2007).
44. W. Lindinger, A. Hansel, A. Jordan, “Proton-transfer-reaction mass spectrometry (PTR-MS): on-line monitoring of volatile organic compounds at pptv levels,*” Chemical Society Reviews,* 27 347-354 (1998).
45. S.G. Lias, J.E. Bartmess, J.F. Liebmann, J.L. Holmes, R.D. Levin, W.G. Mallard, Ion Energetics Data, in: P.J.L.a.W.G. Mallard (Ed.) NIST Chemistry WebBook, NIST
46. W.B. Knighton, T.M. Rogers, B.E. Anderson, S.C. Herndon, P.E. Yelvington, R.C. Miake-Lye, “Quantification of aircraft engine hydrocarbon emissions using proton transfer reaction mass spectrometry,” *J. of Propulsion and Power*, 23 949-958 (2007).
47. National Institute of Occupational Safety and Health Diesel Particulate Matter (as elemental carbon). Method 5040:Issue 3, http://198.246.98.21/niosh/nmam/pdfs/5040.pdf (2003).
48. Z. Yu, D.S. Liscinsky, E.L. Winstead, B.S., True, M.T. Timko, A. Bhargava, S.C Herndon, R.C. Miake-Lye, and B.E. Anderson, “Characterization of lubrication oil emissions from aircraft engines,” *Environ. Sci. Technol.* 44, 9530-9534 (2010).
49. Z. Yu, Z., S.C. Herndon, L.D. Ziemba, M.T. Timko, D.S. Liscinsky, B.E. Anderson and R.C. Miake-Lye, “Identification of lubrication oil in the particulate matter emissions from engine exhaust of in-service commercial aircraft,” *Environ. Sci. Technol*. 46, 9630-9637 (2012).
50. W. B. Knighton, S. C. Herndon, E. Wood, R. C. Miake-Lye, M. Timko, Z. Yu, A. Beyersdorf, E. Winstead, B. E. Anderson, C. Wey, D. Bulzan, “Near-idle organic gas emissions for characterizing aircraft engine exhaust emissions: Assessment of the influence of fuel flow, ambient temperature, and alternative fuels”, Manuscript in preparation (2017).
51. SAE 2017, “Procedure for the Continuous Sampling and Measurement of Non-volatile Particulate Matter Emissions from Aircraft Turbine Engines,” SAE: Warrendale, PA, SAE Aerospace Recommended Practice ARP 6320, In review (2017).

Appendix: Points of Contact

Performer	Organization	Phone/Email	Role in Project
Edwin Corporan	Fuels & Energy Branch (AFRL/RQTF)	937-255-2008 Edwin.corporan@wpafb.af.mil	Principal Investigator
Matthew DeWitt	University of Dayton Research Institute (UDRI)	937-255-6399 Matthew.dewitt.ctr@wpafb.af.mil	Fuels Characterization and Emissions Evaluations
Meng-Dawn Cheng	Oak Ridge National Laboratory (ORNL)	865-241-5918 chengmd@ornl.gov	VPS modeling & characterization, PMP system implementation
Richard Miake-Lye	Aerodyne Research Inc.	978-932-0251 rick@aerodyne.com	Condensation probe & PM chemical characterization
John Kinsey	U.S. Environmental Protection Agency, NRMRL	919-541-4121 kinsey.john@epa.gov	Volatile & non-volatile PM mass and sulfur measurements
W.B. Knighton	Montana State University	406-994-5419 bknighton@chemistry.montana.edu	PTR-MS measurements
Chris Klingshirn	University of Dayton Research Institute (UDRI)	937-255-7301 christopher.klingshirn.ctr@us.af.mil	Emissions Evaluations

LIST OF ACRONYMS, ABBREVIATIONS, AND SYMBOLS

Acronym	Description
AAFEX	Alternative Aviation Fuel Experiment
APEX	Aircraft Particle Emissions Experiment
AFCO	Alternative Fuels Certification Office
AFRC	Air Force Reserve Command
AFRL	Air Force Research Laboratory
AIR	Aerospace Information Report
AMS	Aerosol Mass Spectrometer
ARI	Aerodyne Research Inc.
ARP	Aerospace Recommended Practice
CAA	Clean Air Act
CAEP	Committee on Aviation Environmental Protection
CDP	Condensation Dilution Probe
CFD	Computational Fluid Dynamics
CPC	Condensation Particle Counter
CVS	constant volume sampling
DC	Dilution Chamber
DMA	Differential Mobility Analyzer
DOD	Department of Defense
DOE	Department of Energy
DOP	Dioctyl Phthalate
EC/OC	Elemental Carbon/Organic Carbon
EEPS	Engine Exhaust Particle Sizer
EERF	Engine Environment Research Facility
EI_n	Particle Number Emission Index
EPA	Environmental Protection Agency
EU	European Union
FAA	Federal Aviation Administration
FTIR	Fourier Transform Infrared
GC-MS	Gas Chromatography-Mass Spectrometry
ICAO	International Civil Aviation Organization
LII	Laser Induced Incandescence
LTO	Landing Takeoff
MAAP	Multi-Angle Absorption Photometer
MSS	Micro-Soot Sensor
NAAQS	National Ambient Air Quality Standards
NDIR	Non-Dispersive Infrared

NIOSH	National Institute for Occupational Safety and Health
nm	nanometer
NRMRL	National Risk Management Research Laboratory
NTRC	National Transportation Research Center
ORNL	Oak Ridge National Laboratory
PARTNER	Partnership for AiR Transportation Noise and Emissions Reduction
PM	Particulate Matter
PMP	Particulate Matter Programme
PN	Particle Number
PTFE	Polytetrafluoroethylene
PTR-MS	Proton Transfer Reaction -Mass Spectrometry
SAE	Society of Automotive Engineers
SBIR	Small Business Innovative Research
SMPS	Scanning Mobility Particle Sizer
TRL	Technology Readiness Level
SIPs	State Implementation Plans
UDRI	University of Dayton Research Institute
VPR	Volatile Particle Remover
VPS	Vapor Particle Separator
VTDMA	Volatility Tandem Differential Mobility Analyzer
WPAFB	Wright-Patterson Air Force Base